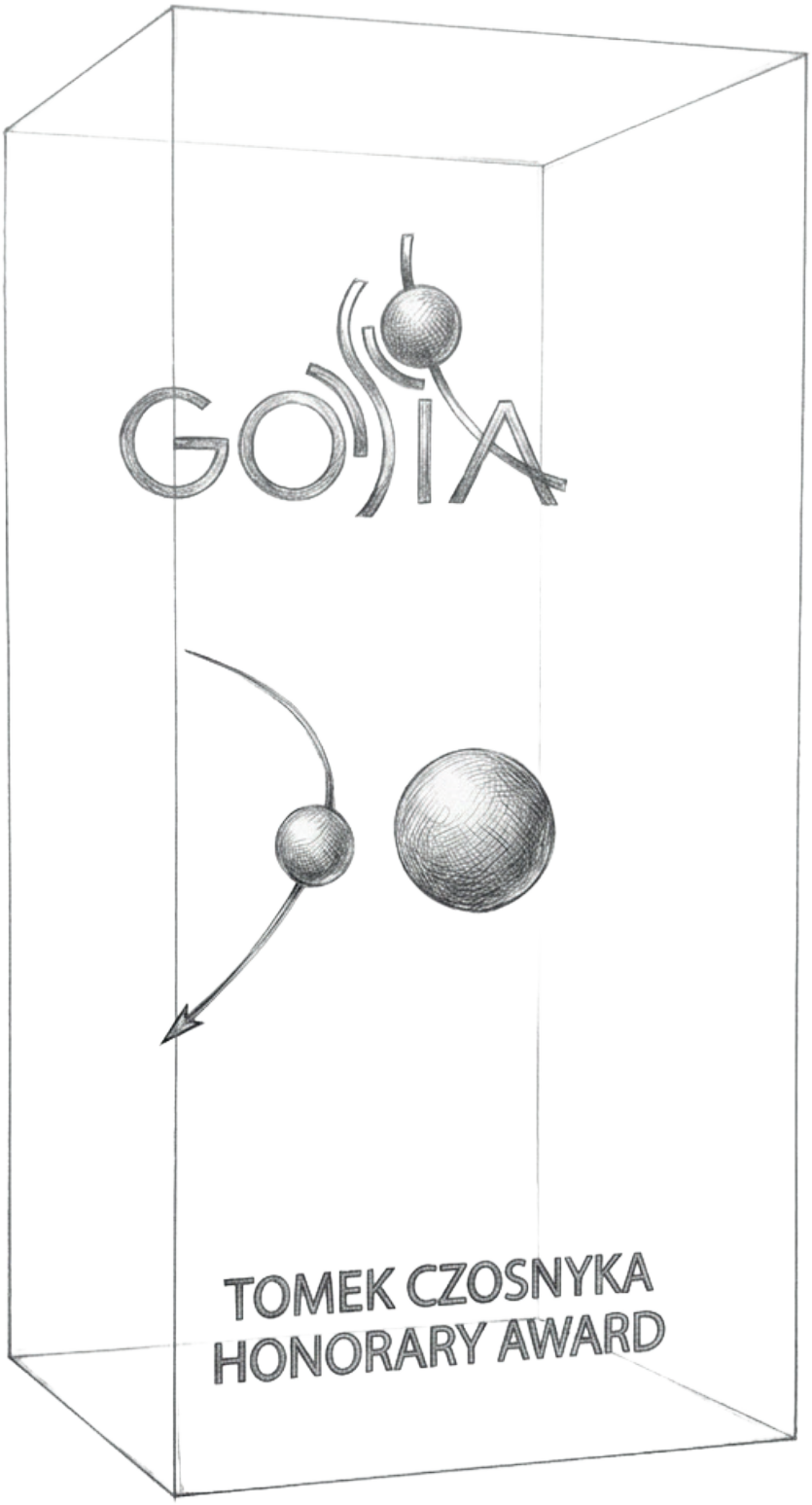
Heavy Ion Laboratory

ANNUAL REPORT 2025





Tomasz Czosnyka
1952 - 2006

UNIVERSITY OF WARSAW

HIL
Heavy Ion Laboratory

Heavy Ion Laboratory

University of Warsaw

Annual Report

2025



Warszawa, May 2026

Annual Report of the
Heavy Ion Laboratory, University of Warsaw
ul. Pasteura 5a, 02-093 Warszawa, Poland
phone (+48)22-8222123, (+48)22-5546000
fax (+48)22-6592714
http://www.slcj.uw.edu.pl

Editors:
Justyna Samorajczyk-Pyśk, Marzena Wolińska-Cichocka,
Andrzej Tucholski, Monika Paluch-Ferszt, Nicholas Keeley
e-mail: raport@slcj.uw.edu.pl
ISSN 1895-6726

Cover design:
Rafał Klęk

On the cover:
Tomek Czosnyka Honorary Award statuette

Contents

Introduction 5
Tomek Czosnyka Honorary Award 2025 Presented to Katarzyna Hadyńska-Klęk 6

A Laboratory overview and technical developments **9**
A.1 Reconstruction of the injection line for the U-200P cyclotron 11
A.2 A standalone station with automatic loading, dedicated to the PETtrace cyclotron 16
A.3 Operation of the ECR ion source and injection beamline at HIL in 2025 . . 18
A.4 New interfaces for magnet power supplies 21
A.5 Application of the Heavy Ion Laboratory Ion Source to low-energy ion implantation 23
A.6 Control application for internal beam irradiation in the cyclotron 25
A.7 HPGe Detector Laboratory 27
A.8 Barium targets for Coulomb excitation of ^{136}Ba studies 28
A.9 Polish Workshop on the Acceleration and Applications of Heavy Ions . . . 31

B Research for medical and biological applications **33**
B.1 Analysis of potential interferents in synthesis of Pd-porphyrin complexes for radiopharmaceutical applications 35
B.2 Polish honeys as a source of selenomethionine 37
B.3 The use of white mulberry extract (Morus alba L.) for the synthesis of selenium nanoparticles 39
B.4 Development and Validation of a Digitized Quantitative Analytical Method for Kryptofix 2.2.2 Determination in ^{18}FDG Radiopharmaceuticals 41
B.5 Optimization of Automated [^{18}F]FAZA Synthesis on the Synthra RN System 44
B.6 Single-Domain Anti-HER2 Antibody Labelled with Theranostic ^{177}Lu - Physicochemical and Biological Characterization for Targeted Radioimmunotherapy 46

C Nuclear physics **49**
C.1 Lifetime studies in neutron-deficient ^{172}Os using the RDDS technique . . . 51
C.2 Gamma-ray Spectroscopy of ^{134}Sm 54
C.3 Lifetime measurement of low-lying excited states in ^{118}Xe 56
C.4 Lifetime measurement of ^{128}Cs I=11^+, 12^+ states with the plunger technique 59
C.5 Search for a new chiral nucleus in the mass 80 region: ^{72}As 61
C.6 Deformation of the $0^+_{1,2}$ states in ^{110}Cd from low-energy Coulomb excitation 64
C.7 Coulomb excitation of ^{104}Pd with the EAGLE + SilCA-DSSD setup. . . . 67
C.8 Measurement of quasielastic barrier distributions of the ^{24}Mg + ^{92,94,95}Mo systems 70
C.9 Dissipation in the ^{20}Ne + ^{92,94,95}Mo systems: the role of transfer channels . 73
C.10 First results from the T-INSIDE experiment 76

C.11 Collective excitations of neutron-deficient Hg isotopes within the framework of the mean-field theory . . . 79
C.12 Coulomb excitation of ^{90}Zr . . . 82

D Appendices **85**
D.1 List of experiments performed at HIL in 2025 . . . 87
D.2 Degrees and theses completed or in progress during 2025 . . . 88
D.2.1 DSc degrees of HIL staff members . . . 88
D.2.2 MSc and BSc theses supervised by HIL staff members . . . 88
D.3 Publications . . . 92
D.4 Seminars . . . 101
D.4.1 Seminars organised at HIL . . . 101
D.4.2 Seminars co-organised by HIL . . . 102
D.4.3 External seminars given by HIL staff . . . 104
D.4.4 Poster presentations . . . 107
D.4.5 Lectures for students and student laboratories . . . 108
D.4.6 Science popularization lectures . . . 110
D.5 Honours and Awards . . . 112
D.6 Laboratory staff . . . 113
D.7 Laboratory Council . . . 114
D.8 Programme Advisory Committee . . . 115
D.9 HIL external users . . . 116

List of Authors **117**

Introduction

The year 2025 brought a number of events that clearly illustrate both the continuity and the future of research carried out at HIL. Of particular importance was the award of the Tomek Czosnyka Honorary Prize to Dr. Katarzyna Hadyńska-Klęk. This distinction, established by Tomasz Czosnyka's former students to honour his memory and preserve his legacy, was presented for the sixth time. It is also the second time the prize has been awarded to a member of our Laboratory—following Dr. Katarzyna Wrzosek-Lipska, who received it in 2019. These recognitions demonstrate that research on nuclear structure using Coulomb excitation methods continues to have a strong foundation and a promising future in Warsaw.

This future also has an instrumental dimension. The new SilCA-DSSD detection system, operating with EAGLE, is now ready for use. Its first physics experiment—Coulomb excitation of ^{104}Pd—was successfully carried out in December 2025. This opens the way for an extensive programme of Coulomb excitation measurements planned for 2026.

The stay of the neutron detector array NEDA in Warsaw is coming to an end. It is therefore no surprise that we look with great interest at the first results of the NEEDLE campaign. The scientific section of this Report presents results from experiments performed with the combined NEDA+EAGLE setup, including studies of the structure of ^{134}Sm and lifetime measurements of excited states in ^{118}Xe.

Alongside gamma-ray spectroscopy, research on barrier distributions and dissipation mechanisms in heavy-ion reactions continues to develop dynamically. In 2025, Dr. Giulia Colucci was awarded funding from the NCN SONATA-20 programme for the project "Near- and sub-barrier fusion reactions: the investigation of the hindrance phenomenon and its link to astrophysics". Her achievements were further recognized with a University of Warsaw Rector's Distinction for outstanding scientific activity, encompassing both research and development work that significantly contributes to the growth and prestige of the University.

The year concluded with an important publication milestone: the article by Martyna Araszkiewicz and collaborators: "Expression of DNA-damage response genes after exposure to high-LET particles used in BNCT in glioblastoma cells with altered radiosensitivity" (Scientific Reports 16 (2025) 2822). This work is the outcome of Dr. Araszkiewicz's doctoral project, conducted under the supervision of Prof. Agnieszka Korgul (Faculty of Physics) and Dr. Katarzyna Tymińska (NCBJ). A significant portion of the research was conducted in the radiobiology laboratory at HIL, led by Dr. Urszula Kaźmierczak, and focuses on the expression of DNA damage response genes following the exposure of glioblastoma cells to high-LET particles used in BNCT.

This year also brought organizational changes at the Heavy Ion Laboratory. New terms began for the Laboratory Council, the Programme Advisory Committee, and the Jury of the Heavy Ion Laboratory Prize, founded by Professor Inamura. In 2026, we will see the first decisions of these bodies, including the selection of new experimental projects recommended for execution using the cyclotron beam, as well as the announcement of the next Prize laureate.



Tomek Czosnyka Honorary Award 2025 Presented to Katarzyna Hadyńska-Klęk

P.J. Napiorkowski for the Award Committee,

Heavy Ion Laboratory, University of Warsaw, Warszawa, Poland

Tomasz Czosnyka was one of the founding fathers of the Warsaw Cyclotron. In 1982, following the dissolution of the Institute for Nuclear Research, he joined the Heavy Ion Laboratory at the University of Warsaw. His work focused on two main research areas: the acceleration of charged particles and the structure of atomic nuclei. After completing his studies, he developed software to simulate ion acceleration in the Warsaw Cyclotron. During a research internship at the University of Rochester in the United States, he created the GOSIA program for Coulomb excitation analysis. Following the successful extraction of the cyclotron beam in 1994, he established a research group and initiated nuclear structure studies at the Heavy Ion Laboratory using Coulomb excitation methods.

Tomasz Czosnyka passed away prematurely in 2006. At that time, his mentor, Prof. Douglas Cline, wrote:
"Tomasz was a brilliant scientist with tremendous drive, dedication and effectiveness. His work led to pioneering advances in the field of Coulomb excitation. His Ph.D. thesis developed sophisticated techniques that solved a problem that many in the field claimed was impossible when started in 1979. This important development now forms the foundation of modern multiple Coulomb excitation analysis and will continue to play a major role in nuclear physics research at new radioactive beam facilities now in operation or under construction. Tomasz was a generous and thoughtful friend and colleague, with a warm, easygoing manner and a great sense of humor. Even though Tomasz is no longer with us in person, he remains with us in spirit, and we continue to hold him in the highest esteem and affection. The legacy of his achievements in nuclear science will endure for many years to come."

To honour Tomasz Czosnyka and his achievements, his four former PhD students - Jędrzej Iwanicki, Jarosław Choiński, Paweł J. Napiorkowski, and Magda Zielińska - established the Honorary Tomek Czosnyka Award in 2014, marking the 20^{th} anniversary of the first beam extraction from the Warsaw Cyclotron. The award recognizes outstanding contributions to the development of Coulomb excitation and accelerator physics. Its recipients are regarded as honorary students of Tomasz Czosnyka and become members of the Award Committee.The laureate is considered an honorary Tomek alumnus and joins the Award Council.

The award has been presented to:

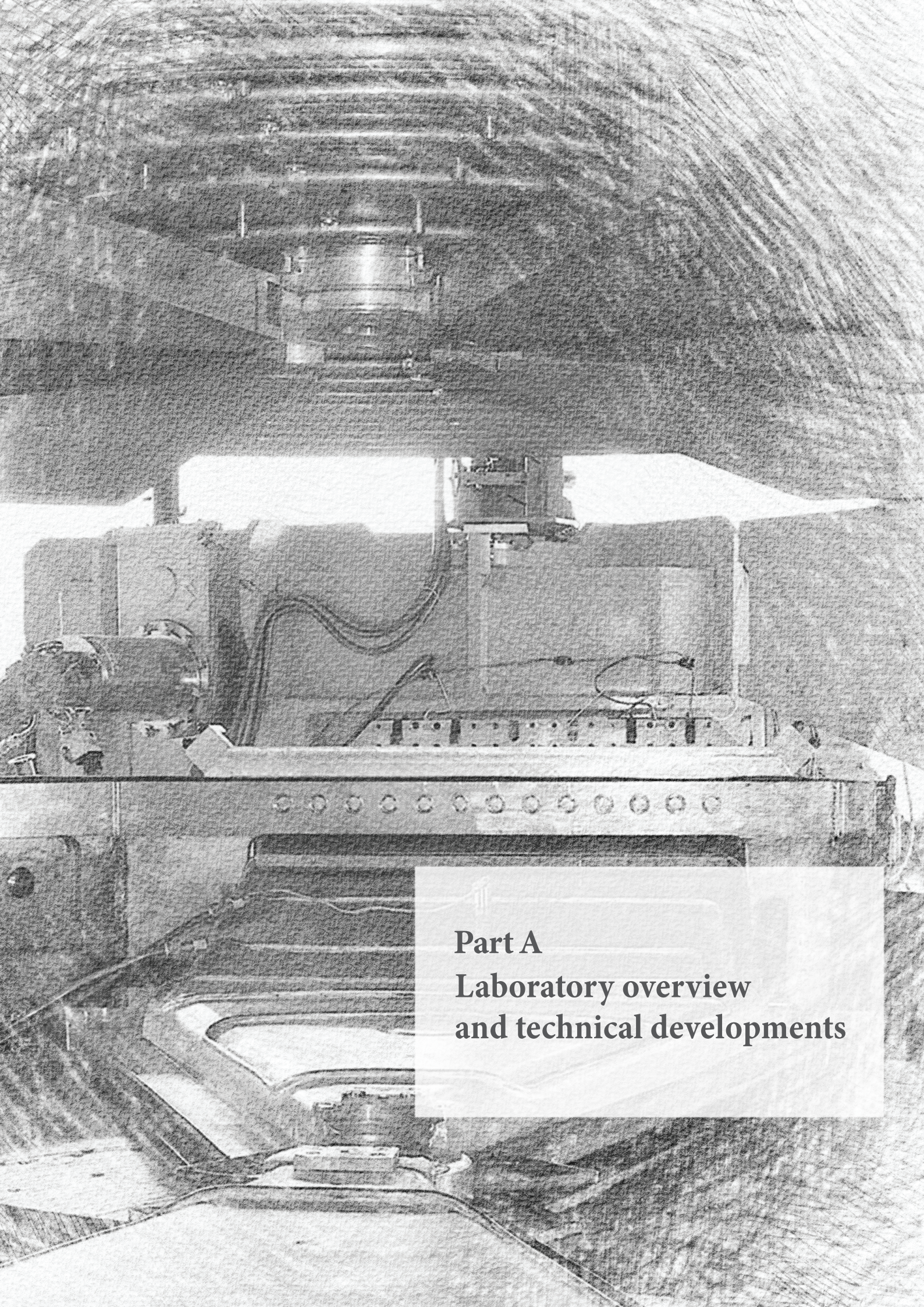
- 2014 – Emmanuel Clément,
- 2015 – Nigel Warr,
- 2017 – Liam P. Gaffney,
- 2019 – Katarzyna Wrzosek-Lipska,
- 2023 – Janne Pakarinen.

In 2025, the Honorary Tomek Czosnyka Award was presented to Katarzyna Hadyńska-Klęk of the Heavy Ion Laboratory. She had already decided to pursue research on atomic nuclei using Coulomb excitation methods during her studies, following her participation in the 2006 Student Workshop. She completed her doctoral thesis at the Heavy Ion Laboratory, focusing on superdeformation in ^{42}Ca. In Warsaw she is now developing experimental infrastructure for

Coulomb excitation studies, including the SILCA chamber. Her expertise and achievements are also highly valued by collaborators in Oslo, Legnaro, Surrey, Florence, Cape Town, and Orsay.

In two years' time - at the next Mazurian Conference on Nuclear Physics in 2028 - the Honorary Tomek Czosnyka Award will be presented to another distinguished researcher.





Part A
Laboratory overview and technical developments

A.1 Reconstruction of the injection line for the U-200P cyclotron

J. Choiński, M. Matuszewski, B. Radomyski, T. Abraham, M. Antczak, P. Jasiński, W. Kalisiewicz, R. Kopik, M. Kopka, W. Kozaczka, P. Krysiak, K. Łabęda, K. Makowski, J. Miszczak, K. Pietrzak, R. Ratyński, Ł. Standyło, M. Szperkiewicz

Heavy Ion Laboratory, University of Warsaw, Warszawa, Poland

The U-200P cyclotron injection line transports the ion beam from the ECR sources to the inflector, which introduces the ion beam into the area of the accelerating structure in the cyclotron. The transport efficiency directly determines the ion beam current delivered to the cyclotron.

Job description

In 2025, from January, employees from the Accelerator Operation, Mechanical Design and Accelerator Development sections collected devices, designed equipment and, based on it, manufactured equipment on their own or through external orders necessary to rebuild the injection line. A work plan was developed, which was to begin during the summer holidays after the experimental campaign planned for the first half of the year was completed.

In the second half of July the designated team of workers (the workers changed over time; taking into account the holiday needs of the workers and their usefulness at a given stage of the reconstruction) started to implement the reconstruction. The renovation began with the dismantling of the vertical section of the injection line. Before the renovation, Fig. 1, the vertical section of the line-between Glaser Lens 1 and Glaser Lens 2-had an electrostatic quadrupole embedded in a magnetic steel tube.

In practice, however, the system failed to fulfill its focusing function. It served primarily as an additional set of corrective magnets operating in the X-Y plane. The quadrupole electrodes narrowed the effective aperture of the injection ion guide. As a consequence, this electrostatic quadrupole actively hindered beam transport on the vertical section of the line. An additional problem was the increased residual gas pressure level on this section ($\approx 10^{-6}$ mbar).

As a result of the work carried out, the vertical section of the line connecting the T-type magnet and the solenoid located within the cyclotron magnet yoke was dismantled including of course the electrostatic quadrupole doublet.

By disassembling the vertical section, the electromagnetic components comprising the ion optics were electrically and mechanically checked. The Glaser 2 focusing magnet was found to have a burnt winding, Fig. 1.

In Fig. 1 there is a diagram of the injection line that has been in operation for the last 13 years.

The injection line system was exposed enough to allow for measurements to be taken to verify the axial alignment of other equipment components. Lasers and laser theodolites were used for this purpose. In the horizontal section of the line connecting the 14.5 GHz ECR to the T-type magnet, no change in position of any of the components was found. However, the T-type bending magnet required a minor horizontal adjustment (approximately 1 mm). The vertical correction was approximately 4 mm for this magnet. After the correction, the T-type magnet assumed the correct position.

The setting of the 10 GHz ECR ion source and its accompanying ion optics also required correction.

After repairing the damaged devices, such as the Glaser 2 winding, which was wound by HIL itself, the vertical section of the injection line was reconstructed, Fig. 2. In addition to the existing equipment in this section, new or repaired elements were installed: Faraday cup No. 3 (repaired), a new electromagnetic quadrupole doublet No. 3, which replaced the electrostatic

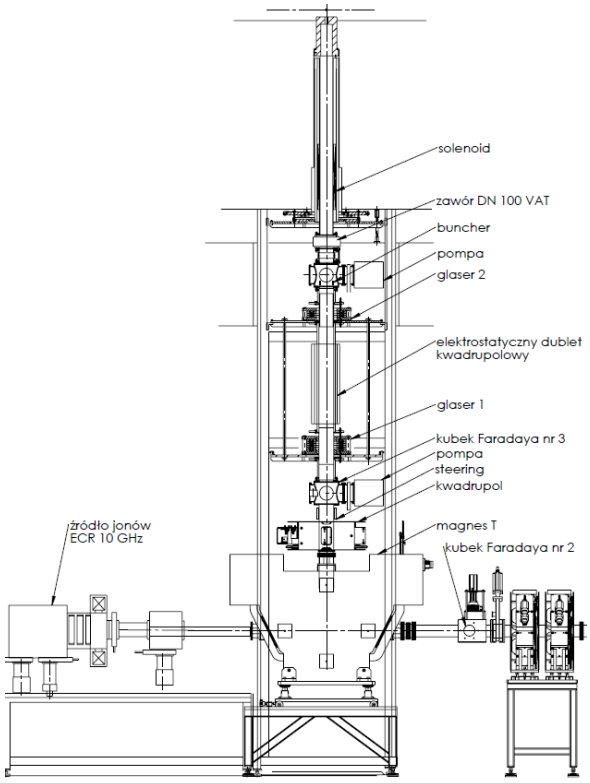


Figure 1: Schematic diagram of the injection line connecting two ECR ion sources to the U-200P cyclotron. The invisible second 14.5 GHz ECR ion source is installed to the right of the vertical part of the line.

quadrupole doublet, Glaser No. 2 (completely new lens winding), Faraday cup No. 4 (new measuring device on the line), turbo molecular pump moved away from the immediate vicinity of the cyclotron magnet yoke, and a DN 100 gate valve (replacing the 37-year-old valve installed in this location). Of course, all electrical connections, compressed air systems and vacuum systems have been recreated.

In the horizontal line next to the position correction of the 10 GHz ECR ion source, Faraday cup No. 2 was repaired and the electrical connections of quadrupole doublets of the 14.5 GHz ECR ion source to their respective power supplies were improved.

Scope of modification carried out

- Removal of the electrostatic quadrupole doublet system - the electrostatic quadrupole and its magnetic steel tube were removed from the vertical section of the line between Glaser 1 and 2.
- Installation of a new ion guide section - the magnetic steel tube was replaced with a section of 316 non-magnetic steel.
- Installation of an electromagnetic quadrupole doublet (Z1/Z2, current range 0–10 A) - replacing the electrostatic quadrupole doublet with an electromagnetic quadrupole doublet is the most important modification. The new quadrupole doublet enlarges the aperture inside the ion guide from 50 mm to 100 mm, and the electromagnetic lenses also allow for greater focusing power. The more efficient quadrupole doublet allows for better matching of the ion beam emittance to the accelerator's acceptance.

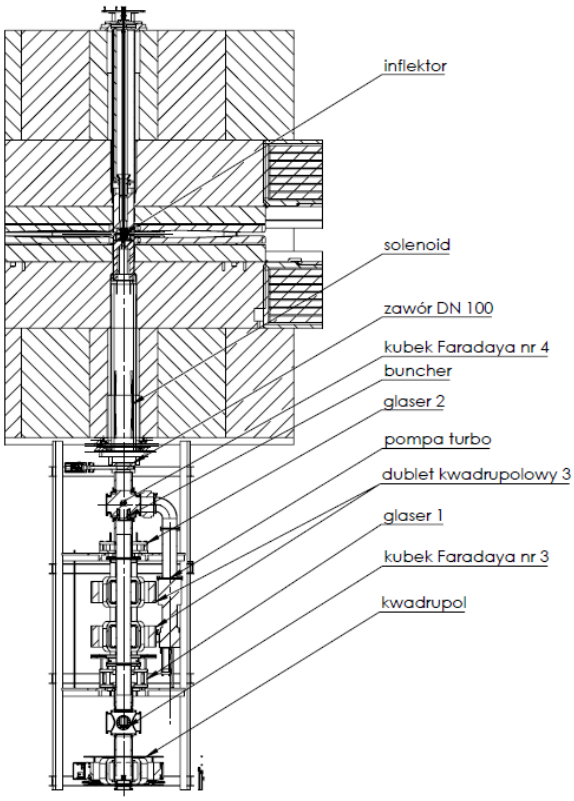


Figure 2: Current state of development of the vertical section of the injection line.

- Vacuum Improvement - After modifications and maintenance, the vacuum section of the line reached a level of $10^{-7} - 10^{-8}$ mbar, an order of magnitude better than before the upgrade.
- Rebuilding Glaser Lens 2 - The magnetic lens located directly below the new quadrupole doublet was revitalized.
- Installation of Faraday Cup No. 4 - A multi-collector Faraday cup was installed on the Buncher chamber, above Glaser 2 and the new Z1/Z2 doublet.
- Replacement of the pressure gate valve - the valve directly below the cyclotron was replaced with a new one.
- Modernization of the compressed air system
- Modernization of the water cooling system
- Modernization of the electrical power supply systems for the vertical line equipment
- Repair of multi-collector Faraday cup no. 3
- Repair of multi-collector Faraday cup no. 2
- Checking and correcting the alignment of injection line components

Independently of the work described above, the Design, Mechanical Engineering, and Accelerator Development team has been modernizing the spiral inflector. Several different

variants of this device have already been developed and are being successively tested.

Benefits of rebuilding the injection line

After completing the installation work, restoring the vacuum in the line and cyclotron, and checking the tightness of the vacuum systems, the cyclotron and ion source were started up to check the correct operation of the entire device. The first check took place on October 14, 2025. To determine the actual focusing properties of the rebuilt line, a phosphor was installed in the center of the cyclotron in the inflector location. It did not allow for simultaneous viewing of the shape of the beam introduced into the cyclotron media plane and measuring the beam intensity, but viewing the shape and the possibility of changing it using the ion optics of the line provided information about the obtained properties of the new line.

Diagnostic methodology of the new injection line

The quality of the beam-to-inflector fit was measured as the voltage deposited by the ion beam on the top electrode of the inflector when the electrode supply voltage was turned off – the so-called offset voltage U_{inf} [kV]. A higher U_{inf} value indicates better beam fit to the inflector geometry and acceptance.

Faraday Cups - Collector Geometry

- Faraday Cup No. 1 (horizontal line, behind the L-shaped magnet, before the wire profiler) - single collector; current reference from the source for all measurements.
- Faraday Cup No. 2 (horizontal line, behind doublets Q1-Q4 and magnets ST1-ST4) - two half-rings, top/bottom (vertical asymmetry diagnostics) + central collector.
- Faraday Cup No. 3 (vertical line, above magnet T, Q5, and ST4) - outer ring, center ring, central collector.
- Faraday Cup No. 4 (vertical line, Buncher chamber, above Glaser 2 and new doublet Z1/Z2) - geometry as Faraday Cup No. 3.

Note: Some ring collectors did not always measure ion currents correctly during testing. Faraday Cup No. 1 reading was considered a reliable current reference.

Injection line test results

He^+ Beam Tests - December 16, 2025.

The current on Faraday Cup No. 1 increased from ≈ 230 μA in the first beams to 370-820 μA after optimization. The inflector offset voltage reached $U_{inf} = 8.40$ kV - very good matching of the He b eam to the inflector. Source settings: U = 22 kV, DC_{bias} = 200 V, puller = 185 V, focu = 380 V, P = 30 W, gen = 14.5259 GHz, $P_{inj} = 6.5 \times 10^{-6}$ mbar.

S^{+5} Beam Tests - December 2025.

Sulfur ion tests were used to determine the optimal settings for the entire line. Source parameters: U_{ekstr} = 14.5 kV, P = 128/1.4 W, gen = 14.5263 GHz, $P_{inj} = 1.83 \times 10^{-4}$ mbar. The procedure involved sequentially setting Faraday Cup No. 1 $\rightarrow$ Faraday Cup No. 4, followed by iterative optimization of all ion optics elements of both line sections.

Table 1: Beam profile S^{+5}: before and after full line optimization (ref. FC1 $\approx$ 82 μA)

Etap	Faraday Cup No.	outer ring [μA]	center ring [μA]	central collector [μA]
Before optimization	II (FC2)	9	69	0
	III (FC3)	8	16	33
	IV (FC4)	1	9	58
After optimization	II (FC2)	4	74	24
	III (FC3)	-	37	36
	IV (FC4)	13	84	31

Before optimization, the inflector offset was just 0.22 kV. After full optimization, it increased to 2.02 kV-a nearly tenfold increase.

Profile analysis reveals the role of the new quadrupole doublet Z1/Z2: before optimization, the central current at the Faraday cup electrode No. 4 was dominant (58 μA) with almost zero current at Faraday cup No. 2 (0 μA), indicating that the beam was focused only on the vertical section, but not centrically. After optimization, the central currents increased in Faraday cup No. 2 (0 $\rightarrow$ 24 μA) and equalized in Faraday cup No. 4, confirming the effective cooperation of the horizontal doublets Q1-Q4 with the new doublet Z1/Z2 and the Glaser lenses in the vertical section.

Summary and most important conclusions from the reconstruction

- The cause of suboptimal ion beam transmission on the vertical section of the line has been eliminated. Replacing the electrostatic doublet with a quadrupole magnetic doublet Z1/Z2 has enabled synergistic cooperation between Glaser 1, Z1/Z2, and Glaser 2 instead of mutual compensation. The performance of the vertical section of the injection line after the modernization is much more promising - the ion optics system is complete and physically feasible, and further increases in transmission seem achievable through systematic optimization of the settings.
- The beam-to-inflector matching efficiency has improved significantly: the U_{inf} offset increased from 0.22 kV to 2.02 kV for S^{+5} ($\times$9) and reached 8.40 kV for He^{+}. The obtained values confirm that the upgraded vertical section operates predictably and delivers the beam to the inflector in a way that allows further optimization for specific ion species.
- The vacuum in the modernized section has improved by an order of magnitude ($\approx 10^{-6} \rightarrow 10^{-7} - 10^{-8}$ mbar), reducing beam losses due to scattering on the residual gas in the line.
- A beam profile diagnostic (Faraday cup no. 4) was installed directly in front of the inflector on the vertical section of the line, enabling non-invasive measurement of the beam's spatial distribution.

A.2 A standalone station with automatic loading, dedicated to the PETtrace cyclotron

J. Choiński, T. Bracha, R. Kopik, J.A. Kowalska, O. Nassar, B. Radomyski, A. Stolarz, Ł. Świątek

Heavy Ion Laboratory, University of Warsaw, Warszawa, Poland

The Radiopharmaceutical Production and Research Center was built and launched by the Heavy Ion Laboratory in 2012. The Center is still leased to an external company which is responsible for daily production of radiopharmaceuticals: fluorodeoxyglucose ^{18}F-FDG and choline based on fluorine ^{18}F. The HIL team, on the other hand, uses a special external station installed there for the irradiation of targets in metal and powder form. It enables the production of a variety of other radioisotopes for research purposes . For the last four years this research work is carried on in cooperation with teams from the Institute of Nuclear Chemistry and Technology in Warsaw and from the Jagiellonian University, Krakow. We are implementing a joint research project entitled "Development of three-photon emitting radiotracers for positronium imaging". The project was launched on 2022-07-21, under the OPUS-2022 edition, contract No. UMO2021/43/B/ST2/02150, where the Jagiellonian University, Faculty of Physics, Astronomy and Applied Computer Science is the leading unit.

In 2025, a total of 9 irradiations of targets were performed, including three irradiations related to the production of $^{44/44m}$Sc, two irradiations related to the production of ^{55}Co and four irradiations of targets for the production of ^{72}As. For irradiation, as in previous years, a target holder was used, enabling irradiation with a beam of ions incident perpendicularly on the target material.

After discussions within the project team, it was agreed that in 2025 the holder allowing for irradiation of the target material with a beam directed obliquely to the target, Fig. 1, will not be used.



Figure 1: View of the new target holder with pressure and twisting rings.

The methodology for making a calcium target (calcium carbonate) corresponding to the changed target exposure geometry has not changed in relation to the description included in the report submitted for 2024. The generated target thickness corresponds to the range of 16 MeV protons for each holder version.

Further tests carried out proved that the addition of 2.5 - 5% graphite (by weight), a chemically inert material that does not interfere with the processing of the target after exposure, ensures full mechanical durability of the disc.

The production of ^{44}Sc needed for the implementation of this research project was planned based on two methods: in the nuclear reaction of ^{44}Ca bombarded with protons (based on a

target prepared from calcium carbonate) and by producing a ^{44}Ti/^{44}Sc generator produced in the nuclear reaction of ^{45}Sc with protons. The methodology for manufacturing target using the second method has also been developed. The target is prepared in a glove box under an argon atmosphere using the target pellet forming method. The $^{\mathrm{nat}}$Sc cut into ≈1-2 mm pieces is pressed in a 10 mm diameter rings (Fig. 2).



Figure 2: View of a 10 mm diameter ^{nat}Sc target.

To produce ^{55}Co, a $^{\mathrm{nat}}$Fe target was used, prepared by forming a pellet from mini Fe grains using a hydraulic press. The ^{72}As production tests were performed using a version of the target holder perpendicular to the incident ion beam.

Bibliography

[1] J. Choiński et al., HIL Annual Report (2024) 25.
[2] J. Choiński et al., HIL Annual Report (2023) 19.
[3] J. Choiński et al., HIL Annual Report (2022) 15.
[4] J. Choiński et al., HIL Annual Report (2021) 18.

A.3 Operation of the ECR ion source and injection beamline at HIL in 2025

Ł. Standyło, M. Antczak, J. Choiński, A. Górecki, P. Jasiński, R. Kopik, M. Kopka, W. Kozaczka, P. Krysiak, K. Łabęda, K. Makowski, M. Matuszewski, J. Miszczak, K. Olejarczyk, K. Pietrzak, B. Radomyski, R. Ratyński, K. Sudlitz, M. Szperkiewicz

Heavy Ion Laboratory, University of Warsaw, Warszawa, Poland

During 2025 the 14.5 GHz Supernanogan ECR ion source at HIL provided ion beams for several experimental campaigns and dedicated source-development runs on the U200-P cyclotron [1]. The source operates in the microwave frequency range 13.75–14.5 GHz with a maximum RF power of 400 W. This report summarises the ion species produced, the key developments in the injection beamline, and the production of metallic magnesium beams.

Ion beams produced in 2025. Table 1 lists the ion species extracted from the ECR source during 2025. The feed materials used were: CH_4 for carbon, m-carborane ($C_2B_{10}H_{12}$) for boron, Ne 5.0 gas for neon, H_2S for sulphur, and metallic Mg pellets for magnesium. The beams supported experiments HIL120 and HIL122 (boron, May–July), the LaBr commissioning run and HIL122 (carbon, June), the Student Workshop (neon, October), and the SILCA preparatory run (^{32}S at 88 MeV, December). Argon and nitrogen beams were produced during beam-development and beamline commissioning runs.

Table 1: Ion beams produced by the 14.5 GHz ECR source in 2025. I_{FC1} is the beam current at Faraday cup FC1. U_{inf} is the inflector offset voltage. Mg beams were produced in January 2026 as part of the 2025 development campaign.

Ion	Feed material	Date	U_s [kV]	P_{RF} [W]	f [GHz]	I_{FC1} [μA]	U_{inf} [kV]
$^{11}B^{2+}$	m-carborane	05.2025	17	70	14.517	57–85	5.8
$^{11}B^{3+}$	m-carborane	05.2025	15	75	14.517	∼65	7.1
$^{12}C^{3+}$	methane	06.2025	22	104	14.506	111	7.9
$^{14}N^{3+}$	N_2 gas	04.2025	22	130	14.528	220	7.0
$^{14}N^{3+}$	N_2 gas	06.2025	22	175	14.530	214	7.2
$^{20}Ne^{3+}$	Ne 5.0 gas	10.2025	14.5	48–57	14.514	60–80	6.6
$^{40}Ar^{7+}$	Ar gas	11.2025	16.5	218	14.529	60	7.3
$^{32}S^{5+}$	H_2S gas	11.2025	14.5	100–178	14.527	58–74	6.8–7.2
$^{24}Mg^{4+}$	metallic Mg	01.2026 (dev.)	14.5	250–270	14.527	50–56	6.5
$^{24}Mg^{4+}$	metallic Mg	02.2026 (HIL135)	14.5	250–270	14.527	65–70	6.5

Injection beamline modification (July–September 2025). The injection beamline consists of a horizontal section housing both ECR ion sources (9.5 GHz and 14.5 GHz) and a vertical section from dipole D2 to the cyclotron entrance, as shown in Fig. 1. The major upgrade carried out in July–September 2025 comprised: removal of a faulty electrostatic quadrupole insert and its magnetic-steel shielding tube; installation of a non-magnetic stainless steel tube with a magnetic quadrupole doublet (QDline, 0–10 A); vacuum rehabilitation ($\sim 10^{-6}$ mbar $\rightarrow 10^{-7}$–10^{-8} mbar); refurbishment of the Glaser magnetic lens; installation of a new three-collector Faraday cup (FC4) for transverse beam-profile diagnostics; and replacement of the main gate valve. Performance was characterised with a $^{20}Ne^{3+}$ beam: the inflector offset voltage U_{inf} (the voltage applied between the inner and outer electrodes of the cyclotron inflector to optimise beam injection) rose from 0.78 kV to **2.34 kV** (threefold increase) after optimisation of the QDline doublet orientation, with beam transmission FC1→FC3 of ≈ 85%.

Metallic magnesium beam development. The first successful production of metallic magnesium beams was achieved using the positioned-crucible technique [2–5] – an approach in

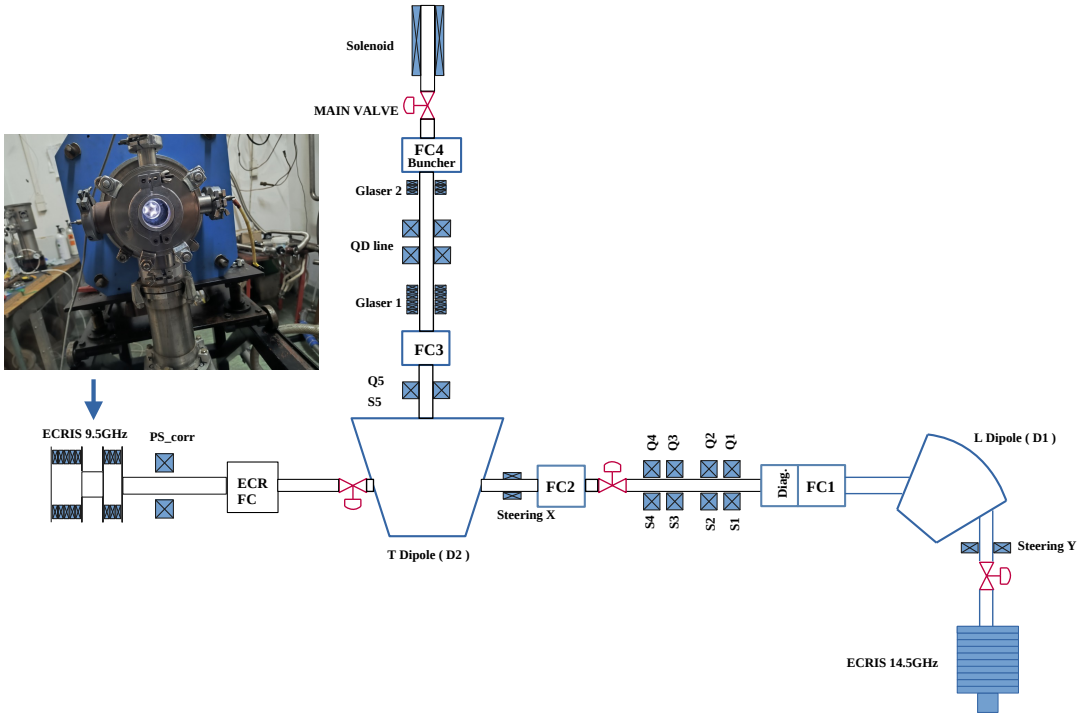


Figure 1: Schematic of the injection beamline with both ECR ion sources. The inset photograph shows the plasma burning inside the reconstructed 9.5 GHz ECR source; the hexagonal pattern reflects the new hexapole magnetic field structure.

which metallic Mg pellets are placed directly inside the plasma chamber and evaporated by the ECR plasma without any external heating, combining the simplicity of solid-feed techniques with the high charge-state performance of an ECR source. The mass spectrum recorded at optimal source tuning is shown in Fig. 2; all three stable isotopes are resolved for charge states $q = +2$ to $+6$. The technique was subsequently used in February 2026 to deliver ^{24}Mg beams at 71–86 MeV for experiment HIL135, with beam $^{24}Mg^{4+}$ currents of 50–56 μA (development tests, January 2026) and 65–70 μA (HIL135). During HIL135 an electrical short forced operation at $\Delta V = 0$ V (equal potentials on the source high voltage and the concentric waveguide extension), yet the beam remained stable for two weeks with only one crucible replacement, demonstrating the robustness of the technique.

Reconstruction of the 9.5 GHz ECR ion source. The 9.5 GHz ECR source underwent a major reconstruction in 2025: new solenoid coils were wound and a new hexapole magnet assembly was installed to restore the required radial magnetic confinement. The first functional test in early July 2025 was performed with an argon plasma; at 250 W of injected microwave power a total extracted current of ≈2.2 mA was measured at the ECR Faraday cup (ECR FC), which is a promising result for an initial commissioning run of a rebuilt source of this type [1]. The source is currently being prepared for integration into the injection beamline and further optimisation runs are planned for 2026.

Plans for 2026. Three beam-development campaigns are planned: (1) production of ^{34}S using SF_6 feed gas, expected to yield higher beam currents and better isotopic purity than H_2S [6]; (2) multiply charged ^{40}Ca beams using the oven technique with metallic pellets, targeting $^{40}Ca^{6+}$

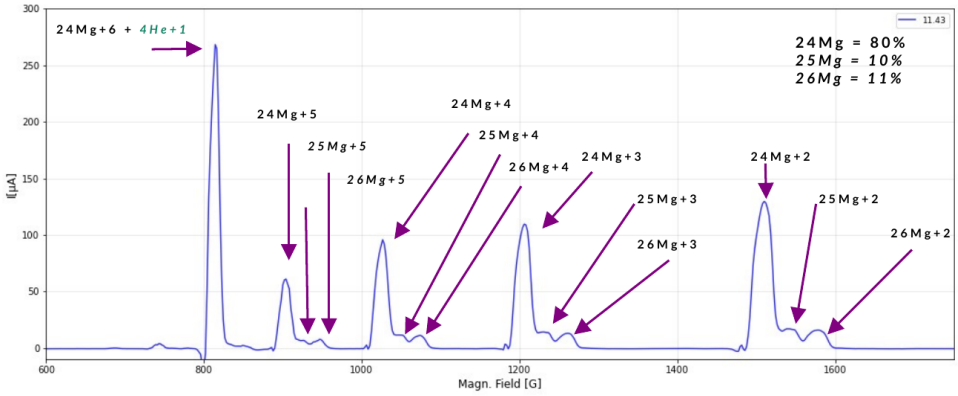


Figure 2: Mass spectrum of the Mg ion beam recorded at optimal source tuning. All three stable isotopes (^{24}Mg 80%, ^{25}Mg 10%, ^{26}Mg 11%) are resolved for charge states $q = +2$ to $+6$. A partial overlap of $^{4}He^{+}$ with $^{24}Mg^{6+}$ is indicated.

or $^{40}Ca^{7+}$ at 20–50 μA; and (3) continued commissioning of the reconstructed 9.5 GHz ECR source towards full integration into the injection beamline.

Bibliography

[1] R. Geller, *Electron Cyclotron Resonance Ion Sources and ECR Plasmas*, IOP Publishing, Bristol, 1996.
[2] H. Koivisto, J. Ärje, M. Nurmia, Rev. Sci. Inst. **69** (1998) 785.
[3] R. Geller, P. Ludwig, G. Melin, Rev. Sci. Inst. **63** (1992) 2795.
[4] H. Koivisto *et al.*, Rev. Sci. Inst. **75** (2004) 1479.
[5] T. Nakagawa *et al.*, Rev. Sci. Inst. **63** (1992) 2872.
[6] R.C. Reid, J.M. Prausnitz, B.E. Poling, *The Properties of Gases and Liquids*, 4th ed., McGraw-Hill, New York, 1987.

A.4 New interfaces for magnet power supplies

K. Olejarczyk

Heavy Ion Laboratory, University of Warsaw, Warszawa, Poland

In previous years the Heavy Ion Laboratory imported a number of 200-amp power supplies from the Svedberg Laboratory in Uppsala. The first step in using them to power the magnets is to integrate the control electronics in each power supply with the control system operating at HIL. The interface design presented here meets this role. Figure 1 shows a simplified schematic diagram.

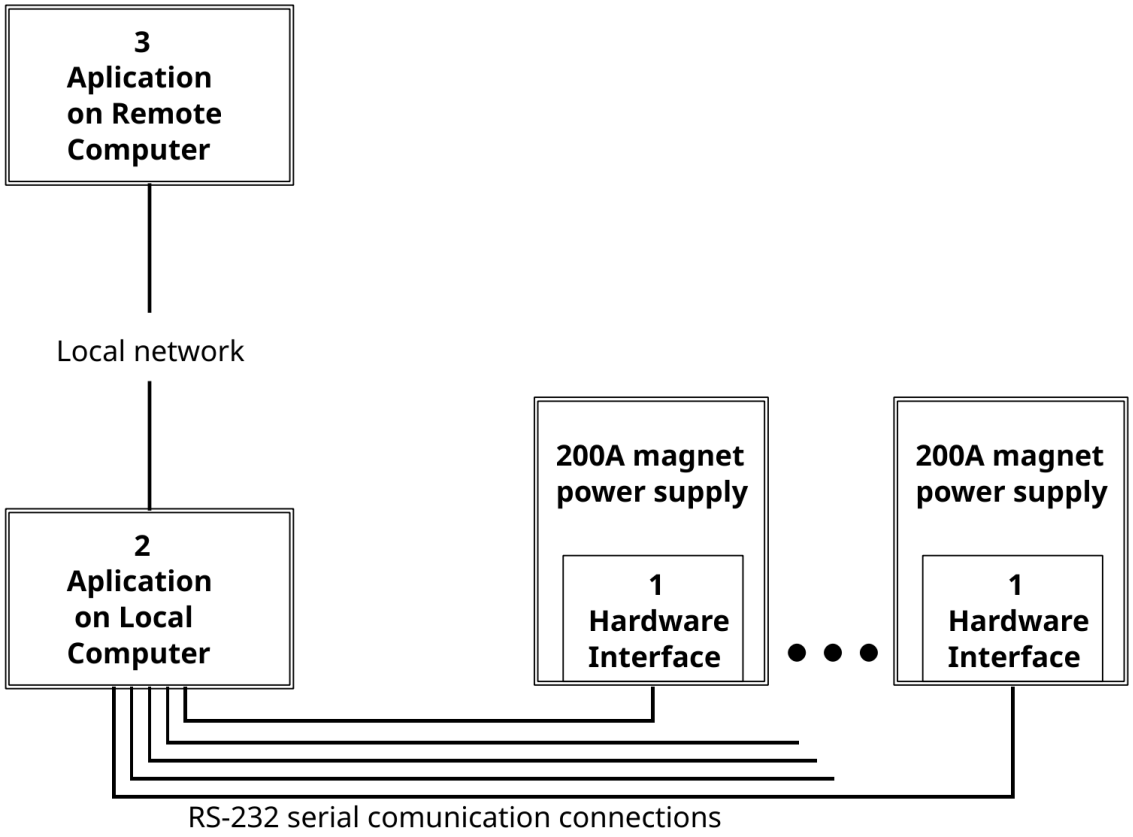


Figure 1: 1. Electronic modules that serve as hardware interfaces, housed inside power supply enclosures. 2. An application enabling local control, designed to monitor and supervise several (up to 16) power supplies. It runs on a computer located near the power supplies. 3. An application designed for remote control of power supplies in the control room.

The hardware interface is equipped with a physical RS232 port for connecting to a supervisory computer. At the logical level, interface (1) acts as a Modbus RTU server (slave). The hardware interface (1) was implemented using a Raspberry Pi Pico microprocessor and integrated into the power supply automation system. The microcontroller software was written in C using the Raspberry Pi SDK and the FreeModbus libraries. The hardware interface was built as a single prototype. The application (2) acts as a Modbus RTU client (master) in relation to individual power supplies with hardware interfaces (1). The application monitors the status of the power supplies and transmits control signals if the user changes the settings. The application (2) can operate in local or remote mode. In local mode, the application enables local control via a GUI. In remote mode, the application only allows monitoring of the status of the power supplies, and

control signals are transferred to the power supplies from the application (3). Application (3) provides all monitoring and control functions, if remote mode is set in application (2). Otherwise the status of the power supplies can only be monitored in the remote computer. Data transfer between applications (2) and (3) is performed via a computer network. Modbus TCP is used at the logical layer. Application (2) acts as a Modbus TCP server (slave) and application (3) acts as a client (master). Applications (2) and (3) differ only in their configuration and have been implemented as a single program capable of performing both functions. This solution reduced implementation and testing time. The program was written in C++ on Linux using the FreeModbus and FLTK libraries. The project was tested using a single power supply. The tests covered typical control and monitoring tasks, as well as known or potential abnormal and emergency situations.

A.5 Application of the Heavy Ion Laboratory Ion Source to low-energy ion implantation

A.J. Kordyasz, Ł. Standyło, A. Bednarek, M. Kisieliński, A. Stolarz
Heavy Ion Laboratory, University of Warsaw, Warszawa, Poland

Production of p – n junctions in thin silicon epitaxial detectors created using the low-temperature technique [1] is possible only by implantation of boron ions into n – type thin silicon wafers. Unfortunately, after the closure of the Institute of Electronic Materials Technology in Warsaw such a process is impossible in Poland. For boron implantation we will use the Pantechnik ion source see, Fig. 1:

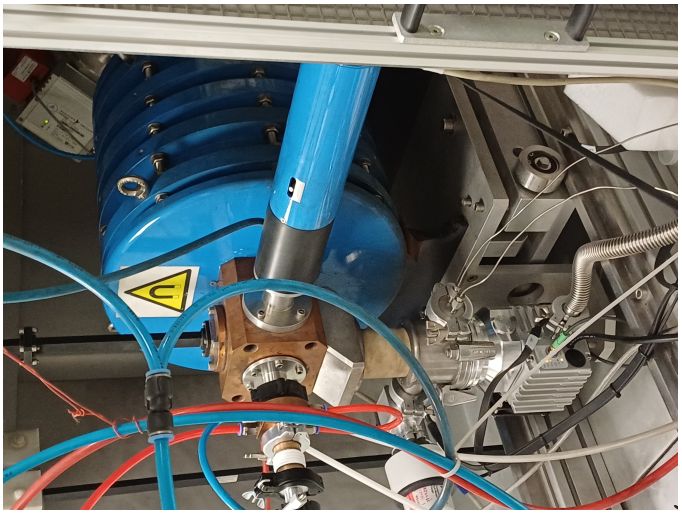


Figure 1: Pantechnik ion source at the Heavy Ion Laboratory of Warsaw University.

Boron ions from the ion source are selected by the deflection magnet, see Fig. 2:

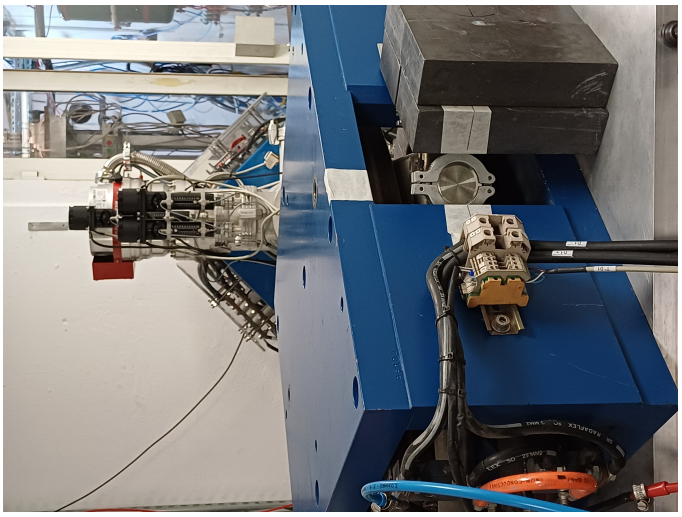


Figure 2: Magnet for a selecting clean boron beam from the ion source.

Clean selected boron ions are introduced into a chamber containing thin 21.5 μm thick 21.5 mm $\times$ 21.5 mm silicon wafers, see Fig. 3:

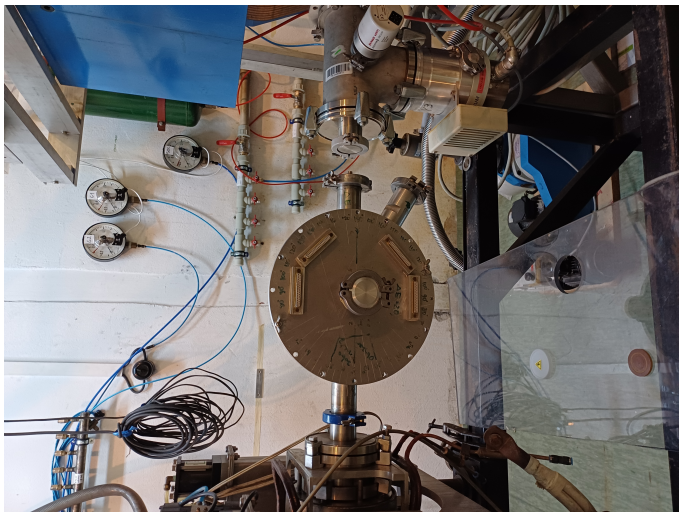


Figure 3: The implantation chamber with thin 21.5 μm thick 21.5 mm $\times$ 21.5 mm silicon wafers, for boron implantation. On this photo the chamber was not yet connected to the right side of the ion beam ion pipe.

To get a good p-n junction a clean boron beam with a dose of $5{\cdot}10^{14}$ ions/cm^2 and energy of about (40 – 50) keV is used. Inside the chamber a circular plate is mounted holding the 21.5 μm Si wafers. The positions of the Si samples for exposure to the boron ions are selected through a vacuum-tight knob on the outer wall of the chamber. The uniform implantation of boron ions will be achieved by X, Y motion of the focused ion beam on the thin silicon samples using electric deflection by two pairs electrodes located about two metres before the implantation chamber. The electronics system was designed and constructed by M. Kisieliński and A. Bednarek. Evaporation 0.5 μm Al layers on both sides of the thin Si detectors will be conducted in the chemical laboratory of A. Stolarz.

Bibliography

[1] A. J. Kordyasz et al., Eur. Phys. J. A (2015) 51: 15

A.6 Control application for internal beam irradiation in the cyclotron

T. Abraham, J. Choiński, J. Miszczak, T. Bracha

Heavy Ion Laboratory, University of Warsaw, Warszawa, Poland

A computer control system for internal beam irradiation experiments was developed to support experiments related to the production of medical radioisotopes at the HIL cyclotron facility. The software provides the operator with a graphical interface for monitoring and controlling elements of the irradiation research station connected to a programmable logic controller (PLC). The program is a newer implementation of an earlier control application that used the wxWidgets library together with Modbus communication. In the current version the graphical interface was rewritten using the Qt framework while maintaining the Modbus-based communication model. The application communicates with the control hardware through an embedded controller based on the Tiva microcontroller (TM4C123GH6PM). The controller acts as an intermediary between the operator application and the PLC as well as other connected devices. Data exchange between the application and the controller is performed using the Modbus protocol over an RS-232 serial connection.

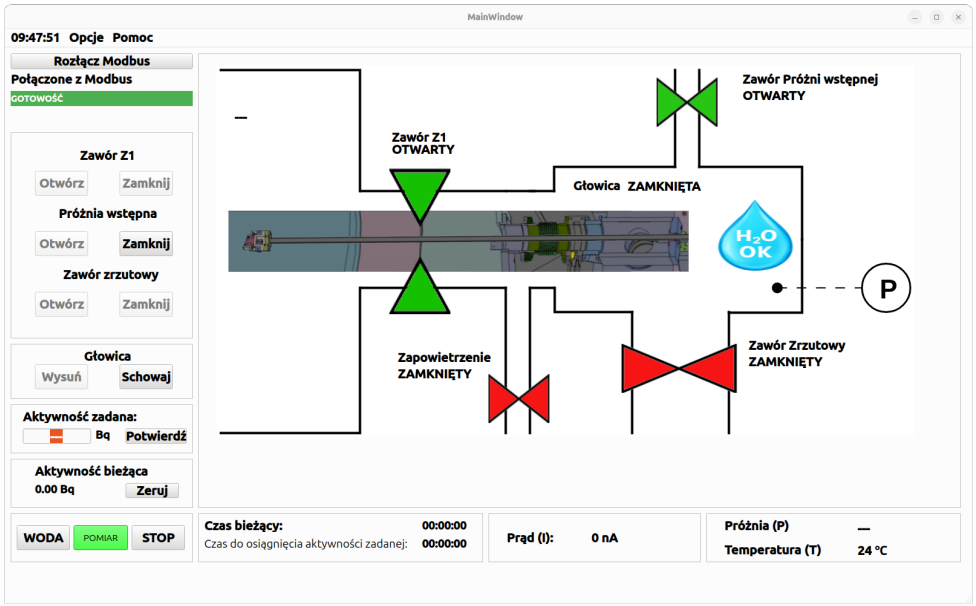


Figure 1: Graphical user interface of the internal beam irradiation control application showing the system connected to the controller and the current status of valves, sensors, and the irradiation head.

The graphical user interface provides a simplified schematic view of the irradiation system and allows the operator to monitor the state of devices connected to the PLC. The displayed components include:

1. valve Z1;
2. pre-vacuum valve;
3. dump valve;
4. venting valve;

5. vacuum pressure in the chamber of the irradiation head;
6. irradiation head and its drive;
7. beam current impinging on the target;
8. accumulated activity produced in the target;
9. cooling water status.

An example of the graphical user interface during operation, with the controller connected and device states indicated by colour markers, is shown in Fig. 1.

In addition to status monitoring, the operator can directly control selected elements of the system through the interface. These include opening and closing valves, moving the irradiation head, and activating control signals such as WODA (cooling water) and STOP. The interface also displays diagnostic signals received from the PLC, including water system status, fault conditions, and information about switching the system to local control mode. The application continuously reads measurement data from the control system and presents them to the operator in real time. The monitored parameters include vacuum pressure, temperature, and beam current. During the experiment the operator may define the desired activity of the produced radioisotope. Using the measured beam current and irradiation time, the application estimates the current activity induced and the time required to reach the requested value. Compared with the earlier implementation based on wxWidgets, the new program provides a redesigned graphical interface and improved maintainability thanks to the use of the Qt framework, while preserving compatibility with the existing Modbus-based control infrastructure.

A.7 HPGe Detector Laboratory

M. Komorowska[1], W. Grochalska[2] M. Kisieliński[1], M. Kowalczyk[1], A. Malinowski[1,3], M. Matuszewski[1], W. Okliński[1], M. Palacz[1], A. Špaček[1], M. Antczak[1], R. Kopik[1]

1) Heavy Ion Laboratory, University of Warsaw, Warszawa, Poland
2) Zespół Szkół Elektronicznych im. Wojska Polskiego, Bydgoszcz, Poland
3) Faculty of Physics, University of Warsaw, Warszawa, Poland

In 2025 the Detector Laboratory continued [1] its maintenance and operational support of the HPGe detectors used in EAGLE experiments. While the large-volume GAMMAPOOL detectors remained an important focus, a growing share of effort was directed towards the repair and refurbishment of smaller-efficiency detectors. Neutron damage and vacuum-related repairs were successfully carried out on 16 detectors in total during the year. FET replacements and preamplifier repairs were also performed as required.

Work continued on two projects reported in the previous year. Assembly of the clean-box glove chamber, designed to allow the safe opening of detector cryostats, is ongoing and expected to extend into 2026. The new unified preamplifier, tailored for the EAGLE digital pulse-processing acquisition system, has reached the assembly and initial testing stage; integration with the detectors is planned for a subsequent phase.

A grant under the Excellence Initiative – Research University (IDUB) programme was acquired for the replacement of worn-out signal and high-voltage cabling for HPGe detectors and the ACS system in the EAGLE setup with higher-quality materials. Following cable production and assembly, the full cable replacement is planned for the first half of 2026.

The liquid nitrogen auto-fill system experienced a significant malfunction requiring the replacement of the Beckhoff CX9001-1001 PLC. Following the repair work, remote monitoring and control of the cooling system became available. A separate malfunction affected the mid-tank filling system, in response to which a full manual control mode for the mid-tank valves was introduced as an additional operational and contingency feature.

The Detector Laboratory was also equipped with a system for monitoring the detector annealing process. The system runs on a Raspberry Pi 4 Model B (Debian GNU/Linux 13 Trixie, kernel 6.12.47) and currently supports vacuum readout from the Alcatel µPascal Display for Penning and Pirani gauges, the Pfeiffer TPG 362 gauge controller, and the Pfeiffer TCP-350 Turbo Pump Controller, all communicating via serial interface. Temperature is read from PT100 or PT500 sensors mounted in the detector cryostats, using MAX31865 resistance-to-digital converter modules optimized for each sensor type. Data acquisition and communication are implemented in Python. All monitored parameters are visualized in the Grafana platform, and the system allows configurable alert thresholds for critical parameter values.

Bibliography

[1] M. Komorowska *et al.*, HIL Annual Report 2024, page 23.

A.8 Barium targets for Coulomb excitation of ^{136}Ba studies

A. Stolarz, J.A. Kowalska, K. Wrzosek-Lipska, K. Hadyńska-Klęk, M. Komorowska, M. Palacz, I. Piętka, A. Špaček

Heavy Ion Laboratory, University of Warsaw, Warszawa, Poland

Barium targets with thickness of 1-2 mg/cm^2 on Ni, Al Cu, or Au metallic backing were required for Coulomb ^{136}Ba excitation studies in reactions with ^{32}S (102 MeV, 1 pnA) and ^{14}N (39 MeV, 3 pnA). Taking into account the chemical character of Ba and the required thickness a target consisting of a Ba compound deposit would be the best solution. Nevertheless, this solution is limited by practically no adherence of pure salts to metallic backings. From earlier experience (HIL annual report 2016) it was known that some Ba compounds adhere to carbon foils, but carbon backing was excluded by the experimentalists due to the nature of the planned studies. Thus, an attempt to build a Ba deposit on a Au foil by evaporation in high vacuum and protecting the deposit against oxygen originating from the atmosphere was undertaken. The latter was necessary as neither the evaporation system nor the experimental setup (target chamber on the beam line) has vacuum tight connections assuring safe Ba transfer and installation in the experimental chamber.

Since Ba enriched isotopes are available as barium carbonate, to achieve metallic Ba the carbonate first has to be decomposed to the oxide and then the reduction to elemental form can take place.

$$BaCO_3 \rightleftharpoons BaO + CO_2 \tag{1}$$

$$2BaO + Zr \rightarrow 2Ba + ZrO_2 \tag{2}$$

where Zr acts as reductant.

Taking into account that both elemental Ba as well as BaO are air sensitive both steps have to be carried out in vacuum with a single load of barium carbonate and reductant (Zr) into the reaction vessel. BaO prepared by separate $BaCO_3$ decomposition when exposed to the air for mixing with reductant would absorb CO_2 from the atmosphere and promptly convert back to carbonate.

Unloading the metallic Ba deposit to be transferred to the target chamber installed on the beam line should also be performed either via an airlock or the deposit must be protected by a tightly covering layer of other air insensitive element. The rapidity of Ba oxidation and further conversion into carbonate is illustrated in Figure 1. Approximately ∼90% of barium deposit is reconverted to carbonate within 1-1.5 h when exposed to air (assessed by sample weighing at short intervals).

$$2Ba + 2O_2 \rightarrow BaO + CO_2 \rightarrow BaCO_3 \tag{3}$$

In the test performed at HIL barium carbonate thoroughly mixed with freshly powdered Zr (with excess to the stechiometric ratio) and compacted into a pellet was placed in a Ta tube and after reaching a vacuum of ∼1-2×10^{-6} mbar was gently heated to decompose the carbonate (decomposition temp 1000°C – 1400°C depending on the data source).

The decomposition step had to be performed carefully as heating the mixture to too high temperature may lead to the creation of barium zirkonate $BaZrO_3$ that can be easily created when hot Ba, carbon dioxide and Zr are in the reaction vessel [1]. During this step barium

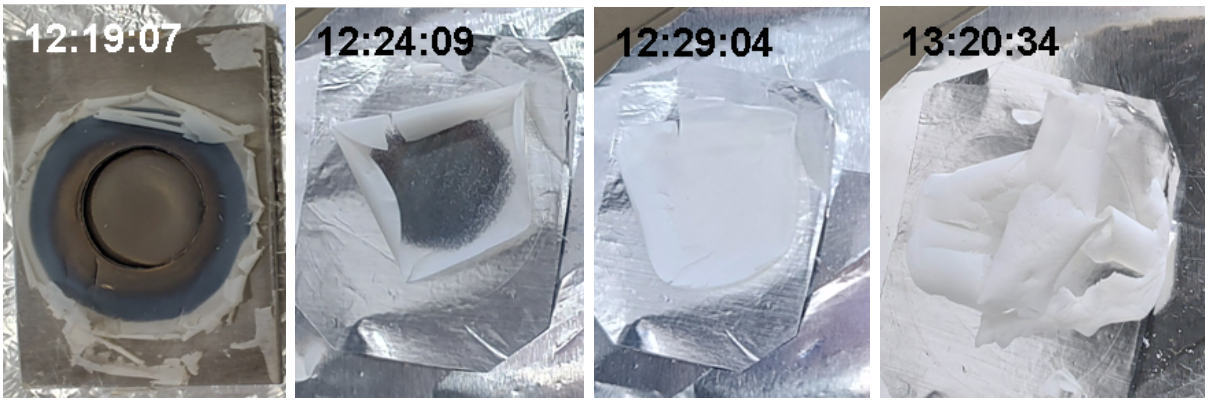


Figure 1: Sample of Ba deposit exposed to the air. As can be seen in the first photo (left) oxidation to the oxide or carbonate (both white) of the thin deposit on the target mask takes ∼1-2 min (time needed for dismounting the deposit from the evaporator).

carbide can also be produced since carbon dioxide reduction can take place in the presence of hot barium metal already at 600°C [2], so it is important to provide high speed pumping to assure quick removal of the carbon dioxide from the reaction vessel. Both side reactions are hard to control and prevent. The products of these processes probably can be seen in the samples presented in Figure 2. To verify this assumption detailed chemical analyses are needed.

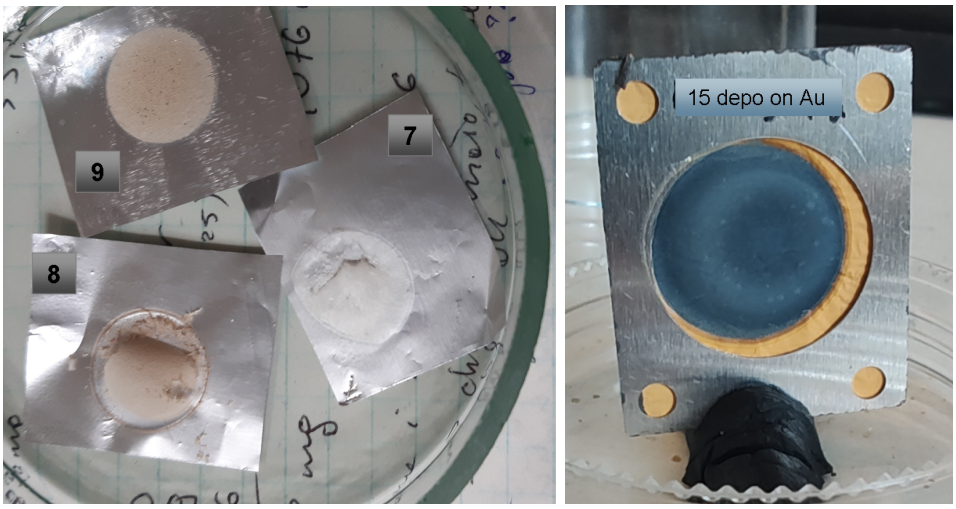


Figure 2: Ba test deposits: 7, 8 and 9 on Al backing and 15 on Au. They remained brownish (8,9) and dark grey (15) even after days of exposure to the air. Deposits 8 and 9 changed their mass (∼5% within the first day) but the colour remained unchanged). Deposit 15 had hardly changed its mass even after a few days of exposure to the air, which means no reaction with oxygen and carbon dioxide.

Therefore it is necessary first to decompose the carbonate and fully evacuate the carbon dioxide from the reaction vessel. After carbonate decomposition (assessed by vacuum changes) the vacuum must be improved to reach at least the level of 10^{-7} mbar and the temperature of the Ta crucible may then be raised.

For testing the Ba target performance in beam deposits on a Au backing were produced. The Au backing foil (5 mg/cm^2) was placed at a distance of 1.7 cm above the reaction crucible on a rotary arm which allows transfer of the Ba deposit over the source of Au for covering with a protective layer without opening the evaporator bell jar and therefore without contact with

air. Deposits of ∼2 mg/cm^2 of barium protected with ∼150 µg/cm^2 and with 300 µg/cm^2 were prepared in this way.

The first one demonstrated a quick mass rise after unloading from the evaporator so was disqualified and the second with a thicker Au protective layer was produced. Unfortunately the target lasted for only 1 h in beam (Figure 3). The target was tested with a ^{12}C beam of 72 MeV energy thanks to the courtesy of A. Špaček sharing his beam time during the $LaBr_3$ commissioning experiment.



Figure 3: The 2 mg/cm^2 Ba deposit between Au layers after 1 h of exposure to the beam.

Unfortunately, either a 300 µg/cm^2 thick layer of Au is not sufficient to prevent air penetration or, what is highly probable, the residues of carbon dioxide and oxygen present under the bell jar of the evaporator were absorbed by the metallic Ba. The latter results with partial Ba conversion back to carbonate that when heated by the beam decomposes. In consequence released carbon dioxide blocked by protective Au layer cause the target rupture.

To complete the request of providing a Ba target in a metallic form with a thickness of 1 - 2 mg/cm^2 either further efforts have to be undertaken or the chemical form of Ba target requested for the planned studies has to be rethought.

Bibliography

[1] Alberto Ubaldini, Vincenzo Buscaglia, Claudio Uliana, Giorgio Costa, and Maurizio Ferretti; J. Am. Ceram. Soc., **86** [1] (2003) 19–25

[2] W. J. Arrol, R. Glascock, J. Chem. Soc.**4** (1948) 1534–1537. doi:10.1039/JR9480001534.

A.9 Polish Workshop on the Acceleration and Applications of Heavy Ions

J. Samorajczyk-Pyśk[1], G. Colucci[1], K. Hadyńska-Klęk[1], M. Kowalczyk[1], K. Kilian[1], M. Komorowska[1], J.A. Kowalska[1], P.J. Napiorkowski[1], O. Nassar[1], M. Palacz[1], I. Piętka[1,2] M. Paluch-Ferszt[1], K. Rani[1], K. Rusek[1], P. Sekrecka[1], A. Stolarz[1], A. Trzcińska[1], M. Wolińska-Cichocka[1] K. Wrzosek-Lipska[1],

1) Heavy Ion Laboratory, University of Warsaw, Warszawa, Poland
2) Faculty of Physics, University of Warsaw, Warszawa, Poland

The 19^{th} edition of the National Workshop on the Acceleration and Applications of Heavy Ions has come to an end, marking 20 years since the initiation of these now traditional meetings.

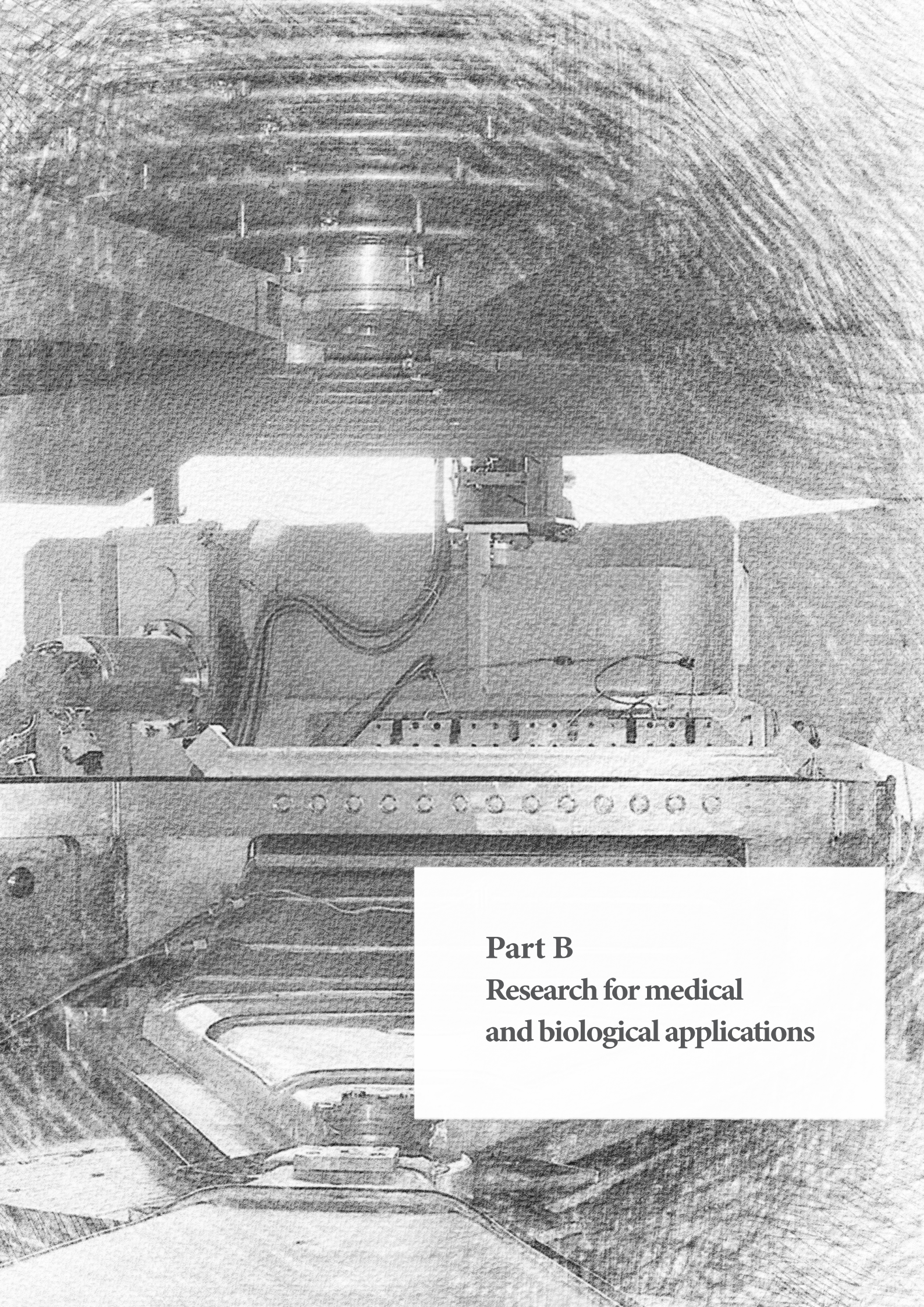
This year we hosted 12 participants from six research institutions: the University of Warsaw, Warsaw University of Technology, the University of Gdańsk, AGH University of Science and Technology, the University of Łódź, and Trinity College Dublin.

The young researchers worked in three four-person groups, demonstrating great interest and strong engagement in their tasks. Before undertaking the practical work, they had the opportunity to broaden their knowledge during lectures tailored to the exercises carried out by the students. Experimental tasks and measurements performed using specialized equipment available in the laboratory provided an opportunity to become familiar with the HIL infrastructure. As is traditional, the workshops concluded with student presentations—each group prepared a presentation on their measurements and the results obtained.

The workshops were aimed at third- and fourth-year physics students interested in nuclear physics. Their main objective was to create a unique opportunity to gain experience in data acquisition and analysis, cyclotron operation, and techniques for the detection of charged particles and gamma radiation.



Figure 1: Participants in the 19^{th} Polish Workshop on the Acceleration and Applications of Heavy Ions (photo. P. Jasiński and K. Łabęda).



Part B
Research for medical and biological applications

B.1 Analysis of potential interferents in synthesis of Pd-porphyrin complexes for radiopharmaceutical applications

M. Pęgier[1], K. Kilian[1], K. Pyrzyńska[2]

1) Heavy Ion Laboratory, University of Warsaw, Warszawa, Poland
2) Faculty of Chemistry, University of Warsaw, Warszawa, Poland

Bifunctional ligands are highly valued in nuclear medicine for both diagnostic and therapeutic purposes. While they can effectively bind suitable radioactive nuclides, they also enable their targeted delivery to specific tissues or their inclusion selected metabolic pathways. The porphyrins are a group of macrocycles that can be applied in diagnostic techniques such as positron emission tomography (PET), as well as in radiotherapy [2]. Porphyrin complexes also occur naturally in living organisms-for example, iron-containing heme and cobalt-containing cobalamin. The palladium radioisotope ^{103}Pd ($T_{1/2}$ = 16.99 days), which is already used clinically in brachytherapy in the form of metallic seeds, is considered a promising candidate for therapeutic applications. In recent years, it has also been proposed for targeted Auger electron therapy [2]. During its decay to ^{103m}Rh ($T_{1/2}$ = 56.1 min), it emits Auger electrons; the daughter isotope further decays with additional Auger electron emission, ultimately forming stable ^{103}Rh. Therefore, ^{103}Pd can act as an in vivo generator of these radionuclides. It can be produced in a cyclotron via the ^{103}Rh(p,n)^{103}Pd reaction. Another palladium radionuclide of potential interest in radiopharmaceutical applications is ^{109}Pd ($T_{1/2}$ = 13.7 h). It undergoes β^- decay to ^{109m}Ag ($T_{1/2}$ = 39.6 s), which subsequently emits a cascade of conversion and Auger electrons. This makes ^{109}Pd a possible in vivo generator of ^{109m}Ag [3]. In this study the complexation of palladium(II) with porphyrin was investigated. The hydrophilic anionic porphyrin meso-tetrakis(4-sulfonatophenyl)porphyrin (TSPP) served as ligand for the reaction. Previous studies showed that optimal conditions for the reaction were acetate at pH 4 with microwave heating to 120°C [4]. The structure of the investigated porphyrin and corresponding UV-VIS spectra are presented in Fig. 1.

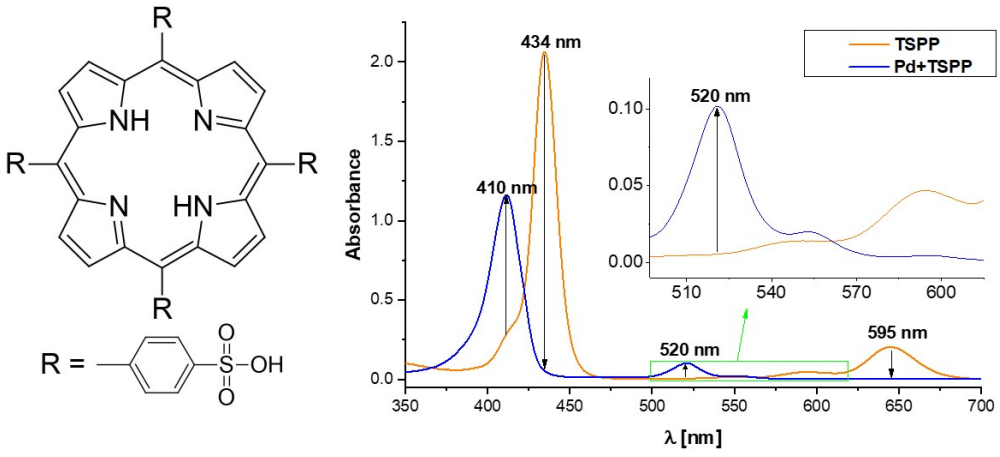


Figure 1: Structure of TSPP and changes in UV-VIS spectra after formation of palladium complex of TSPP

Due to the time and cost associated with cyclotron operation, another important factor that must be considered before conducting experiments is the effect of potential interferents present in the reaction mixture. Even trace amounts of other metals in the rhodium used for the reaction

may adversely affect the interaction between porphyrin and palladium. Because the radioactive isotope is present at very low chemical concentrations in the solution, these trace impurities can occur at concentrations several orders of magnitude higher than that of palladium. At such a large excess, competing complexes with other metal ions may form, and the reaction itself may be significantly slowed by their presence in the solution. Possible impurities in metallic rhodium include primarily other platinum group elements (PGEs), such as Pt, Ru, Ir, and Os. Other potential contaminants are common metals such as Fe, Cu, Zn, and Pb. Zinc, copper, and lead relatively easily form complexes with TCPP in aqueous solution. However, the optimal reaction conditions correspond to a pH of approximately 9. Under acidic conditions, protonation of the porphyrin hinders the formation of these complexes, which is beneficial from the perspective of synthesizing the Pd-TSPP complex.

The study aimed to determine whether the most likely impurities present in natural rhodium negatively affect the formation of the Pd–TSPP complex. Standard solutions of the following metals were used: Pt, Ru, Rh, Ir, Os, Fe, Cu, Zn, and Pb. In the first stage, it was examined whether these metals form complexes with TSPP under the conditions used for Pd-TSPP synthesis. Solutions of TSPP and the respective metal ions at a concentration of 5×10^{-6} mol/L were mixed in an acetate buffer at pH 4. The mixtures were then heated at 120°C for 20 minutes. A summary of the results is presented in Table 1.

Table 1: Reaction of potential interfering ions with TSPP.

Rh	Minimal decrease of TSPP bands
Pt	No change
Ru	No change
Ir	No change
Os	No change
Fe	No change
Cu	Minimal decrease of TSPP bands, formation of Cu-TSPP bands
Zn	No change

Only in the case of Cu ions was a slight decrease in the intensity of the TSPP absorption bands observed, accompanied by the formation of bands characteristic for the Cu-TSPP complex. In the case of Rh ions, only minimal changes in the spectrum were observed.

In the next step, the synthesis of the Pd-TSPP complex was carried out in the presence of a fivefold excess of the investigated metal ions. In all cases, the synthesis was successful, and no significant decrease in the efficiency of Pd-TSPP complex formation was observed. These experiments confirm the potential of the proposed synthesis strategy.

Bibliography

[1] K. Pyrzyńska, K. Kilian, M. Pęgier, Molecules 27 (2022), 3311.
[2] D. Filosov, E. Kurakina, V. Radchenko, Nuclear Medicine and Biology 94-95 (2021), 1-19.
[3] J. Pineau et al., Chemistry A European Journal 28 (2022), e202200942.
[4] M.Pęgier, K.Kilian, K.Pyrzyńska, HIL Annual Report 2024, page 38.

B.2 Polish honeys as a source of selenomethionine

M. Janiszewski[1], A. Sentkowska[2]

1) Faculty of Chemistry, University of Warsaw, Warszawa, Poland
2) Heavy Ion Laboratory, University of Warsaw, Warszawa, Poland

Selenium is a crucial trace element for the proper functioning of the human body. Recently, it has been proven that selenium can prevent the development of cancer and slow down the ageing process [1]. The recommended daily allowance (RDA) of selenium for adults is 55 micrograms per day; however, the content of this element in food tends to reflect the level of selenium in the soil, which is relatively low. Therefore, selenium deficiency remains a problem in many human populations, and selenium-enriched foods and supplements have been proposed as a means to circumvent this issue [2]. It should therefore not be surprising that natural sources of this element, which can effectively supplement its dietary deficiencies, are still being sought. In food, selenium occurs mainly in the form of organic compounds, e.g. selenomethionine. Selenomethionine is an organic form of selenium, where selenium replaces sulphur in the amino acid methionine. It was found in food, including cereal grains (such as wheat, maize, and rice), soybeans, and yeast. SeMet is well known for its antioxidative properties [3]. In the described study, the content of selenomethionine (SeMet) in Polish honeys was determined. The exact location of the honeys used in the study is shown in Fig. 1.



Figure 1: Place of origin of the honeys used in the study.

Selenium speciation analysis was performed using hydrophilic interaction chromatography coupled with mass spectrometry detection (HILIC-MS). Identification of SeMet in the samples was performed based on a knowledge of its fragmentation paths and comparison of its retention time with the standard. The results obtained are summarised in Table 2.

Table 1: Selenomethionine content in various types of Polish honeys.

Type of honey	Sample number	SeMet content [μg/g]
Acacia nectar	20	1.97 ± 0.03
Phacelia nectar	5	0.84 ± 0.02
	7	0.19 ± 0.01
Linden nectar	1	0.43 ± 0.02
	2	0.62 ± 0.07
	8	0.31 ± 0.02
	9	0.54 ± 0.02
	16	0.17 ± 0.01
Goldenrod nectar	11	0.59 ± 0.02
	17	0.72 ± 0.01
Blueberry Nectar	13	0.36 ± 0.19
Dandelion Nectar	6	0.54 ± 0.06
Rapeseed nectar	4	0.03 ± 0.01
	12	0.81 ± 0.01
	21	1.79 ± 0.27
	22	0.55 ± 0.03
Honeydew-Virginia	14	0.71 ± 0.02
Multifloral nectar	3	0.05 ± 0.01
	10	0.27 ± 0.02
	15	1.32 ± 0.02
Cream multifloral	18	0.93 ± 0.01
Multifloral honeydew	19	1.54 ± 0.05

SeMet contents ranged from 0.03 to 1.97 μg per one g of honey. SeMet is the dominant form of selenium in most of the honeys tested. This is particularly noticeable in acacia, linden, and rapeseed honeys. This correlation of results may indicate that the honey species has a significant impact on the form in which selenium occurs in honey. This research has shown that honey can be a good dietary supplement containing selenium.

Bibliography

[1] M. Kieliszek, Molecules 24 (2019) 1298.
[2] K. Ivory and C. Nicoletti Trends Food Sci. Tech. 62 (2017) 190. *Selenium is a source of aliment and ailment: Do we need more?*
[3] L. Reyes et al. Antioxidants 13 (2019) 546.

B.3 The use of white mulberry extract (Morus alba L.) for the synthesis of selenium nanoparticles

N. Szoblik[1], A. Sentkowska[2]

1) Faculty of Chemistry, Warsaw University of Technology, Warszawa, Poland
2) Heavy Ion Laboratory, University of Warsaw, Warszawa, Poland

Selenium nanoparticles (SeNPs) are becoming increasingly popular due to their high antioxidant and antibacterial properties. The latest research shows that due to their multifaceted action, they can be an effective drug in the fight against infections caused by antibiotic-resistant bacteria [1]. It should therefore not be surprising that new methods for their synthesis are still being developed. One of the most demanding ways of obtaining them is the so-called green method using plant material [2]. Despite the difficulties and certain limitations of this type of syntheses, they are increasingly being developed due to their environmental friendliness. The lack of the need to use toxic reagents, the ability to conduct the reaction at room temperature and the high stability of the nanoparticles obtained distinguish green methods from others.

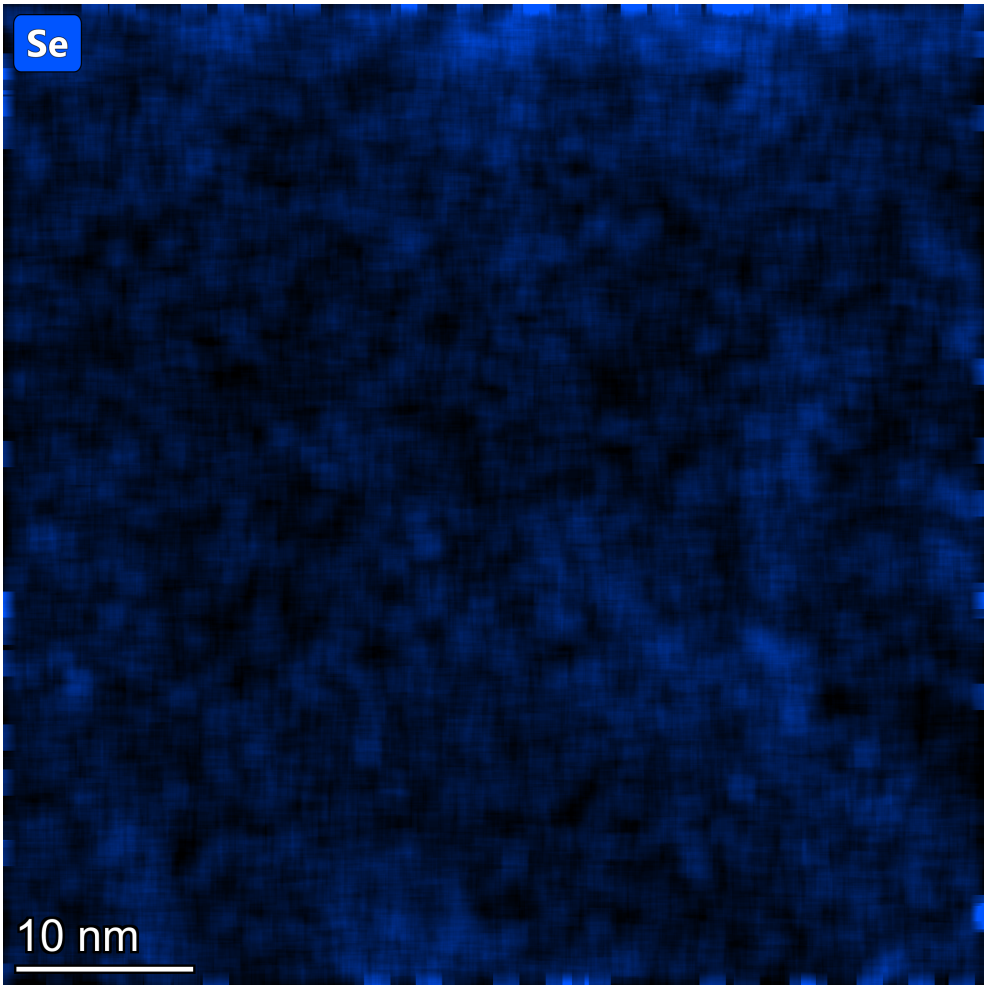


Figure 1: SI EDS-HAADF image of obtained SeNPs.

The research examined the potential of white mulberry (Morus alba L.) extract for the synthesis of selenium nanoparticles. The plant material was obtained from organic farming conducted near Jasło. The extraction procedure involved pouring 5 g of ground mulberry leaves

into 50 mL of boiling water and infusing for 30 minutes. The resulting extract was filtered using a paper filter. The synthesis procedure consisted of adding 2.5 mL of mulberry extract to 2.5 mL of sodium selenate solution (0.1 mol/L) and 20 mL of deionised water. The reaction mixture was stirred vigorously for 1 hour. After the reaction, the nanoparticles were tested for their physical properties. TEM studies revealed the formation of small, spherical nanoparticles with sizes of less than 10 nanometers, and SI EDS-HAADF confirmed the presence of SeNPs, as shown in Fig. 1.

The small-sized nanoparticles obtained have potential for biomedical applications, as their size is closely related to their ability to pass through biological membranes [3]. Further research into their antioxidant and antibacterial properties is ongoing.

Bibliography

[1] N. Filipović et al. Front. Bioeng. Biotechnol. 8 (2021) 1591
[2] K. Pyrzyńska & A. Sentkowska J. Nanostr. Chem. 12 (2022) 467.
[3] A. Haleem et al. Global Health J. 2 (2023) 70.

B.4 Development and Validation of a Digitized Quantitative Analytical Method for Kryptofix 2.2.2 Determination in ^{18}FDG Radiopharmaceuticals

W. Dworak[1] , K. Kilian[2]

1) Faculty of Chemistry, University of Warsaw, Warszawa, Poland
2) Heavy Ion Laboratory, University of Warsaw, Warszawa, Poland

The dynamic growth of the nuclear medicine market, which tripled in value between 2020 and 2024, has intensified the demand for efficient and precise quality control (QC) protocols. Positron Emission Tomography (PET) remains a cornerstone of modern oncological and neurodegenerative diagnostics, with 18fluorodeoxyglucose (^{18}FDG) accounting for nearly 40% of the global PET tracer market. The synthesis of ^{18}FDG primarily utilizes nucleophilic substitution, where Kryptofix 2.2.2 (a cyclic ether) acts as a phase-transfer catalyst to enhance the reactivity of the fluoride-18 ion. Despite its chemical utility, Kryptofix 2.2.2 is a toxic compound; even sub-lethal doses can induce neuromuscular symptoms, such as tremors and impaired motor coordination. To ensure patient safety, the European Pharmacopoeia mandates a strict concentration limit of 2.2 mg per maximum container volume (approximately 0.147 mg/ml for a standard 15 ml vial). While various high-end techniques like LC-MS/MS or GC-NPD offer high sensitivity, their adoption in routine clinical settings is often hindered by high operational costs and lengthy analysis times.

The primary goal of this research was to develop an innovative, cost-effective, and rapid quantitative method by digitizing the traditional qualitative "spot test". The objective was to transform a visual, subjective assessment into a robust analytical tool capable of precise Kryptofix quantification in radiopharmaceutical matrices.

Experimental Methodology

The methodology utilizes TLC silica gel plates pre-treated with a potassium iodoplatinate (K_2PtI_6) solution. Samples of 2.5 μl were applied to the plates. Following application, the plates were digitized using a high-resolution optical scanner (1200 dpi) in .png format. Digital image analysis was conducted using ImageJ software, where the mean intensity of the spot centre was measured as the primary dependent variable.

System Optimization and Hardware Stability

Extensive optimization was performed to ensure the reliability of the digital signal:

- Bit Depth: Analysis of 8-bit, 16-bit, and 32-bit images revealed that while bit depth does not significantly alter the regression coefficients, 32-bit depth provides the most comprehensive colour data retention.
- Variable Selection: Comparing the "mode" and "mean intensity" of both the whole spot and its centre, it was determined that the mean intensity of the spot centre yielded the highest correlation ($R^2 > 0.9$).
- Scanner Stability: The impact of scanner lamp heating over successive cycles was investigated. The relative error in signal intensity remained below 0.34%, which is negligible for routine analytical purposes.

Analytical Validation and Results

The method underwent a full validation according to ICH and pharmacopoeial guidelines:

- Linearity and Matrix Effects: The method was validated in the concentration range of 0.0294 - 0.1470 mg/ml. A significant matrix effect was observed; while aqueous solutions followed a linear model, samples in a phosphate buffer matrix (simulating the final ^{18}FDG product) showed a superior fit using a quadratic regression model ($R^2 = 0.997$).
- Precision: Repeatability studies showed a maximum Relative Standard Deviation (%RSD) of 1.04%. Intermediate precision (inter-operator) was confirmed at 3.87%, demonstrating the method's robustness.
- Sensitivity: The Limit of Detection (LOD) was determined to be 0.005 mg/ml based on blank signal standard deviation.
- Selectivity: Signal intensity proved highly dependent on pH levels, particularly within the pharmacopoeial range of 4.5-8.5. This necessitates strict pH control or matrix matching during calibration.

Practical Application to Industrial Batches

The method was applied to five production batches of ^{18}FDG post-decay. Due to low native concentrations, a standard addition technique was utilized. The analysis confirmed that all batches complied with the 0.147 mg/ml limit, with batches 4 and 5 showing concentrations of 0.075 mg/ml and 0.062 mg/ml respectively, while the others fell below the LOD.

Comparative Discussion and Conclusions

Compared to gold-standard techniques like LC-MS/MS, this digitized spot test is approximately 80 times less sensitive but offers substantial advantages in terms of cost-efficiency, accessibility, and speed (analysis time $<$ 10 minutes). It provides a bridge between purely qualitative screening and expensive quantitative instrumentation. The successful validation of this method demonstrates its potential for routine integration into radiopharmaceutical quality control, with future applications targeting other tracers like ^{18}FCH.

Table 1: Summary of Analytical Validation Parameters for the Digitized Spot Test

Parameter	Value / Result
Linear Range	0.0294 - 0.1470 mg/ml
Regression Model (Buffer)	Quadratic ($y=488.31^2$-344.44x+205.87)
Coefficient of Determination (R^2)	0.997
Limit of Detection (LOD)	0.005 mg/ml
Repeatability (%RSD)	1.04%
Intermediate Precision (%RSD)	3.87%
Recovery Efficiency	86.4% - 106.1%

Table 2: Comparison of Kryptofix 2.2.2 Determination Methods

Method	Type	R^2	LOD [mg/ml]	Analysis Time	Cost
HPLC (UV)	Quantitative	0.999	0.0002	≈20 min	$$$
LC-MS/MS	Quantitative	0.998	0.000001	≈5 min	$$$$
Standard Spot Test	Qualitative	-	-	≈10 min	$
Proposed Method	Quantitative	0.997	0.005	≈ 10 min	$

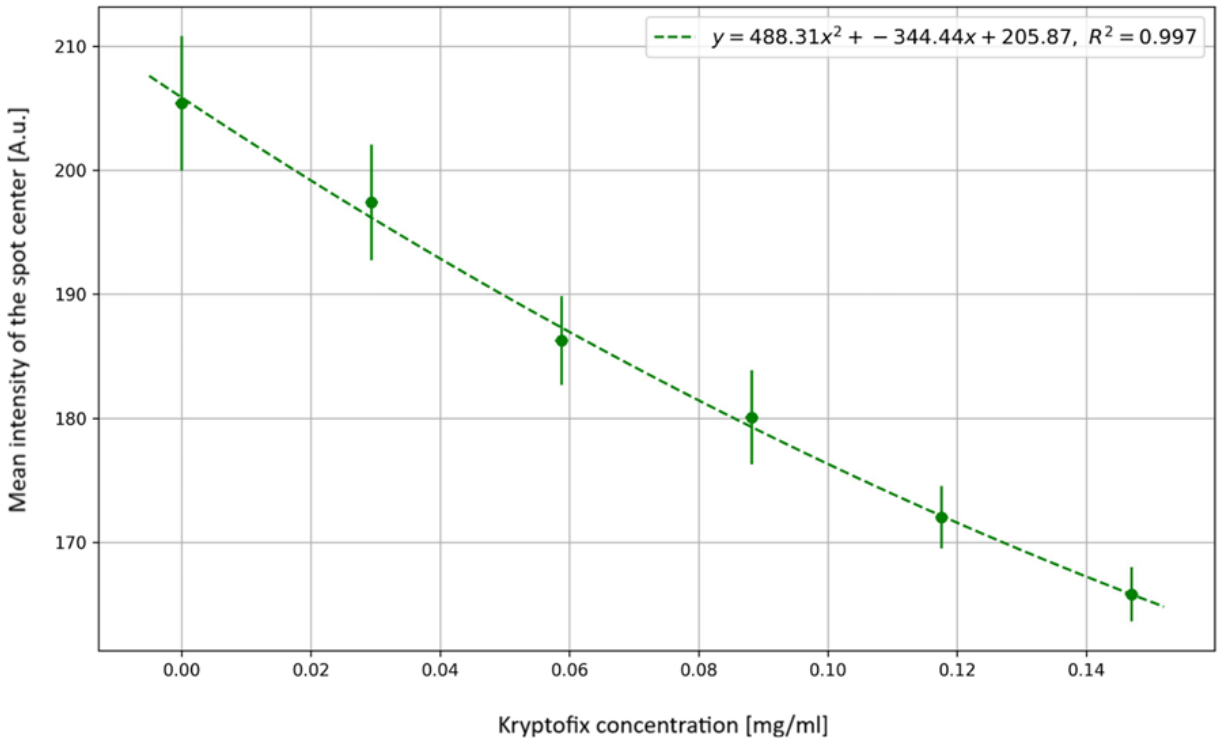


Figure 1: Dependence of the average (N=6) spot centre brightness on the concentration of the Kryptofix solution in the buffer matrix, approximated by quadratic regression.

B.5 Optimization of Automated [^{18}F]FAZA Synthesis on the Synthra RN System

K. Głazowska[1] , K. Kilian[2]

1) Faculty of Chemistry, University of Warsaw, Warszawa, Poland
2) Heavy Ion Laboratory, University of Warsaw, Warszawa, Poland

Introduction

[^{18}F]Fluoroazomycino-arabinoside ([^{18}F]FAZA) is a second-generation 2-nitroimidazole derivative used in Positron Emission Tomography (PET) for the non-invasive imaging of tumour hypoxia. Its mechanism of accumulation is based on the intracellular reduction of the nitro group in oxygen-deprived environments, leading to the covalent binding of the tracer to cellular macromolecules. Compared to the standard [^{18}F]FMISO, [^{18}F]FAZA exhibits superior pharmacokinetics, including faster diffusion and more efficient clearance from normoxic tissues, resulting in a higher tumour-to-background ratio. This report details the development and optimization of an automated synthesis method for [^{18}F]FAZA using the Synthra RN synthesizer, focusing on increasing efficiency and reproducibility for clinical applications.

Experimental Setup The experiments were performed using the Synthra RN automated system, which features two reaction vessels (5 ml and 11 ml) with a temperature range from -50°C to 200°C, and an integrated HPLC system with UV and radiometric detection. The [^{18}F] isotope was produced using a GE PETrace 840 cyclotron via the ^{18}O(p,n)^{18}F nuclear reaction. For the optimization trials, residual activity (approximately 1-2 GBq) from routine production was used. The precursor employed was 1-(2,3-diacetyl-5-tosyl-alpha-D-arabinofuranosyl)-2-nitroimidazole. Synthesis preparation involved thorough chemical cleaning of the system with acetone at 80°C followed by helium drying.

Experimental Optimization (Probes I–XI) The optimization process involved eleven experimental trials where various reaction parameters were modified to identify the most effective synthesis conditions:

- Probes I-III (Initial Protocols): The first trials followed established literature procedures, using 5 mg of precursor in DMSO (100°C-120°C for 10 min) and hydrolysis with 0.1 M NaOH. These attempts failed to yield the target product, with HPLC chromatograms showing predominantly free fluorides and unidentified impurities. The introduction of an Al_2O_3 column to remove fluorides and switching the neutralizing agent from HCl to H_3PO_4 did not improve the outcome.

- Probes IV-VII (Solvent and pH Modifications): The solvent was changed from DMSO to acetonitrile to facilitate easier evaporation. Despite this, the tracer was not obtained. Subsequent trials focused on the influence of pH, including additional buffering of the samples and removing the neutralization step entirely, which resulted only in further unidentified signals and injection-related issues.

- Probes VIII-IX (Enhanced Anhydrous Conditions): Assuming that trace amounts of water were inhibiting nucleophilic substitution, drying times were significantly increased (up to 8 min at 70°C and 3 min at 95°C). However, these rigorous anhydrous conditions alone were insufficient to catalyze the reaction.

- Probes X-XI (Successful Synthesis): A critical breakthrough was achieved by drastically reducing the amount of Kryptofix 2.2.2 (down to 100 μl in Probe X and 50 μl in Probe XI).

Drying parameters were also refined (5 min at 70°C and 2 min at 95°C). Under these optimized conditions, a peak corresponding to [^{18}F]FAZA was observed at a retention time of approximately 13.7 minutes, consistent with the reference standard.

Quality Control and Results The identity of the final product was confirmed using an analytical HPLC system (Shimadzu) with a C18 column, a mobile phase of H_2O:EtOH (90:10), and UV detection at 225 nm.

- **Radiochemical Yield (RCY):** The optimized process yielded an RCY of **22.3%** for Probe X and **26.8%** for Probe XI, which are comparable to values reported in international literature.
- **Radiochemical Purity (RCP):** The radiochemical purity was calculated based on the ratio of the [^{18}F]FAZA peak area to the sum of all radioactive peaks, consistently exceeding 95%.
- **Stability:** Stability studies showed that [^{18}F]FAZA remains highly stable (99%) in a saline solution for at least 12 hours post-synthesis, indicating it is suitable for clinical use even several hours after production.

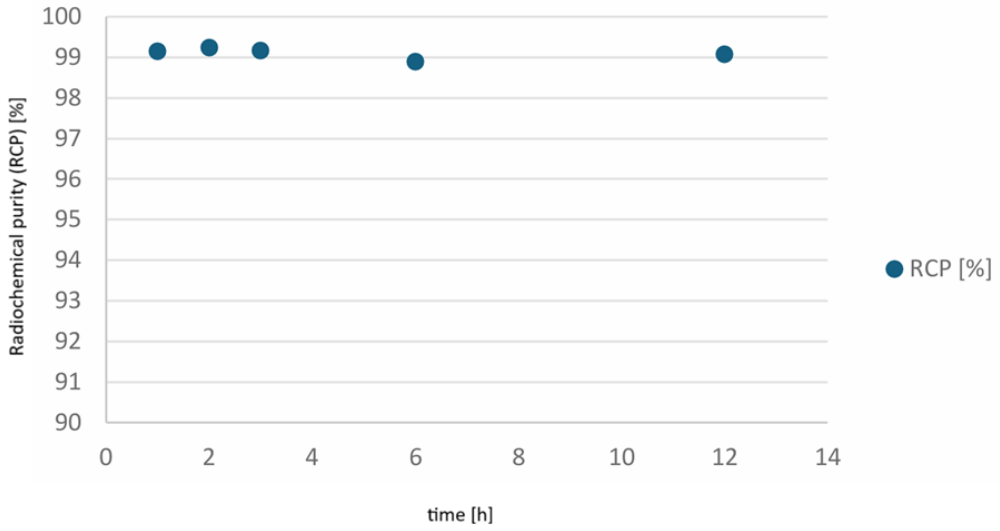


Figure 1: Radiochemical purity and stability of [^{18}F]FAZA 1-12h. Determination: HPLC, Column C18 (Agilent, Eclipse XDB-C18, 150 mm × 4,6 mm × 5 μm), Detection: UV (225 nm) and radiometric Raytest-Gabistar, mobile phase ethanol:water 10:90 v/v, flow: 1 mL/min

Conclusions An efficient and automated method for the synthesis of [^{18}F]FAZA has been successfully developed for the Synthra RN synthesizer. The study demonstrated that precise control over the Kryptofix 2.2.2 concentration and specific drying parameters are the most critical factors for successful radiollabeling. The high stability and competitive yields achieved allow for the potential implementation of this method in routine radiopharmaceutical production at HIL to support advanced preclinical studies.

B.6 Single-Domain Anti-HER2 Antibody Labelled with Theranostic ^{177}Lu - Physicochemical and Biological Characterization for Targeted Radioimmunotherapy

Z. Napora[1], K. Kilian[2], M. Pruszyński[3]

1) Faculty of Chemistry, University of Warsaw, Warszawa, Poland
2) Heavy Ion Laboratory, University of Warsaw, Warszawa, Poland
3) Institute of Nuclear Chemistry and Technology, Warszawa, Poland

Introduction

Breast and ovarian cancers characterized by the overexpression of human epidermal growth factor receptor 2 (HER2) represent a significant challenge in modern oncology. Despite the success of targeted therapies using monoclonal antibodies such as trastuzumab, approximately 70% of patients develop resistance within one year. Radioimmunotherapy (RIT), which combines the molecular precision of vectors with the destructive power of ionizing radiation, offers a potential solution. This study utilized the 2Rb17c nanobody-a small (12-15 kDa), highly stable antibody fragment that provides rapid pharmacokinetics and deep tumour penetration. Lutetium-177 (^{177}Lu) was chosen as the isotope due to its therapeutic β-emissions and γ-radiation, which allows for diagnostic imaging (theranostics).

Experimental Section

Materials and Molecular Vectors Two variants of the 2Rb17c nanobody were used: 2Rb17c-His (for lysine-mediated conjugation) and 2Rb17c-His-linker-Cys (for cysteine-mediated conjugation). The nanobodies were purified and desalted using Vivaspin 500 centrifugal concentrators with a 5 kDa molecular weight cut-off (MWCO), and their concentrations were determined via UV-VIS spectroscopy at 280 nm. Bioconjugation Strategies Two paths for functionalizing the nanobody with the DOTA chelating ligand were implemented:

- Lysine Conjugation: The bifunctional ligand p-SCN-Bn-DOTA was reacted with the primary amine groups of the nanobody's lysine residues in a borate buffer (pH 8.5) using a 10-fold molar excess.
- Cysteine Conjugation: This process required initial reduction of the 2Rb17c-His-linker-Cys dimers to reactive monomers using TCEP-HCl in the presence of EDTA. Subsequently, a Michael addition was performed between the cysteine thiol group and the maleimide group of the mal-DOTA ligand.

Radiolabelling with ^{177}Lu The resulting bioconjugates were labelled with lutetium(III) chloride $^{177}LuCl_3$ in 0.8 M acetate buffer at pH 4.5. Incubation was carried out at 37-42°C for 1.5-3 hours. Radiochemical yield (RCY) was monitored using radio-iTLC in 0.05 M citrate buffer. The final product was purified on PD-10 columns filled with Sephadex G-25 medium.

In Vitro Biological Studies The SK-OV-3 cell line (ovarian adenocarcinoma) with HER2 overexpression served as the experimental model.

- Stability: Investigated in PBS, human serum (HS), and cell medium over 72 hours.
- Specificity: Evaluated by comparing the binding of the radiobioconjugate in cells blocked with an excess of unmodified nanobody or trastuzumab versus unblocked cells.

- Affinity (K_d): Determined from a receptor saturation curve using varying concentrations of the preparation (0.046-100 nM) at 4°C to prevent internalization.

- Cytotoxicity: Assessed using a clonogenic assay by counting colonies formed after 4 and 24 hours of exposure to activities ranging from 0.063 to 8 MBq/mL.

Results and Discussion

Physicochemical Characterization of Bioconjugates ESI-MS mass spectrometry confirmed the success of bioconjugation for both variants. For the lysine pathway, an average of 0.7 ligands per nanobody molecule was achieved. In the cysteine variant, SEC-HPLC showed 100% reduction of the dimer to the monomer, and ESI-MS confirmed the formation of the desired product with only 5% of unreacted nanobody remaining.

Labelling Efficiency and Stability Despite successful bioconjugation, the cysteine variant (2Rb17c-His-linker-Cys-mal-DOTA) exhibited low and inconsistent labelling yields (below 30%), precluding further biological studies. Conversely, the ^{177}Lu-DOTA-Bn-SCN-p-His-2Rb17c (lysine variant) was obtained with a labelling yield of 87.6–90.6%. After PD-10 purification, the preparation reached a radiochemical purity of 99.0% and a specific activity of 0.2 MBq/μg. Stability studies demonstrated that the radiobioconjugate remained fully stable in PBS, cell medium, and human serum for the entire 72-hour period.

Specificity and Receptor Affinity Specificity tests confirmed that modification and labelling did not disrupt the nanobody's target recognition. Binding to SK-OV-3 cells in the unblocked variant was 2.15%, while blocking with an excess of nanobody or trastuzumab reduced this value to approximately 0.2%. The fact that trastuzumab effectively blocked nanobody binding confirms that both vectors compete for the same IV epitope of the HER2 receptor. The dissociation constant determined from the saturation curve was $K_d = 40.04 \pm 10.52$ nM. This result is comparable to the value for the unmodified nanobody (49.6 nM), proving that high affinity for the molecular target is maintained.

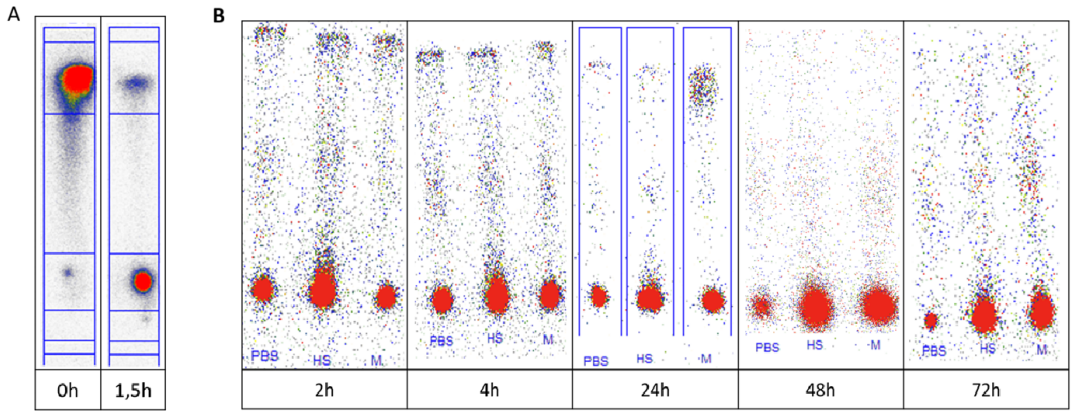


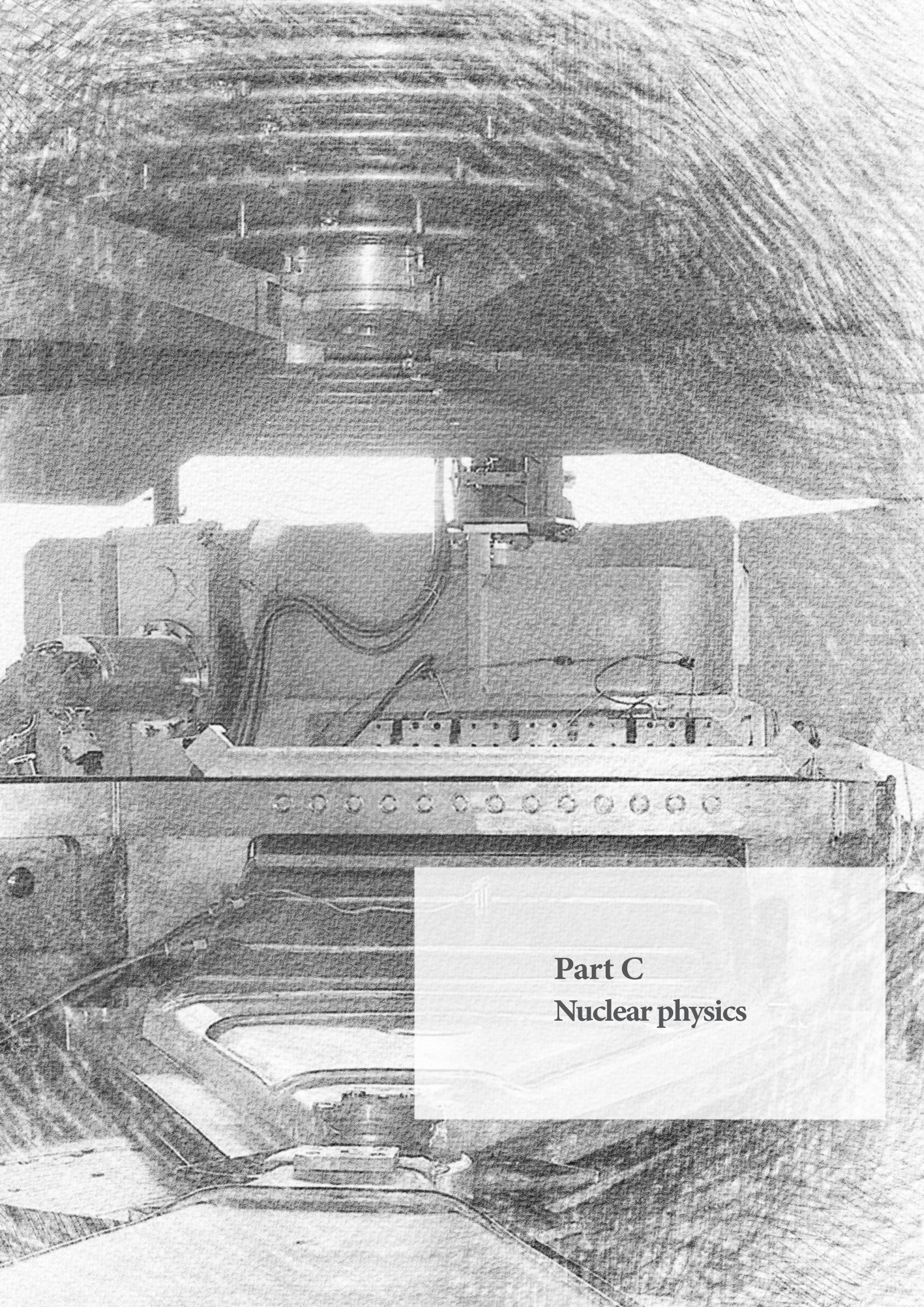
Figure 1: A-Radio-TLC of 2Rb17c-His-p-SCN-Bn-DOTA labeled with ^{177}Lu after t=0h and t=1,5h. Conditions: 0,05mol/L citrate buffer pH = 4,5. ^{177}Lu-DOTA-Bn-SCN-p-His-2Rb17c (Rf = 0,0), ^{177}Lu (Rf = 1,0). B - Stability of ^{177}Lu2Rb17c-His-p-SCN-Bn-DOTA in PBS (PBS), human serum (HS) and McCoy medium (MC) after t=2 h, 4 h, 24 h, 48 h and 72 h incubation

Cytotoxic Effect The clonogenic assay showed a strong dependence of cell survival on radiation dose and incubation time.

- After 4 hours of incubation at the highest dose (8 MBq/mL), colony-forming ability dropped to 65.5%.
- After 24 hours, the effect was much more pronounced-at the same activity level, only 5.5% of cells survived relative to the control. The IC_50 value (activity causing 50% cell death) for the 24-hour incubation was 1.65 MBq/mL.

Conclusions

The study successfully synthesized and characterized the new radiobioconjugate ^{177}Lu-DOTA-Bn-SCN-p-His-2Rb17c. It was demonstrated that the preparation possesses high radiochemical purity, excellent stability, and preserved affinity and specificity for the HER2 receptor. The significant cytotoxic effect confirmed in in vitro tests positions this compound as a promising candidate for targeted radioimmunotherapy of HER2-positive cancers, including breast and ovarian cancer.



Part C
Nuclear physics

C.1 Lifetime studies in neutron-deficient ^{172}Os using the RDDS technique

A. Didik[1], C. Fransen[1], T. Abraham[2], D. Al Daas[1], A. Blazhev[1], B. Cederwall[4], M. Doncel Monasterio[6], T. Grahn[3], J. Grębosz[7], K. Hadyńska-Klęk[1], C. Heymer[1], G. Jaworski[2], J. Jolie[1], M. Komorowska[2], M. Kowalczyk[2], A. Krzysiek[2], C.-D. Lakenbrink[1], A. Malinowski[2], C. Müller-Gatermann[5], A. Nałęcz-Jawecki[2], P.J. Napiorkowski[2], R. Novak[1], M. Palacz[2], J. Parkarinen[3], I. Piętka[2], P. Ruotsalainen[3], K. Rusek[2], P. Sekrecka[2], A. Špaček[2], F. von Spee[1], J. Srebrny[2], A. Tucholski[2], E.T.E. Uusikyla[3], K. Wrzosek-Lipska[2]

1) Institute for Nuclear Physics, University of Cologne, Germany
2) Heavy Ion Laboratory, University of Warsaw, Warszawa, Poland
3) Department of Physics, University of Jyväskylä, Finland
4) Department of Physics, KTH - The Royal Institute of Technology, Stockholm, Sweden
5) Argonne National Laboratory, Argonne, USA
6) Department of Physics, Stockholm University, Sweden
7) The H. Niewodniczański Inst. of Nucl. Phys. PAN, Kraków, Poland

The neutron-deficient osmium isotopes in the mass region $A \sim 170$ represent an important testing ground for investigations of the evolution of nuclear collectivity and shape. Systematics of excitation energies and electromagnetic transition strengths indicate a gradual transition from well-deformed rotational structures near mid-shell towards softer and more transitional configurations at lower neutron numbers. However, the detailed behaviour of transition strengths in the lighter osmium isotopes reveals a complex and not yet fully understood picture.

In particular, previously reported lifetime measurements and transition quadrupole moments in ^{172}Os suggested an unusual evolution of collectivity along the yrast band [1]. While the lowest excited states exhibit rotor-like properties, enhanced collectivity at higher spins has been interpreted as a possible signature of band mixing or the onset of shape coexistence in this nucleus [2]. It should be noted that the available lifetime data might be affected by unobserved delayed side-feeding contributions [1]. Therefore, a new precise determination of yrast level lifetimes in ^{172}Os is required in order to clarify the structural evolution in this region.

Motivated by these considerations, a lifetime measurement was performed at the Heavy Ion Laboratory (HIL), University of Warsaw. Excited states in ^{172}Os were populated via the fusion–evaporation reaction ^{144}Nd(^{32}S,4n)^{172}Os at a beam energy of about 170 MeV. Level lifetimes were measured using the recoil-distance Doppler-shift (RDDS) technique with the Cologne coincidence plunger device [5] coupled to the EAGLE γ-ray spectrometer [4]. Data were collected for a range of target–stopper distances between approximately 5 and 1000 μm in order to enable a reliable extraction of level lifetimes.

Within the present PhD project, the analysis of the experimental data has been continued. The $\gamma\gamma$ coincidence events were sorted into ring-wise matrices, allowing the extraction of shifted and unshifted components of the main yrast transitions. Coincidence gates on flight components of feeding transitions were applied to eliminate systematic uncertainties related to unobserved side feeding, which represented a major limitation of earlier measurements. An example of the spectra obtained is shown in Fig. 1.

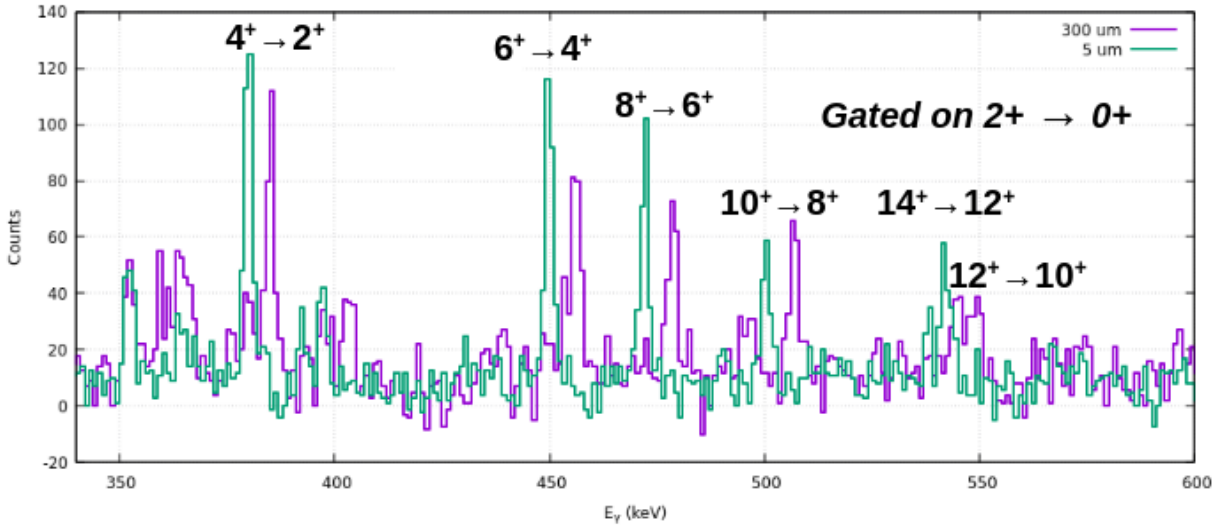


Figure 1: Example of γ-ray spectra gated on the $2_1^+ \rightarrow 0_1^+$ transition obtained for two different target–stopper distances (5 and 300 μm). The main transitions in the ground-state band of ^{172}Os are indicated. The change of relative peak intensities with distance forms the basis of the lifetime determination using the RDDS method.

Preliminary level lifetimes have been determined for several states in the ground-state band up to spin 10^+. The results obtained are in agreement with previously reported values [1] but show improved statistical precision and a more systematic behaviour along the yrast sequence. Based on the extracted lifetimes, reduced transition probabilities $B(E2)$ and transition quadrupole moments Q_t were deduced and are presented in Fig. 2.

The resulting Q_t systematics indicate a smooth evolution of collectivity and support the interpretation that ^{172}Os is located close to the border of a rapid structural change observed in the lighter osmium isotopes towards a region with "anomalous" $B_{4/2} = B(E2; 4_1^+ \rightarrow 2_1^+)/B(E2; 2_1^+ \rightarrow 0_1^+)$ values, i.e., $B_{4/2} < 1$, with ^{172}Os the lightest isotope state inhibiting "regular" collective properties of the lower yrast states.

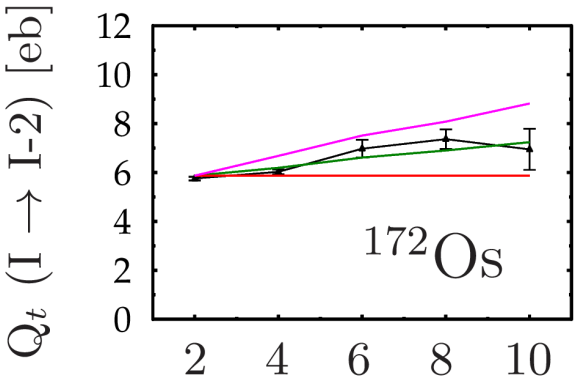


Figure 2: Transition quadrupole moments Q_t as a function of spin for the ground-state band in ^{172}Os obtained in the present analysis. The purple, green and red lines give the expectation values for rotor, X(5) and vibrator nuclei, respectively.

A comparison with theoretical calculations based on symmetry-conserving configuration-mixing approaches shows that the general trends of excitation energies and transition strengths between the lowest yrast states in ^{172}Os can be well reproduced and yielded a slight triaxial defor-

mation [3]. Nevertheless, a consistent description of the structural behaviour of neutron-deficient osmium isotopes remains challenging and further experimental input is required.

The analysis is still in progress. Future work will focus on a detailed evaluation of systematic uncertainties and on extending the lifetime information to higher-spin states. Final results are planned to be presented in a forthcoming journal publication.

Bibliography

[1] P. Virtanen et al., Nucl. Phys. A **591**, 145 (1995).
[2] J. Gascon et al., Nucl. Phys. A **470**, 230 (1987).
[3] A. Goasduff et al., Phys. Rev. C **100**, 034302 (2019).
[4] J. Mierzejewski *et al.*, Nucl. Instrum. Methods Phys. Res. A 659, 84 (2011)
[5] A. Dewald, O. Möller, P. Petkov, Prog. Part. Nucl. Phys. **67**, 786 (2012)

C.2 Gamma-ray Spectroscopy of ^{134}Sm

P. Sekrecka[1], A. Malinowski[1,2], M. Palacz[1], A. Fijałkowska[2], G. Jaworski[1], I. Kuti[3], B. Saygı[4], P. Bednarczyk[5], M. Ciemała[5], G. Colucci[1], G. de France[6], A. Goasduff[7] J. Grębosz[5], V. Guadilla[2], K. Hadyńska-Klęk[1], E. Karanfil[4], M. Komorowska[1], A. Korgul[2], M. Kowalczyk[1], J.A. Kowalska[1], A. Krakó[3], M. Matejska-Minda[5], K. Miernik[2], J. Molnar[3], A. Nałęcz-Jawecki[8], P. Napiorkowski[1], W. Okliński[2], A. Otręba[2], I. Piętka[1], M. Regulska[2], J. Samorajczyk-Pyśk[1], A. Špaček[1], A. Stolarz[1], N. Toniolo[7], A. Tucholski[1], K. Wrzosek-Lipska[1], E. Yeltepe[9]

1) Heavy Ion Laboratory, University of Warsaw, Warszawa, Poland
2) Faculty of Physics, University of Warsaw, Warszawa, Poland
3) HUN-REN Institute for Nuclear Research, ATOMKI, Debrecen, Hungary
4) Ankara University, Institute of Nuclear Sciences, Ankara, Turkey
5) The H. Niewodniczański Inst. of Nucl. Phys. Kraków, Poland
6) GANIL, Caen, France
7) INFN, Laboratori Nazionali di Legnaro, Legnaro, Italy
8) National Centre for Nuclear Research, Świerk, Poland
9) Proton Accelerator Facility, Turkish Energy, Nuclear and Mineral Research Agency, Ankara, Turkey

An experiment aiming at the investigation of the excited states of ^{134}Sm was performed in January 2024, see Ref. [1] and references therein. Analysis of the collected data is continuing at HIL.

Detailed stability checks of all the collected correction parameters have been completed. The resulting correction factors have been determined and, together with the calibration factors, applied during a presort of the entire data set. Several preselected data sets have also been created, with conditions on the detected particles and the number of γ rays.

The conditions for the detection and identification of protons and α particles in the DIAMANT detectors were optimised. Three recorded parameters were used for this purpose: energy, time, and the PID parameter (which relates to the pulse shape) [2]. Example gates for a proton, two protons registered in one detector, and a α-particle are shown in Fig. 1.

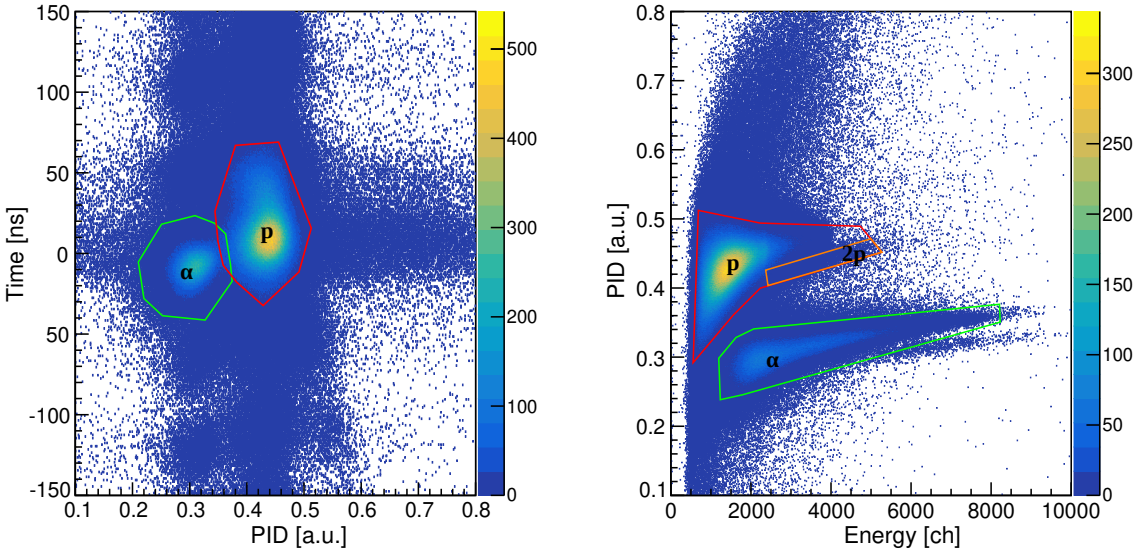


Figure 1: Time vs. PID and PID vs. energy spectra from one of the DIAMANT forward wall detectors. Gates used to identify single protons, two protons registered in the same detector, and an α particles are marked.

The analysis of the γ-ray spectra indicated inconsistencies in the efficiency of the detectors at low energies, determined earlier using a standard approach to the data collected with ^{133}Ba and ^{152}Eu radioactive sources. Thus, the efficiency curve was carefully re-examined, using in addition on-line data and the weak 160 keV of the ^{133}Ba source.

Presently, work is in progress on the level scheme of ^{134}Sm, which includes attempts to identify new states as well as the verification of the properties of the known ones. Double and triple γ-ray coincidence matrices gated on the detected neutrons and α particles are used for this purpose.

The efficiency values for detecting and identifying 1 and 2 neutrons in the NEDA detectors were determined: $\epsilon_{1n} = 22.8(4)\%$, and $\epsilon_{2n} = 4.3(1)\%$ respectively (only statistical effects are taken into account for the error bars).

This work is partly supported by the National Science Centre (NCN), Poland, grant Nos. 2020/39/D/ST2/00466 and 2023/51/D/ST2/02816.

Bibliography

[1] P. Sekrecka *et al.*, HIL Annual Report 2024, page 57
[2] I. Kuti *et al.*, Acta Phys. Pol. B Proceedings Supplement **17** (2024) 3-A13

C.3 Lifetime measurement of low-lying excited states in ^{118}Xe

K.D. Duan[1], B.F. Lv[1], C.M. Petrache[1,2,3], C.-D. Lakenbrink[4], G. Jaworski[5], M. Palacz[5], A. Astier[2], G. Colucci[5], K. Hadyńska-Klęk[5], M. Komorowska[5], M. Kowalczyk[5], K. Krutul-Bitowska[5], P.J. Napiorkowski[5], M.M. Palkowski[5], W. Poklepa[5], J. Samorajczyk-Pyśk[5], J. Srebrny[5], A. Tucholski[5], K. Wrzosek-Lipska[5], C. Fransen[4], M. Beckers[4], F. Dunkel[4], L. Kornwebel[4], F. von Spee[4], S. Basak[1], I. M. Bhat[1], S. Guo[1], P.M. Jodidar[1], K.K. Zheng[1], E. Grodner[6], A. Nałęcz-Jawecki[6], J. Grębosz[7], E.T.E. Uusikyla[8], T. Grahn[8], J. Sarén[8], J. Uusitalo[8], A. Briscoe[9], A. McCarter[9], P. Spagnoletti[9], N. McDonalds[10], C. Andreoiu[3], F. Wu[3], B. Kruzsicz[11], I. Kuti[11], D. Sohler[11], J. Timar[11], A. Goasduff[12], N. Toniolo[12]

1) Institute of Modern Physics, Chinese Academy of Sciences, Lanzhou, China
2) Université Paris-Saclay, CNRS/IN2P3, IJCLab, Orsay, France
3) Department of Chemistry, Simon Fraser University, Burnaby, Canada
4) Institute for Nuclear Physics, University of Cologne, Germany
5) Heavy Ion Laboratory, University of Warsaw, Warszawa, Poland
6) National Centre for Nuclear Research, Świerk, Poland
7) Institute of Nuclear Physics Polish Academy of Sciences, Krakow, Poland
8) Department of Physics, University of Jyväskylä, Finland
9) Oliver Lodge Laboratory, University of Liverpool, Liverpool, UK
10) Department of Physics, University of Surrey, Guildford, UK
11) HUN-REN Institute for Nuclear Research (HUN-REN ATOMKI), Pf. 51, 4001 Debrecen, Hungary
12) INFN, Laboratori Nazionali di Legnaro, Legnaro, Italy

The lifetimes of low-lying excited states are key physical quantities that directly reflect the internal structure of the nucleus. By measuring these lifetimes, one can derive reduced electromagnetic transition probabilities, which provide crucial insights into nuclear deformation. Since theoretically predicted transition probabilities are calculated from the wave functions of the initial and final states, they are inherently sensitive to the underlying assumptions of the nuclear structure model. Consequently, measuring lifetimes provides a rigorous and direct test of these theoretical frameworks. In the specific case of ^{118}Xe with $N = 64$, the number of valence neutrons is close to the middle of the $N = 50-82$ major shell, and therefore the proton-neutron interactions are predicted to be enhanced and result in significant quadrupole deformations, for which Nilsson intruder and extruder orbitals originating from the $1h_{11/2}$ and $1g_{9/2}$ spherical sub-shells are near the Fermi level [1]. The low-lying level structure of ^{118}Xe is interesting to study, precisely to establish the deformation. The $E1$ strengths connecting the negative-parity bands to the ground-state band will also provide validation of the predicted enhancement of octupole correlations [2]. Also, the energy staggering of the levels with even and odd spins in the γ bands of the proton-rich Xe nuclei is largest in ^{118}Xe, indicating a pronounced γ softness which, in combination with a large quadrupole deformation, can give rise to unexpected structural effects.

A plunger experiment measuring the lifetimes of excited states in ^{118}Xe utilizing the recoil distance Doppler-shift (RDDS) technique [3] was performed at the Heavy Ion Laboratory (HIL) in March 2023, using the EAGLE+NEDA+Plunger setup (experiment HIL106). The HPGe detectors of the EAGLE array are located in rings at backward angles of 101°, 117° and 143° with respect to the beam direction. In the RDDS technique, recoil nuclei travel at a velocity v between the thin target and the thick stopper. The γ rays emitted in flight are Doppler shifted, while the γ rays emitted in the stopper are not. Lifetime information is obtained by measuring the change in intensity of the shifted and unshifted peaks as the target-to-stopper distance is varied.

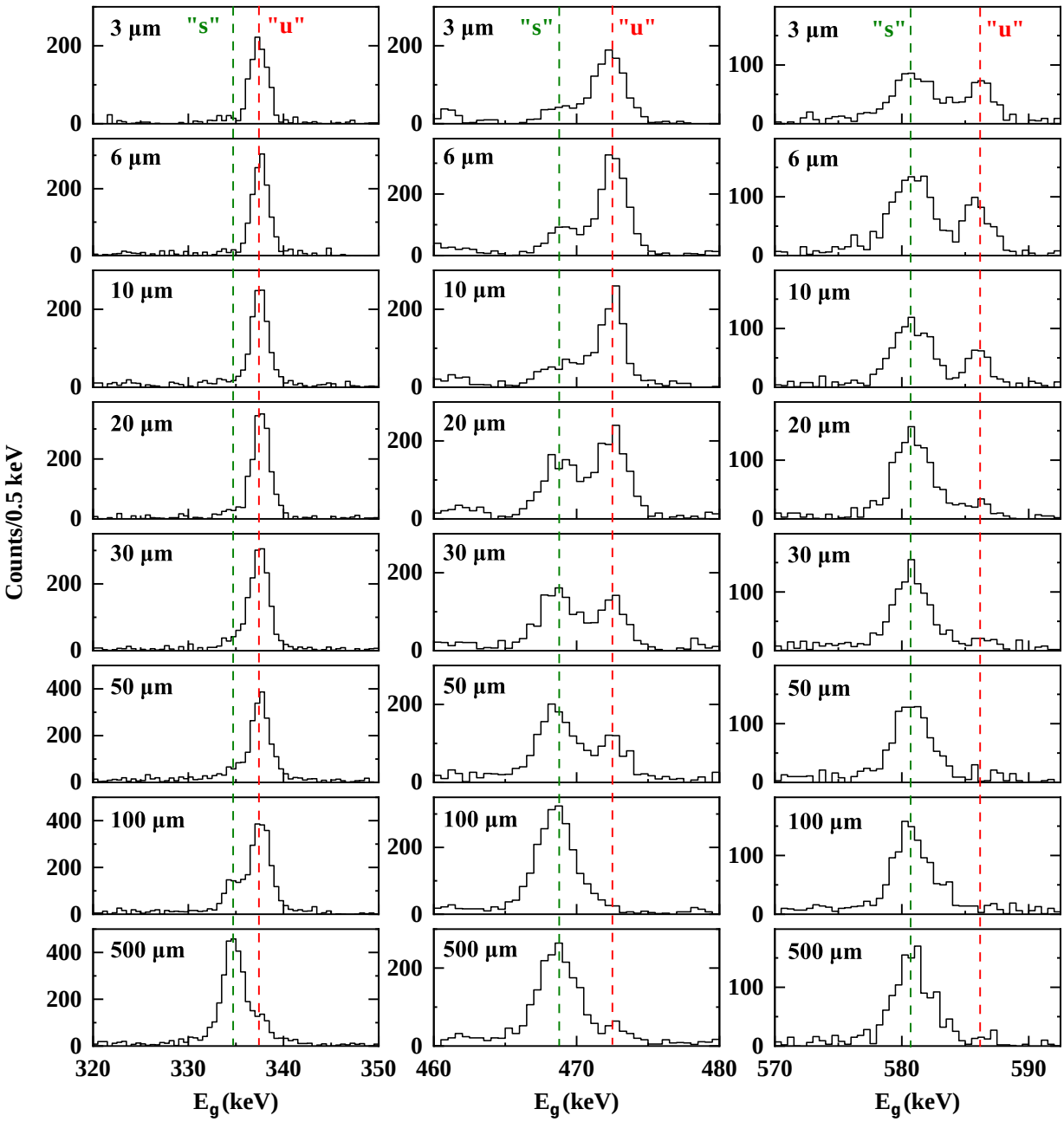


Figure 1: Evolution of the shifted ("s", dashed green line) and unshifted ("u", dashed red line) components. Left: the 338-keV $2^+ \rightarrow 0^+$ transition obtained by gating on the shifted component of the 473-keV $4^+ \rightarrow 2^+$ γ ray. Centre: the 473-keV $4^+ \rightarrow 2^+$ transition obtained by gating on the shifted component of the 586-keV $6^+ \rightarrow 4^+$ γ ray. Right: the 586-keV $6^+ \rightarrow 4^+$ transition obtained by gating on the shifted component of the 676-keV $8^+ \rightarrow 6^+$ γ ray. The indicated distances are relative to the electrical contact point to which an offset has to be added.

The excited states in ^{118}Xe were populated in the fusion-evaporation reaction ^{106}Pd(^{16}O,4n)^{118}Xe, at a beam energy of 85.7 MeV. Measurements were performed at eight different target-to-stopper distances, ranging from 3 to 500 microns. With the mean velocity of the traveling recoils determined to be $v/c = 1.1$ %, this corresponds to times of flight ranging from 0.9 to 152 ps.

Spectra measured at each distance at backward angles ($\approx 143°$) for the 338-keV $2^+ \rightarrow 0^+$ transition gated above on the 473-keV γ ray, 473-keV $4^+ \rightarrow 2^+$ transition gated above on the

586-keV γ ray, and 586-keV $6^+ \rightarrow 4^+$ transition gated above on the 676-keV γ ray are shown in Fig. 1.

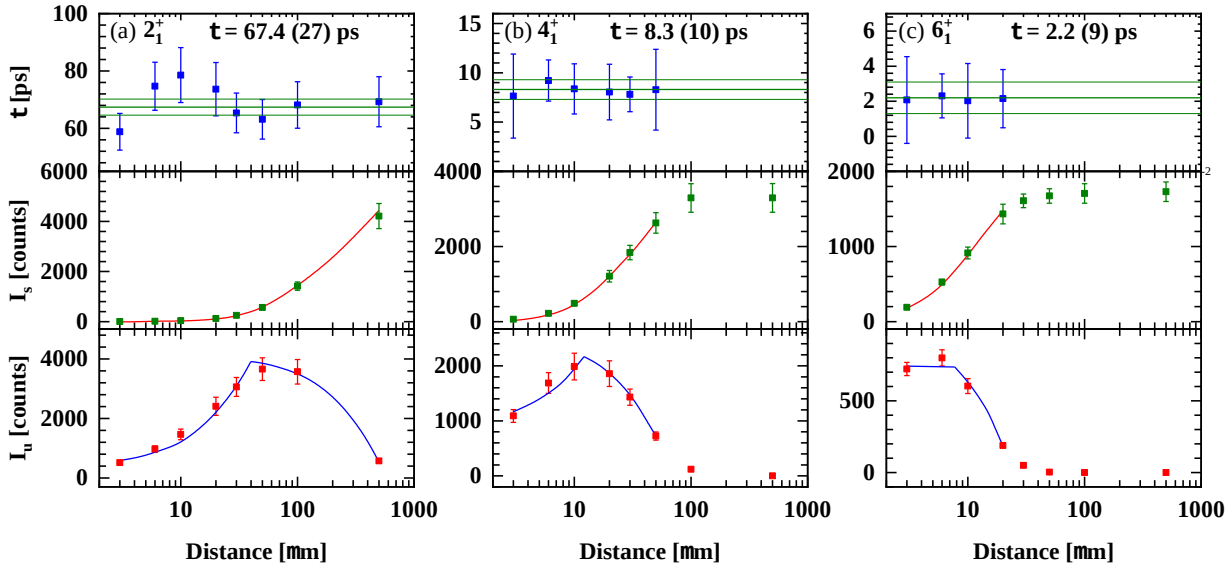


Figure 2: Determination of the lifetimes of the 2^+, 4^+ and 6^+ yrast states in ^{118}Xe using the DDCM technique. The intensities of the shifted (I_s) and unshifted (I_u) components of the depopulating transition are obtained from the spectra produced by gating on the shifted component of transitions feeding the state of interest, and measured with detectors placed at backward angles ($\approx 143°$) with respect to the beam direction. The extracted lifetimes τ are also shown, obtained from fits with second degree polynomials of the I_s and I_u intensities measured at selected distances corresponding to the maximum sensitivity of the method for a given lifetime.

The lifetimes of the 2^+, 4^+, and 6^+ yrast states in ^{118}Xe have been extracted using the differential decay curve method (DDCM) [3, 4], performed with the computer code NAPATAU [5], as shown in Fig. 2. The lifetimes of the 2^+, 4^+, and 6^+ yrast states, extracted from the present measurement, of 67.4(27), 8.3(10), and 2.2(9) ps respectively, are in good agreement with the previous values of 68.6(10), 8.46(17) and 2.18(9) ps, as reported in Ref. [6]. The present results confirm the collective behavior of ^{118}Xe and a ratio of reduced transition probabilities $B_{4/2} = 1.55$. The $B_{4/2}$ ratio is similar to those of the heavier Xe neighbours, but definitely larger than the questionable $B_{4/2} = 1$ value in ^{114}Xe [7].

The analysis of the data from the HIL106 experiment is still in progress, and new results on several other nuclei populated in the same reaction will be reported in the near future.

The installation and use of NEDA at HIL were supported by the National Science Centre (NCN), Poland (grant No. 2020/39/D/ST2/00466). Additional support from the NCN is acknowledged through grants 2023/51/D/ST2/02816.

Bibliography

[1] P. Möller *et al.*, At. Data Nucl. Data Tables **94** (2008) 758.
[2] B.F. Lv *et al.*, Phys. Rev. C **105** (2022) 044319.
[3] A. Dewald, O. Möller, and P. Petkov, Progress in Particle and Nuclear Physics **67** (2012) 786.
[4] G. Böhm *et al.*, Nucl. Instrum. Methods Phys. Res. A **329** (1991) 248.
[5] B. Saha, Ph.D. thesis, Universität zu Köln (2004).
[6] C. Müller-Gatermann *et al.*, Phys. Rev. C **102** (2020) 064318.
[7] G. de Angelis *et al.*, Phys. Lett. B **535** (2002) 93.

C.4 Lifetime measurement of ^{128}Cs I=11^+, 12^+ states with the plunger technique

E. Grodner[1], M. Kowalczyk[2], M. Komorowska[2], J. Srebrny[2], Ch. Droste[3] A. Nałęcz-Jawecki[1], C. Fransen[4], C. Lakenbrink[4], C. Mueller Gattermann[4], Q.B. Chen[5], C. M. Petrache[6,7,8], A. Stolarz[2], A. Tucholski[2], L. Próchniak[2]

1) National Centre for Nuclear Research
2) Heavy Ion Laboratory, University of Warsaw, Warszawa, Poland
3) Faculty of Physics, University of Warsaw, Warszawa, Poland
4) Institut für Kernphysik, Universität zu Köln, Köln, Germany
5) School of Physics, East China Normal University, Shanghai 200241, China
6) Institute of Modern Physics, Chinese Academy of Sciences, Lanzhou, China
7) Université Paris-Saclay, CNRS/IN2P3, IJCLab, Orsay, France
8) Department of Chemistry, Simon Fraser University, Burnaby, Canada

The ^{128}Cs isotope is one of the best-studied nuclei in the context of chiral symmetry breaking in low energy nuclear collective states. Specific structures, i.e., the rotational partner bands, have already been found in ^{128}Cs [1] indicating its possible chiral nature. The first lifetime measurements in these rotational bands were performed at the Heavy Ion Laboratory [2, 3] using the Doppler Shift Attenuation method. The DSA results confirmed the predicted chiral electromagnetic selection rules [4] making ^{128}Cs the first nucleus experimentally recognized as chiral. The EM selection rules are valid for systems invariant with respect to an additional S-symmetry operation [5] and reveal themself in the existence of B(M1) staggering of the electromagnetic transition probability values along the rotational partner bands. The chiral symmetry breaking deals with the time-reversal operation T thus requiring a dynamics on which the T operator may act for the nuclear chirality to exist. The DSA results showed that the chiral dynamics exists for high spin states while below spin 15$\hbar$ the B(M1) staggering in one band of ^{128}Cs increases while in the other band it vanishes. A new observation presented in [6] shows that such an effect could be expected for an isotope losing its chiral dynamics and undergoing a transition from chiral to non-chiral geometry with decreasing spin while still maintaining the additional S-symmetry invariance. The g-factor measurements at the head of the partner bands [7–9] - i.e.: in the lowest spin state in the partner bands - clearly showed that ^{128}Cs does not possess chiral geometry for the lowest possible rotational frequency and such a transition most likely happens in the spin range 9-15 $\hbar$. The experiment covered in this report was designed to measure the lifetimes of these super-picosecond states in ^{128}Cs. The plunger technique with the Cologne-PLUNGER device was used instead of the DSA method, providing sensitivity range from a few up to 500 ps. A gamma spectroscopy experiment using the Doppler effect requires the highest precision of the energy spectra. In contrast to the previous analysis [10] where small non-linearities of energy spectra prevented setting precise energy gates, the results presented in this report were obtained using data from the parallel SMAN aquisition system. Summation of precise multiple gates allowed the stop- and Doppler-shifted components of relevant transitions to be extracted with significant help from the 18 HPGe configuration of the EAGLE array, see Fig. 1.

These data which allow the determination of the lifetimes of the excited states given the full beam time assumed in the submitted proposal. Due to cyclotron failure the effective beam time was less than 50 percent of that requested and did not allow the collection data for more than 4 plunger distances needed for unobserved parameters (like plunger offset) to be fitted with enough precision.

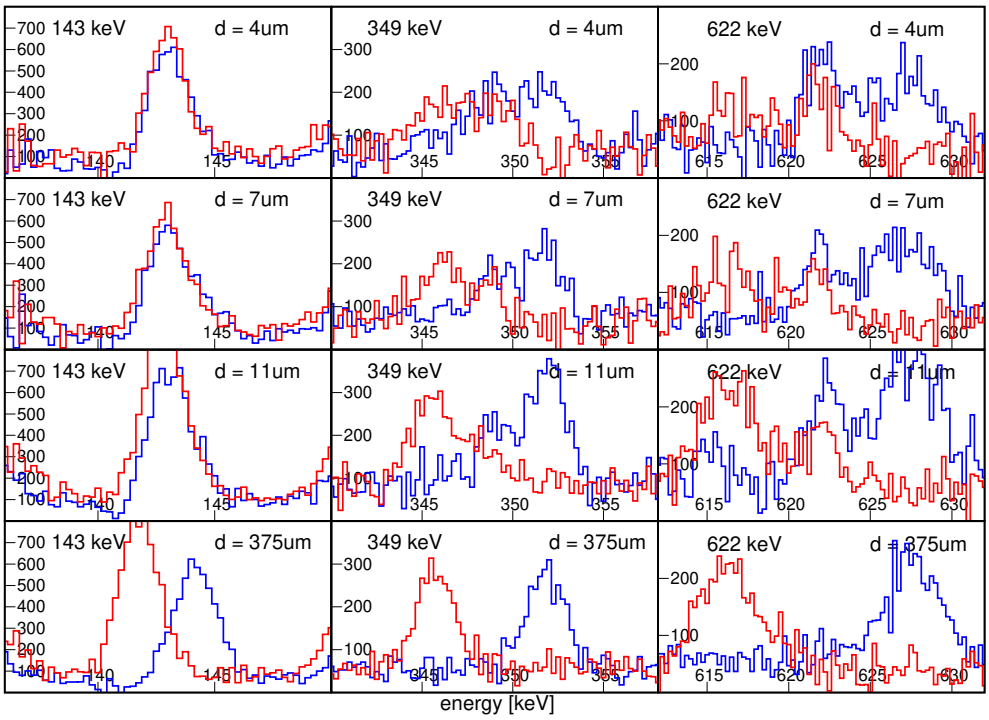


Figure 1: Spectra of 10^+,11^+,12^+ transitions in the partner band of the ^{128}Cs isotope. Rows: plunger distances $4\mu m$, $7\mu m$, $11\mu m$, $375\mu m$. Columns: gamma transition energies: 143keV, 359keV, 622keV. Red colour: backward spectrum (143° with respect to beam direction). Blue colour: forward spectrum (37° with respect to beam direction). All spectra gated on 114.3 + 142.8 + 151.7 + 158.7 +187.9 keV transitions.

Bibliography

[1] T. Koike *et al.*, Phys. Rev. C63, 061304(R) (2001)
[2] E. Grodner *et al.*, Phys. Rev. Lett.97, 172501 (2006)
[3] E. Grodner *et al.*, Phys. Lett. B 703 46–50 (2011)
[4] T. Koike *et al.*, Phys. Rev. Lett.93, 172502 (2004)
[5] L. Próchniak *et al.*, Acta Phys. Pol. B42, 465 (2011)
[6] E. Grodner, Chirality and Wobbling in Atomic Nuclei, Chapter 7, CRC Press, Taylor & Francis Group. (2024)
[7] E. Grodner *et al.*, Phys. Rev. Lett.120, 022502 (2018)
[8] E. Grodner *et al.*, Phys. Rev. C106, 014318 (2022)
[9] E. Grodner *et al.*, Frontiers of Physics, Topical Review, Volume 19 / Issue 3 (2024)
[10] A. Nałęcz-Jawecki *et al.*, HIL Annual Report (2024).

C.5 Search for a new chiral nucleus in the mass 80 region: ^{72}As

C. Liu[1,2], H.Y. Zhang[1], W.B. Zeng[1], S.Y. Wang[1,2], E.H. Wang[1], X.C. Han[1], W.Z. Xu[1], G.Y. Li[1], Z.Y. Wang[1], J. Grębosz[3], E. Grodner[4], K. Hadyńska-Klęk[5], G. Jaworski[5], M. Komorowska[5], M. Kowalczyk[5], A. Malinowski[5], M. Palacz[5], I. Piętka[5], J. Samorajczyk-Pyśk[5], P. Sekrecka[5], A. Špaček[2], A. Stolarz[5], J. Srebrny[5], K. Wrzosek-Lipska[5]

1) Shandong Provincial Key Laboratory of Nuclear Science, Nuclear Energy Technology and Comprehensive Utilization, Weihai Frontier Innovation Institute of Nuclear Technology, School of Nuclear Science, Energy and Power Engineering, Shandong University, Shandong 250061, People's Republic of China
2) WeiHai Research Institute of Industrial Technology, Shandong University, Weihai 264209, People's Republic of China
3) Institute of Nuclear Physics Polish Academy of Science
4) National Centre for Nuclear Research, 05-540 Świerk, Poland
5) Heavy Ion Laboratory, University of Warsaw, Warszawa, Poland

Chirality in atomic nuclei has attracted extensive attention. The $A \approx 80$ mass region is a relatively new territory for the investigation of chirality, and several chiral doublet bands (Refs. [1–4] and the references therein) have been reported in this region. Based on the systematic investigation of nuclei in the $A \approx 80$ mass region, ^{72}As is considered to be a promising candidate to search for chiral doublet bands. In Ref. [5], the g-factor of the 8^+ state at 981.6 keV in ^{72}As was measured by the time-integral perturbed angular distributions method. Based on the measured g-factor value ($g = -(0.534 \pm 0.035)$), the angular momentum geometry for I = 8^+ in ^{72}As can be deduced. It is found that an obviously aplanar rotation appears in the lowest observed state of the positive parity band (981.1 keV state at 8^+) in ^{72}As. Based on the above discussion, we performed an experiment at HIL UW in July 2025 using the EAGLE-NEDA setup. A 51.4 MeV ^{11}B beam impinged on a ^{65}Cu target. The target was made of 5 mg/cm^2 enriched ^{65}Cu evaporated onto a 10.21 mg/cm^2 Pb backing. The average beam intensity was about 0.3 enA and approximately 7.4×10^9 γ-γ coincidence events were accumulated during 36 shifts.

Part A: The candidate chiral doublet bands in ^{72}As

A preliminary level scheme of ^{72}As has been constructed based on the γ-γ coincidence relationships. A pair of nearly degenerate positive parity doublet bands have been identified. Similar band structures have also been reported in the neighbouring isotopes ^{74}As [6] and ^{76}As [2], and were interpreted as chiral doublet bands. Figure 1 shows the gated spectra of the 200.0 keV and 418.3 keV transitions in ^{72}As, and nearly all transitions belonging to ^{72}As can be observed in these two spectra. The excitation energies $E(I)$ and the energy staggering parameters $S(I)$ of the doublet bands are shown in Fig. 2. As shown in Fig. 2, the $E(I)$ and $S(I)$ of the two bands exhibit certain similarities, implying that these two bands possess similar structural properties. Therefore, we preliminarily suggest that the doublet bands in ^{72}As are a pair of chiral doublet bands. Further systematic data analysis and theoretical calculations are needed to confirm this conjecture.

Part B: Lifetime measurement of excited states in ^{73}As

In addition, a large number of γ-ray transitions from ^{73}As were observed in the present data. This provides an opportunity to use the Doppler-shift attenuation method (DSAM) to determine the lifetimes of excited states and to deduce the deformation of ^{73}As. An analysis of the experimental lineshapes was carried out using an updated version of the computer code lineshape for DSAM [7]. The code was used to generate 10000 Monte Carlo simulations for the velocity history of recoiling nuclei traversing the backed target in time steps of 0.01 ps with recoil velocities of the order of 1.44%c in the present work. Electronic stopping powers were taken from Ziegler's tabulation with low-energy modifications [8]. A χ^2 minimization for the observed Doppler shifted lineshapes was then carried out using the level lifetimes, side-feeding lifetimes, background and

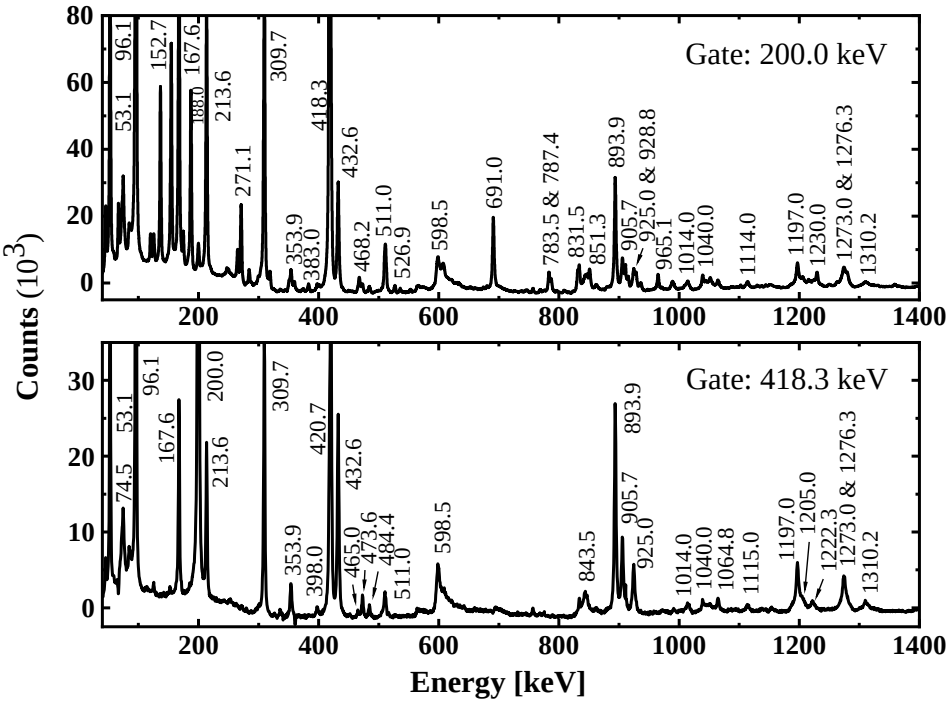


Figure 1: The γ-γ coincidence spectra gated on the 200.0 and 418.3 keV transitions in ^{72}As.

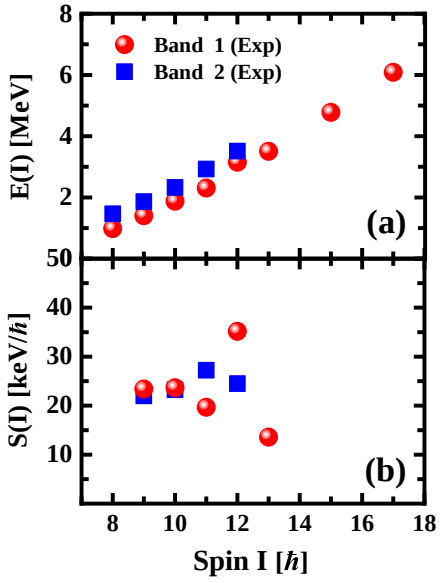


Figure 2: The experimental excitation energies $E(I)$ and the energy staggering parameters $S(I)$ as a function of spin for the nearly degenerate bands in ^{72}As. The two bands are labelled as bands 1 and 2, respectively.

contaminant peaks as input parameters. The lifetimes of four states in a cascade, labelled as Band B1 in Ref. [9], have been extracted. Preliminary results are shown in Fig. 3.

A detailed data analysis is in progress.

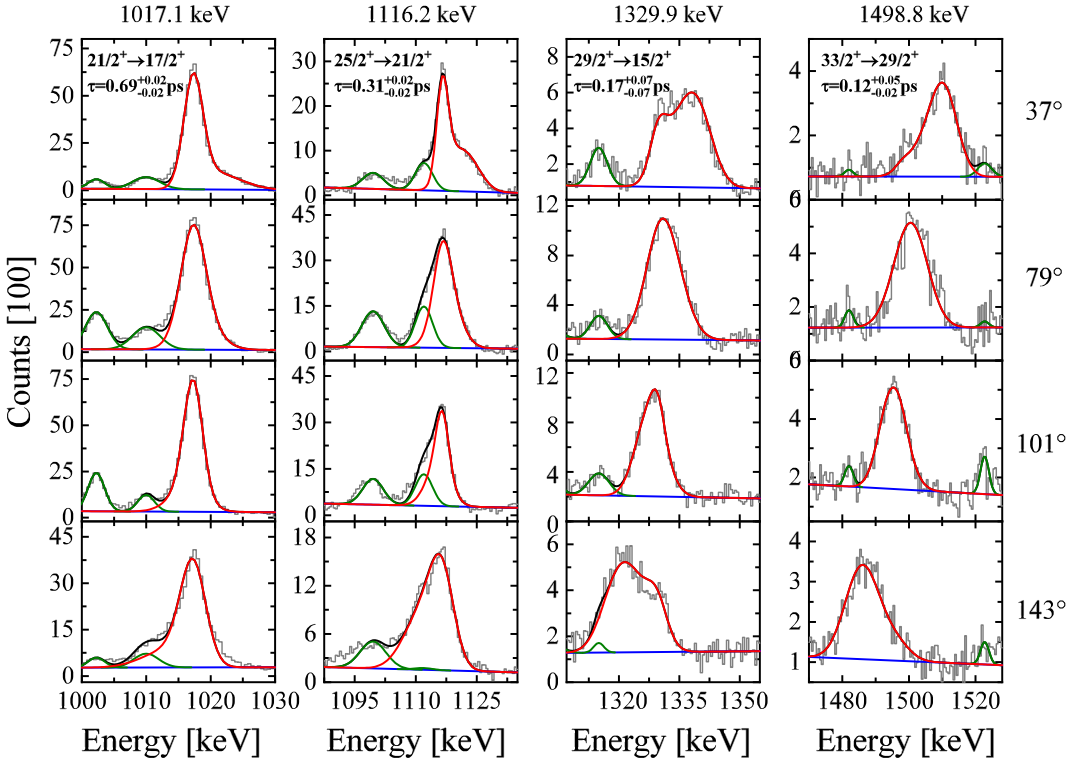


Figure 3: Doppler broadened lineshapes of γ rays calculated at angles of 37°, 79°, 101° and 143° with respect to the beam direction are shown as the red lines. The contamination peaks are presented in green. Black lines shows fits to the experimental data plotted in grey. Blue lines represent the background.

Acknowledgements

This work is partly supported by the National Natural Science Foundation of China (Grant No. 12225504) and the National Science Centre, Poland under Grant Agreement No. 2020/39/D/ST2/00466.

Bibliography

[1] S.Y. Wang *et al.*, Front. Phys. **18** (2023) 64601.
[2] W.Z Xu *et al.*, Phys. Rev. C **109** (2024) 044303.
[3] R.J Guo *et al.*, Phys. Rev. Lett. **132** (2024) 092501.
[4] W.B. Zeng *et al.*, Phys. Rev. C **112** (2025) 034330.
[5] D. Pantelică *et al.*, Phys. Rev. C **82** (2010) 044313.
[6] X. Xiao *et al.*, Phys. Rev. C **106** (2022) 064302.
[7] A.D. Ayangeakaa *et al.*, Phys. Rev. Lett. **110** (2013) 102501.
[8] J.F. Ziegler *et al.*, Pergamon Press, New York vols. 3 and 5 (1980).
[9] M.K. Raju *et al.*, Phys. Rev. C **92** (2015) 064324.

C.6 Deformation of the $0^+_{1,2}$ states in ^{110}Cd from low-energy Coulomb excitation

K. Wrzosek-Lipska[1], I. Piętka[1], L. Próchniak[1], P. E. Garrett[2,3], M. Zielińska[4], T. Abraham[1], J. M. Allmond[5], F. L. Bello Garrote[6], H. Bidaman[2], V. Bildstein[2], S. Buck[2], C. Burbadge[2,1], M. Chiari[7], R. Coleman[2], G. Colombi[2,8], G. Colucci[1] A. Diaz Varela[2], D. T. Doherty[9,3], S. Dutt[10,11], B. Greaves[2], K. Hadyńska-Klęk[1], J. Heery[12], M. Hlebowicz[13], D. Hymers[2,26], J. Iwanicki[1], G. Jaworski[1], B. Jigmeddorj[2,15], D. Kalaydjieva[4,2], M. Kisieliński[1], M. Komorowska[1], N. Kopeć[1,16], M. Kowalczyk[1], J. A. Kowalska[1], K. Krutul-Bitowska[1], R. Kumar[10,1], A. Mai Quynh[17], N. Marchini[7], T. Marchlewski[1], K. R. Mashtakov[2], M. Matejska-Minda[1,18], C. Michelagnoli[8], A. Nannini[7], P.J. Napiorkowski[1], B. Olaizola[2,19], F. Oleszczuk[13], M. Palacz[1], E. Pasquali[20], E.E. Peters[21], M. Rocchini[2,7], E. Sahin[6], J. Samorajczyk-Pyśk[1], M. Saxena[22,1], A. Stolarz[1], J. Srebrny[1], A. Tucholski[1], A. Trzcińska[1], M. Venhart[23], J. L. Wood[24], S. W. Yates[21,25], T. Zidar[2]

1) Heavy Ion Laboratory, University of Warsaw, Warszawa, Poland
2) Department of Physics, University of Guelph, Guelph, N1G2W1, ON, Canada
3) University of the Western Cape, South Africa
4) IRFU, CEA, Université Paris-Saclay, Gif-sur-Yvette, France
5) Oak Ridge National Laboratory, Oak Ridge, TN, USA
6) Department of Physics, University of Oslo, Oslo, Norway
7) INFN Sezione di Firenze, Firenze, Italy
8) Institut Laue Langevin, Grenoble, France
9) University of Surrey, Guildford, GU2 7XH, United Kingdom
10) Inter University Accelerator Centre, New Delhi, India
11) Department of Physics, Aligarh Muslim University, Aligarh, India
12) Department of Physics, University of Surrey, Guildford, UK
13) Faculty of Physics, Warsaw University of Technology, Warszawa, Poland
14) Institut für Kernphysik, Universität zu Köln, Köln, Germany
15) School of Natural Science, Laurentian University, Sudbury, ON P3E2C6, Canada
16) Texas A&M University, College Station, TX 77842-1185, USA
17) Nuclear Research Institute, Dalat, Vietnam
18) Institute of Nuclear Physics Polish Academy of Sciences, Kraków, Poland
19) Instituto de Estructura de la Materia, CSIC, Madrid, ES-28006, Spain
20) Università di Camerino, Camerino, Italy
21) Department of Chemistry, University of Kentucky, Lexington, KY, USA
22) Dep. of Phys. and Astrophysics, U. of Delhi, New Delhi, India
23) Inst. of Physics, Slovak Academy of Sciences, Bratislava, Slovakia
24) School of Physics, Georgia Institute of Technology, Atlanta, GA, USA
25) Department of Physics and Astronomy, University of Kentucky, Lexington, KY, USA
26) Institut für Kernphysik, Universität zu Köln, D-50937 Köln, Germany

For over 40 years even-mass cadmium isotopes have played a key role in the study of collective behaviour in atomic nuclei. Initially, it was believed that their structures could be described within a collective vibrational model, in which the surface of the nucleus oscillates around a spherical equilibrium shape. This view was challenged in Ref. [1] by proposing an alternative interpretation that was supported by the comprehensive spectroscopy of the ^{110,112,114,116}Cd nuclei using the (n,n$'\gamma$) reaction [2–6] as well as highly sensitive β-decay studies [4, 7] and g-factor measurements [8]. These experimental findings led to a fundamental question regarding the nature of the collectivity of the low-lying states in Cd nuclei (see, e.g., Ref. [9]) and inspired new calculations using advanced theoretical models of atomic nuclear structure. The level schemes of ^{110,112}Cd were reorganised in terms of rotational structures [10, 11] and, with guidance from symmetry-conserving configuration mixing (SCCM) calculations, various ellipsoidal shapes were ascribed to them. In parallel, alternative theoretical approaches were developed, based on the interacting boson model (IBM) [12] involving, in its most recent version, configuration mixing with a partial

dynamical symmetry [13–15]. The latter were able to reconcile, to a certain extent, the existing experimental data on these nuclei with their quasi-spherical shapes.

Recent experiments at the Heavy Ion Laboratory, University of Warsaw, enabled discrimination between these two fundamentally different interpretations of the structure of cadmium nuclei by determining the quadrupole moments of excited 2^+ states and the shapes of two key 0^+ states in the ^{110}Cd nucleus. To this end, we used the Coulomb-excitation technique, and by applying the Kumar-Cline quadrupole sum rules formalism [16, 17] to the experimentally determined $E2$ matrix elements we determined the nuclear deformation in a model-independent way.

Within this experimental programme, two Coulomb-excitation experiments to study ^{110}Cd were performed at the Heavy Ion Laboratory, using 91-MeV ^{32}S and 35-MeV ^{14}N beams delivered by the U-200P cyclotron. The γ rays emitted by Coulomb-excited states were detected by the EAGLE γ-ray spectrometer [18], working in coincidence with an array of Si PIN-diode detectors for scattered beam particles [19]. From the measured γ-ray intensities, a set of reduced matrix elements in ^{110}Cd was extracted using the semi-classical Coulomb-excitation least-squares fitting code GOSIA [20, 21].

The results obtained on the shapes of the two lowest-lying 0^+ states in ^{110}Cd were recently published in Physics Letters B [22]. The overall deformation of the 0_1^+ and 0_2^+ states was found to be equal within the experimental uncertainties ($\langle Q^2 \rangle$ values of 0.442(13) e^2b^2 and 0.61(18) e^2b^2, respectively), and the upper limit for the 0_3^+ state is not much higher ($\langle Q^2 \rangle \leq 0.9$ e^2b^2). The obtained triaxiality parameter of the ground state of ^{110}Cd, $\delta = 21.2(20)^\circ$, provides the first experimental evidence for its non-axial character. Moreover, the spectroscopic quadrupole moment of the 2_2^+ state and the $B(E2; 0_2^+ \rightarrow 2_1^+)$ value were determined for the first time, and a more stringent limit for the decay of the 0_3^+ state was obtained. The spectroscopic quadrupole moments of the 2_1^+ and 2_2^+ states were found to be nearly identical in magnitude ($Q_{sp}(2_1^+) = -0.49(11)$ eb and $Q_{sp}(2_2^+) = +0.45(8)$ eb) and their large values clearly rule out a spherical vibrational interpretation.

New theoretical calculations for ^{110}Cd were performed within the General Bohr Hamiltonian (GBH) model for two variants of the interaction: SLy4 and UNEDF0. Overall agreement between theoretical and experimental quadrupole deformation parameters was found; in particular, the non-axiality of the ground state is very well reproduced by the model, independently of the interaction used. Similar to earlier SCCM calculations [10, 11], the GBH model with the SLy4 interaction predicts that the multiple shape coexistence in ^{110}Cd will manifest in a different degree of triaxiality of the $0_{1,2,3}^+$ states. To verify this scenario, follow-up measurements are needed, aiming at experimental determination of non-axiality parameters for the 0_2^+ and 0_3^+ states in ^{110}Cd.

The presented study of ^{110}Cd is part of a broad international research programme aimed at determining the shapes of the low-excited 0^+ states in even-even cadmium nuclei, using a variety of complementary experimental techniques and the most advanced detection systems. Within this programme, Iwona Piętka is preparing a PhD thesis based on experimental data [23] collected with the state-of-the-art γ-ray spectrometer AGATA [24]. Her work is carried out at the Heavy Ion Laboratory, within the Doctoral School of Exact and Natural Sciences of the University of Warsaw, under the supervision of Dr. Katarzyna Wrzosek-Lipska and Dr hab. Leszek Próchniak.

Bibliography

[1] P.E. Garrett and J.L. Wood, J. Phys. G: Nucl. Phys. **37** (2010) 064028, J. Phys. G: Nucl. Phys. **37** (2010) 069701.
[2] P.E. Garrett *et al.*, Phys. Rev. C **86** (2012) 044304.
[3] M. Kadi *et al.*, Phys. Rev. C **68** (2003) 31306(R).
[4] P.E. Garrett *et al.*, Phys. Rev. C **75** (2007) 054310.
[5] D. Bandyopadhyay *et al.*, Phys. Rev. C **76** (2007) 054308.
[6] P.E. Garrett, K.L. Green, and J.L. Wood, Phys. Rev. C **78** (2008) 044308.
[7] J. C. Batchelder *et al.*, Phys. Rev. C **80** (2009) 054318.

[8] A.E. Stuchbery, S.K. Chamoli, and T. Kibedi, Phys. Rev. C **93** (2016) 31302(R).
[9] P.E. Garrett *et al.*, Phys. Scr. **93** (2018) 063001.
[10] P.E. Garrett *et al.*, Phys. Rev. Lett. **123** (2019) 142502.
[11] P.E. Garrett *et al.*, Phys. Rev. C **101** (2020) 044302.
[12] A. Arima and F. Iachello, Annals of Physics **99** (1976) 253.
[13] A. Leviatan, N. Gavrielov, J.E. Garcia-Ramos, and P. Van Isacker, Phys. Rev. C **98** (2018) 031302(R).
[14] N. Gavrielov, J.E. Garcia-Ramos, P. Van Isacker, and A. Leviatan, Phys. Rev. C **108** (2023) L031305.
[15] K. Nomura and J. Jolie, Phys. Rev. C **98** (2018) 024303.
[16] D. Cline, Annu. Rev. Nucl. Part. Sci. **36** (1986) 683.
[17] K. Kumar, Phys. Rev. Lett. **28** (1972) 249.
[18] J. Mierzejewski *et al.*, Nucl. Inst. and Meth. A **659** (2011) 84.
[19] M.B. Würkner *et al.*, Nucl. Phys. A **725** (2003) 3.
[20] T. Czosnyka, D. Cline, and C.Y. Wu, Bull. Am. Phys. Soc. 28 (1983) 745.
[21] T. Czosnyka, D. Cline, and C.Y. Wu, *Gosia User's Manual*, available from slcj.uw.edu.pl/gosia
[22] K. Wrzosek-Lipska *et al.*, Phys. Lett. B **875** (2026) 140315.
[23] I.Z. Piętka *et al.*, Acta Phys. Pol. B Proc. Suppl. **18** (2025) 2–A26.
[24] S. Akkoyun *et al.*, Nucl. Inst. and Meth. A **668** (2012) 26.

C.7 Coulomb excitation of ^{104}Pd with the EAGLE + SilCA-DSSD setup.

K. Hadyńska-Klęk[1], G. Szymanek[1,2], I. Piętka[1], S. Panasenko[1], M. Komorowska[1], M. Palacz[1], K. Wrzosek-Lipska[1], G. Jaworski[1], J. Grębosz[4], A. Goasduff[3], C. Hiver[1], G. Colucci[1], P. Dey[1], D. Duda[4], A. Fijałkowska[2], J. Iwanicki[1], K. Jakowinicz[2], M. Kowalczyk[1], J. Kowalska[1], A. Kundu[5], I. Kuti[6], A. Krzysiek[1,2], A. Malinowski[1,2], M. Matuszewski[1], J. Mierzejewski[1], P. Napiorkowski[1], W. Okliński[1,2], J. Samorajczyk-Pyśk[1], P. Sekrecka[1], G. Singh[7], S. Socha[2], K. Solak[2], A. Špaček[1], A. Stolarz[1], N. Toniolo[3].

1) Heavy Ion Laboratory, University of Warsaw, Warszawa, Poland
2) Institute of Experimental Physics, University of Warsaw, Warszawa, Poland
2) INFN, Laboratori Nazionali di Legnaro, Legnaro, Italy
4) Institute of Nuclear Physics Polish Academy of Sciences, Kraków, Poland
5) Saha Institute of Nuclear Physics, Kolkata, India
6) HUN-REN Institute for Nuclear Research, ATOMKI, Debrecen, Hungary
7) National Centre for Nuclear Research, Otwock, Poland

The versatile SilCA (Silicon Coulex Array) scattering chamber, was developed at the Heavy Ion Laboratory in Warsaw to accommodate various particle detectors, including a CD-like annular DSSD detector (Double-Sided Silicon Strip Detector) [1]. It was assembled at HIL Warsaw with the EAGLE array [2] in late 2023, after a successful experimental campaign performed at the IJC Lab in Orsay [3]. The experimental setup is presented in Fig. 1 (left panel). The array was commissioned in-beam in November 2024 with the EAGLE spectrometer using the digital readout of the CAEN V1725 modules with the XDAQ system [4]. In December 2025, the first physical experiment with this setup was performed to study the structure of the ^{104}Pd isotope using the Coulomb excitation technique. The γ rays emitted from the Coulomb-excited ^{104}Pd target nuclei were measured for 8 days in coincidence with the ^{32}S projectiles delivered from the Warsaw cyclotron at an energy of 88 MeV and an intensity of 0.35 pnA.

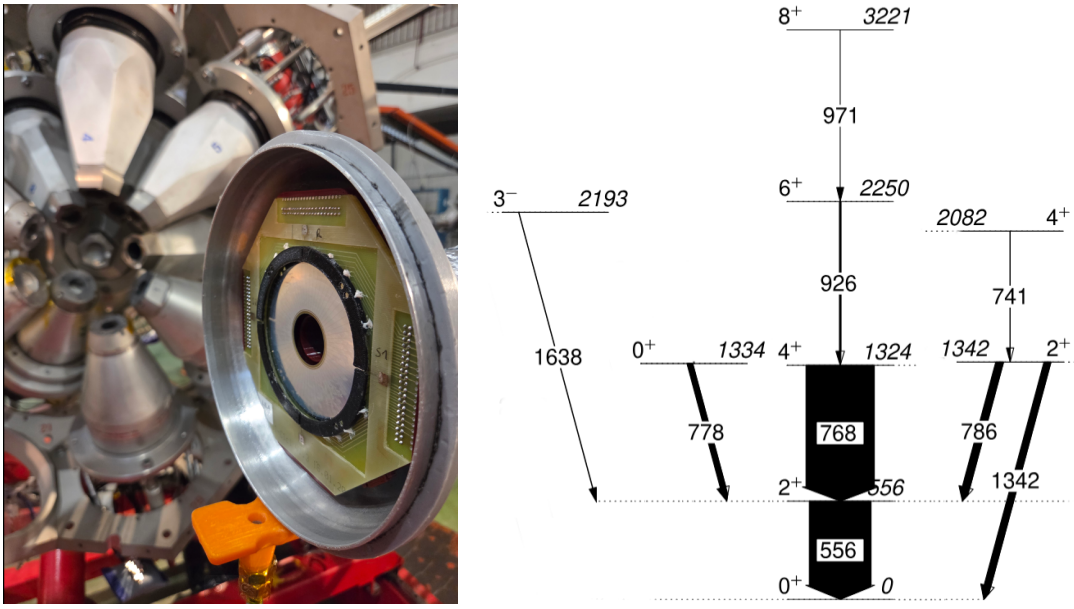


Figure 1: Left panel: The Warsaw DSSD detector in the SilCA scattering chamber, placed in the EAGLE frame. Righ panel: ^{104}Pd level scheme [6].

Similarly to the commissioning experiment in 2024, the signals from the DSSD array were collected using three Mesytec MPR16 preamplifiers – one for the 15 (out of 16) ring channels

(R), two for 29 (out of 32) channels of the radial sectors - the readout from the left and right sides of the DSSD array, denoted S1 and S2, 16 channels each. The signals were then transferred through differential-to-single-ended converters to CAEN V1725 digitizer modules, used for the final electronic data processing. In the present experiment, two digitizers were used for the readout of the 10 EAGLE HPGe detectors (8 from the GAMMAPOOL consortium loan) and three cards of the same type for the DSSD array. An additional card was included in the data stream for the signals from the 6 NEDA fast scintilator detectors [5] and the trigger signal.

The preliminary γ-ray spectrum collected in the first 4 days of data taking is presented in Fig. 2. The full data set is currently being processed to improve Doppler correction and background subtraction. At this stage of the analysis we can distinguish the lines coming from the excited 2_1^+ state at 555 keV, 2_2^+, 4_1^+, 0_2^+ states (a triplet of γ lines of energy of about 750-800 keV), as well as the 1342 and 1638 keV transitions deexciting the 2_2^+ and 3_1^- levels. Additionally, we observed hints of 741, 926 and 971 keV transitions depopulating the 4_2^+, 6_1^+ and 8_1^+ states, respectively (see the level scheme presented in the right panel of Fig. 1). Lines coming from ^{105,106,108}Pd contaminants of the target were also visible. As a reference point, we are using the data from the ^{104}Pd Coulomb excitation reaction with the ^{32}S beam, performed at HIL Warsaw in 2015 in similar conditions, published in Ref. [6], and the SilCA-DSSD commissioning experiment performed in late 2024, see Ref [4].

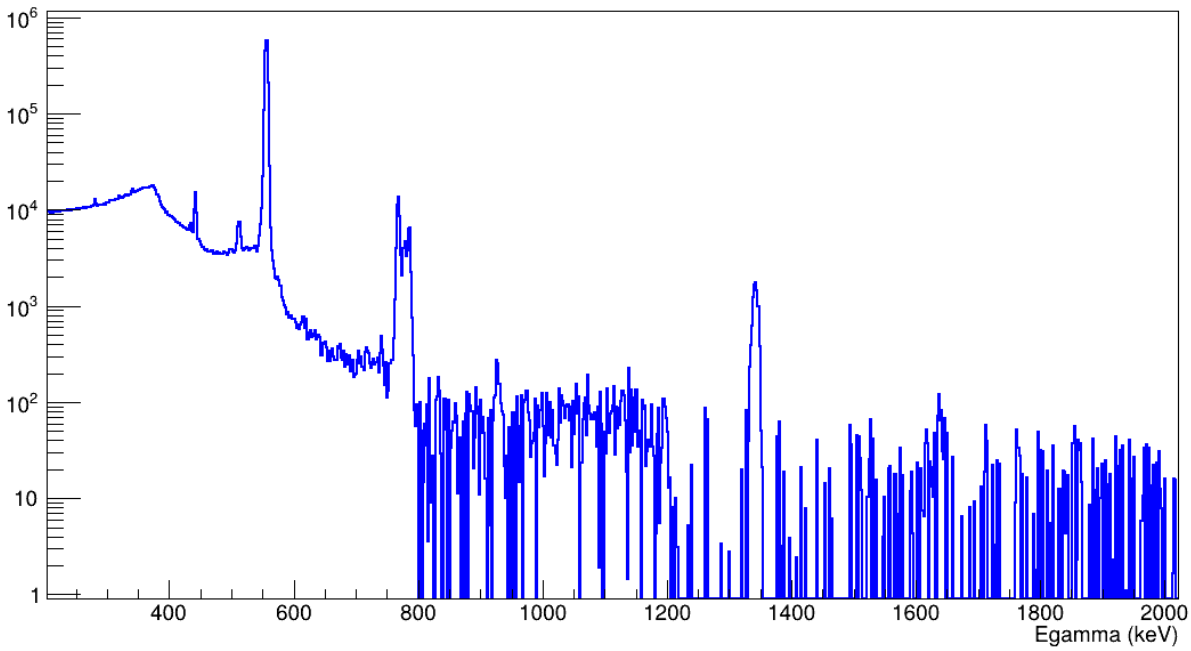


Figure 2: The γ-ray spectrum, background-subtracted, particle–γ coincidence-gated, and Doppler-corrected for the ^{104}Pd velocity.

The analysis of the present data set is the subject of the M.Sc. thesis of Grzegorz Szymanek.

The authors acknowledge the support of the GAMMAPOOL Consortium for providing the HPGe detectors with ACS. The work was supported by the National Science Centre (NCN), Poland (grant Nos. 2020/39/D/ST2/00466 and 2023/51/D/ST2/02816).

Bibliography

[1] K. Hadyńska-Klęk et al., *SilCA – Silicon Coulomb excitation Array at the Heavy Ion Laboratory*, HIL Annual Report 2022, p. 20-22, (2023)
[2] J. Mierzejewski et al. Nucl. Instr. Meth. A659, 84, (2011)
[3] K. Hadyńska-Klęk et al., *The experimental campaign with the Warsaw SilCA(DSSD) array at the IJC Lab, Orsay, France*, HIL Annual Report 2023, p. 65-67, (2024)

[4] K. Hadyńska-Klęk et al., *First report on the SilCA(DSSD) + EAGLE (+NEDA) in-beam commissioning at the HIL Warsaw: Coulomb excitation of* ^{104}*Pd*, HIL Annual Report 2024, p. 70-72, (2025)
[5] J. Valiente-Dobon et al., NIM A 927 (2019) 81 and G. Jaworski et al., Acta Phys. Pol. 50(3) (2019) 585
[6] S. Dutt et al., Acta Physica Polonica Series B 47(3):917 (2016)

C.8 Measurement of quasielastic barrier distributions of the ^{24}Mg + ^{92,94,95}Mo systems

E. Piasecki[1], Y. Cheng[2], G. Colucci[1], H.M. Jia[2], C.J. Lin[2], N.R. Ma[2], K. Rani[1], A. Trzcińska[1], M. Wolińska-Cichocka[1], P.W. Wen[2], L. Yang[2], H.Q. Zhang[2]

1) Heavy Ion Laboratory, University of Warsaw, Warszawa, Poland
2) China Institute of Atomic Energy, Xinzhen, Fangshan, Beijing, China

Barrier distributions extracted from quasielastic scattering provide a sensitive probe of the reaction dynamics in heavy-ion collisions at energies around the Coulomb barrier. Within the coupled-channels (CC) framework, couplings between the relative motion of the interacting nuclei and their intrinsic excitations lead to a distribution of barriers whose structure reflects both nuclear properties and reaction mechanisms. However, the role of additional processes remains not fully clarified, particularly the contribution of weak channels such as transfer reactions and non-collective excitations to the shape of the barrier distribution and to fusion dynamics.

Experimental quasielastic barrier distributions (D_{qe}) measured for some systems have been found to be significantly smoother (without any structure) than predicted by standard CC calculations. This phenomenon was observed for the ^{20}Ne + ^{92}Zr, ^{20}Ne + ^{61}Ni, ^{20}Ne + ^{94}Mo [1, 3, 5] systems, and it was suggested that dissipation could explain the nature of the observed effect. According to this hypothesis, in some systems the shape of the barrier distribution is significantly influenced by the dissipation of part of the kinetic energy into "heat," that is, excitation of a multitude of internal non-collective levels of the system. The coupling of these levels to the relative motion is much weaker than that of the collective ones. However, non-collective excitations are so numerous that they can still influence the barrier penetrability and thus the shape of the barrier distribution.

So far, the code CCRMT [4, 5] is the only existing tool capable of performing CC calculations taking into account the coupling to single-particle (s.p.) excitations, by combining the CC method with Random Matrix Theory. Calculations performed with CCRMT have successfully explained the shapes of barrier distributions for several studied systems [5]. In these studies, ^{20}Ne was chosen as projectile due to its strong deformation. Indeed, based on standard CC calculations, the strong deformation of ^{20}Ne is expected to dominate the structure of the barrier distribution, giving rise to strongly structured shapes for any system involving this projectile. This feature allows changes in the D_{qe} shape to be easily observed in comparison with the predictions and related to the structure of the target nuclei. Similarly, ^{24}Mg is a good candidate for D_{qe} studies, being strongly deformed and alpha-clustered, with six alpha particles compared to five in ^{20}Ne.

The experimental D_{qe} for the ^{24}Mg + ^{90,92}Zr systems was measured [4] and confirmed the influence of dissipation due to non-collective excitations. The structure of the D_{qe} was preserved for the ^{24}Mg + ^{90}Zr system, while it was smoothed out for the ^{24}Mg + ^{92}Zr system, where the high s.p. level density in ^{92}Zr enhances the dissipation. Qualitative agreement between the experimental D_{qe} and CCRMT predictions was observed, although the calculated distributions remain narrower than the experimental ones, and the cause of this quantitative difference is not yet clear. One possible explanation for this discrepancy may lie in the nature of the projectile, and examining the D_{qe} of other systems with ^{24}Mg as the projectile could help test this hypothesis.

Recently, quasielastic barrier distributions for ^{20}Ne + ^{92,94,95}Mo were measured at the Heavy Ion Laboratory (HIL) of Warsaw, showing good agreement between CCRMT predictions and the experimental D_{qe}, particularly for the ^{94}Mo isotope [5]. Based on these results, a similar level of agreement is expected when ^{24}Mg is used as the projectile.

As in the previously studied cases, standard CC calculations predict that the shapes of the barrier distributions for all three systems should be similar and mainly determined by the structure of the ^{24}Mg projectile. However, the influence of the larger number of s.p. excitations in the heavier Mo isotopes is expected to manifest itself through a progressive smoothing of the barrier

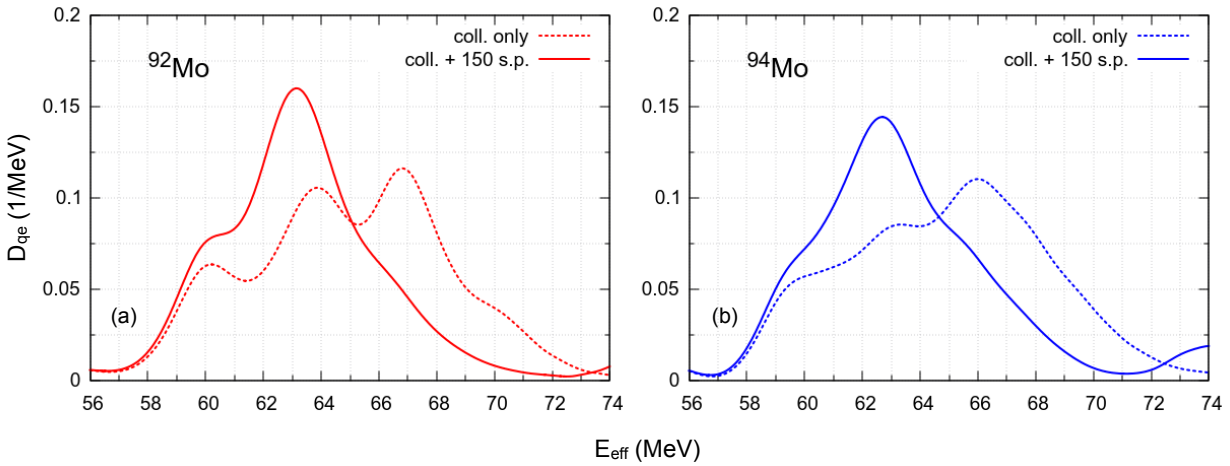


Figure 1: Theoretical barrier distributions for ^{24}Mg + ^{92}Mo (a) and ^{24}Mg + ^{94}Mo (b). The dashed lines show distributions calculated using the standard CC method where only collective excitations were taken into account. The solid lines describe the CCRTM calculations where the dissipation (non-collective excitations – 150 s.p.) was also included.

distributions. Theoretical predictions obtained with the CCRMT model for the ^{24}Mg + ^{92,94}Mo systems are shown in Fig. 1. The expected effect of dissipation on the D_{qe} shape is significant and becomes more pronounced for the ^{94}Mo target, where the s.p. level density is higher. In this case, the predicted barrier distribution becomes almost completely structureless.

In this framework, an experiment was performed at the China Institute of Atomic Energy (CIAE) to measure D_{qe} for the ^{24}Mg + ^{92,94,95}Mo systems. The HI-13 tandem accelerator provided a ^{24}Mg beam with an average current of 50 enA and energies in the range 71–93 MeV, in 1 MeV steps. Thin metallic self-supporting targets of ^{92}Mo (enriched to 99.93%), ^{94}Mo (98.97%), and ^{95}Mo (95.40%), each 100 μg/cm^2 thick, were used.

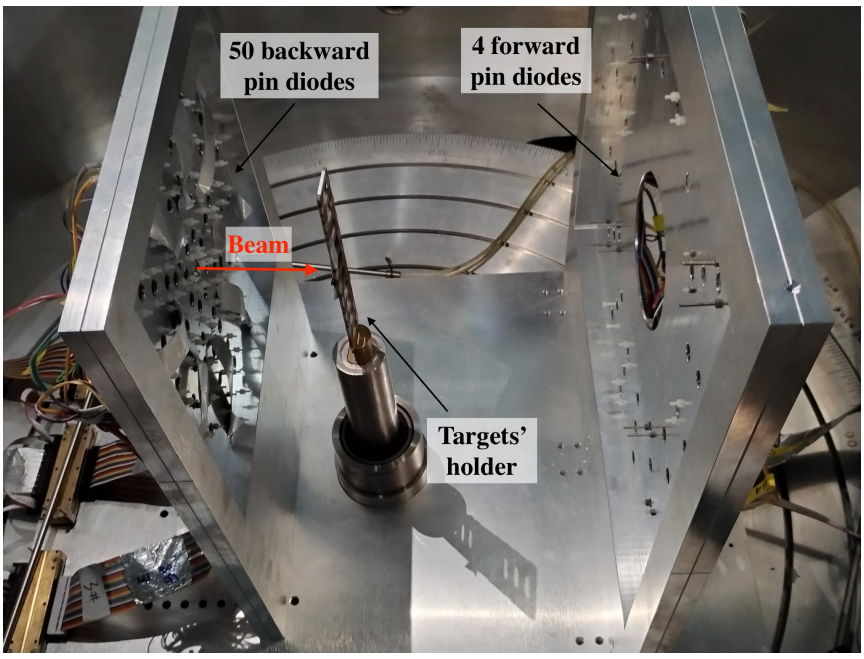


Figure 2: Experimental setup used for the measurement of quasielastic scattering for the ^{24}Mg + ^{92,94,95}Mo systems at CIAE.

The experimental setup (Fig. 2) consisted of 50 silicon detectors arranged in five concentric rings covering backward angles of 139°, 146°, 154°, 160°, and 170°, complemented by four additional detectors placed at a forward angle of 30°. This arrangement allowed a comprehensive measurement of quasielastic scattering over a wide angular range, ensuring precise determination of the barrier distribution. In particular, the backward detectors provided the energy and number of the backscattered projectiles, while the forward detectors were used for beam energy determination and normalization via Rutherford scattering. The analysis of the collected data is currently ongoing.

Bibliography

[1] E. Piasecki *et al.* Phys. Rev. C **80** (2009) 054613.
[2] A. Trzcińska *et al.* Phys. Rev. C **92** (2015) 034619.
[3] G. Colucci *et al.*, Acta Phys. Pol. **17**(2023) 3-A23.
[4] S. Yusa, K. Hagino and N. Rowley Phys. Rev. C **82** (2010) 024606.
[5] E. Piasecki *et al.* Phys. Rev. C **100** (2019) 014616.
[6] A. Trzcińska *et al.* Phys. Rev. C **102** (2020) 034617.
[7] T. Tamura Rev. Mod. Phys. **37** (1965) 679.
[8] N. Rowley, G. R. Satchler and P. H. Stelson Phys. Lett. B **254** (1991) 25.
[9] K. Hagino, N. Rowley, and A. T. Kruppa, Comp. Phys. Comm. **123** (1999) 143.

C.9 Dissipation in the ^{20}Ne + ^{92,94,95}Mo systems: the role of transfer channels

G. Colucci[1], A. Trzcińska[1], E. Piasecki[1], M. Wolińska-Cichocka[1], A. Barbon[2,3], G. D'Agata[2], E. De Filippo[2], Z. K. Czerski[4], R. Dubey[4], E. Geraci[2,3], K. Hadyńska-Klęk[1], G. Jaworski[1], M. Kisieliński[1], P. Koczoń[5], M. Kondzielska[6], M. Kowalczyk[1], Y. Leifels[5], B. Lommel[5], M. Matuszewski[1], N. S. Martorana[2], E. V. Pagano[7], L. Quattrocchi[2], P. Russotto[7], J. Samorajczyk-Pyśk[1], A. Stolarz[1], G. Tiurin[8], W. H. Trzaska[8], A. Tucholski[1], B. Zalewski[1]

1) Heavy Ion Laboratory, University of Warsaw, Warszawa, Poland
2) INFN Sezione di Catania, Catania, Italy
3) Department of Physics and Astronomy, University of Catania, Catania, Italy
4) Institute of Physics, University of Szczecin, Szczecin, Poland
5) GSI Helmholtz Center for Heavy Ion Research, Darmstadt, Germany
6) Faculty of Physics, University of Warsaw, Warszawa, Poland
7) INFN Laboratori Nazionali del Sud, Catania, Italy
8) Department of Physics, University of Jyväskylä, Finland

Barrier distributions extracted from quasielastic scattering are a sensitive probe of heavy-ion reaction dynamics near the Coulomb barrier. In several cases, the experimental quasielastic barrier distributions (D_{qe}) appear significantly smoother than predicted by standard coupled-channels (CC) calculations [1–4]. This behaviour has been attributed to dissipation of part of the kinetic energy into numerous non-collective excitations, expected to be enhanced in nuclei with a high density of single-particle (s.p.) levels.

A similar situation was observed for the ^{20}Ne + ^{92,94,95}Mo systems [5]. The comparative analysis of the D_{qe} indicates that the ^{92}Mo target, characterized by a relatively low s.p. level density, exhibits a well-defined distribution consistent with CC model predictions. In contrast, the distributions measured for ^{94}Mo and ^{95}Mo are much smoother and nearly structureless, deviating from the expectations of the standard CC approach. Calculations including couplings to non-collective excitations reproduce well the measured distributions for the ^{20}Ne + ^{92,94}Mo systems, while for ^{95}Mo the agreement remains less satisfactory than for the lighter isotopes. Interestingly, the experimental distribution for ^{94}Mo is even broader and smoother than that of ^{95}Mo, despite the latter having a higher level density.

Besides non-collective excitations, dissipation in near-barrier reactions may also originate from nucleon transfer processes. Couplings to transfer channels are known to play an important role in heavy-ion reactions near and below the Coulomb barrier, although their quantitative influence on fusion dynamics is still under discussion [6–9]. Recent developments in the CCFULL-sc code have improved the treatment of transfer couplings in calculations of fusion and quasielastic backscattering [10, 11] by introducing coupling strengths that depend on both the type of transferred particle and the experimental Q-value distributions. The results show that the transfer channels contributing to the smoothing of the D_{qe} may vary with the projectile energy, highlighting the importance of including an explicit energy dependence of the transfer couplings in theoretical descriptions of the reaction dynamics. Within this context, measurements of transfer cross sections provide a direct method to investigate the role of transfer-induced dissipation. By comparing transfer channels for neighbouring isotopes and studying their evolution with the projectile energy, it is possible to evaluate whether these couplings may influence the barrier distributions.

Following these considerations, an experiment was performed at the Heavy Ion Laboratory (HIL) of the University of Warsaw to investigate transfer reactions in the ^{20}Ne + ^{92,94,95}Mo systems. A ^{20}Ne beam with an average intensity of about 25 enA was accelerated by the U200-P cyclotron to laboratory energies of 73 and 71 MeV, while lower energies of 68 and 66 MeV were obtained using thin degraders made of natural Ni and Au foils. The chosen energies cover the region around the Coulomb barrier, located at approximately 68 MeV in the laboratory frame, and allow the evolution of transfer channels to be studied as a function of the projectile kinetic

energy.

The measurements were carried out in the ICARE scattering chamber. Reaction products were detected at a backward angle of 142° using a Microchannel Plate (MCP) detector combined with an array of thirteen silicon detectors providing measurements of the residual energy and time-of-flight (ToF). Since transfer angular distributions at near-barrier energies are nearly flat at backward angles, measurements at this single angle allow the relative contributions of the different transfer channels to be evaluated. Charge identification was obtained using an E-ΔE gas telescope placed at the same angle as the MCP and silicon detectors. The combined analysis of the E-ToF and E-ΔE information provides the identification of the mass (A) and charge (Z) of the detected particles, allowing an unambiguous assignment of the reaction channels. Additional silicon detectors placed at forward angles were used for precise monitoring of the beam energy.

The resulting E–ToF matrices for the three systems at the four energies investigated are shown in Fig. 1 and Fig. 2. At the highest beam energy of 73 MeV the dominant transfer channels for all three systems correspond to reaction products with masses A = 19 and A = 16, associated with one-proton and one-alpha stripping processes. In the ^{20}Ne + ^{95}Mo system an additional channel corresponding to A = 21, attributed to one-neutron pickup, is also observed. At 71 MeV, the channel leading to A = 18 is more clearly visible for all molybdenum isotopes, indicating an increasing contribution from other transfer processes as the reaction approaches the Coulomb barrier. More pronounced differences among the systems appear at the lower energies of 68 and 66 MeV. For the ^{20}Ne + ^{92}Mo system the dominant transfer channels remain essentially unchanged over the investigated energy range. In contrast, the reactions involving the heavier isotopes exhibit additional neutron pickup channels at lower energies. At 68 MeV reaction products corresponding to A = 21 and A = 22 appear in the ^{20}Ne + ^{94}Mo and ^{20}Ne + ^{95}Mo systems, respectively, indicating the presence of one- and two-neutron pickup processes. At the lowest beam energy of 66 MeV the A = 22 channel also becomes visible for the ^{94}Mo target, while the set of transfer channels observed for ^{95}Mo remains essentially unchanged. These observations indicate a different evolution of the transfer dynamics for the three isotopes as the projectile energy approaches the Coulomb barrier.

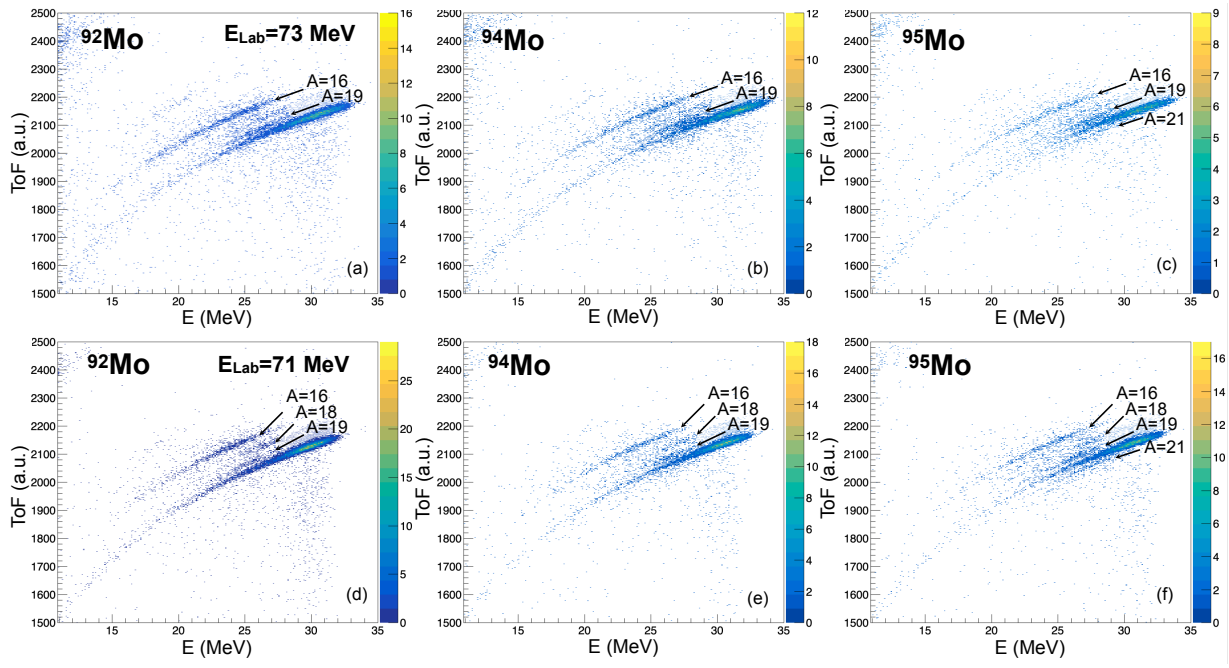


Figure 1: Transfer product identification in mass for the ^{20}Ne + ^{92,94,95}Mo systems at beam energies of 73 MeV (upper panels) and 71 MeV (lower panels).

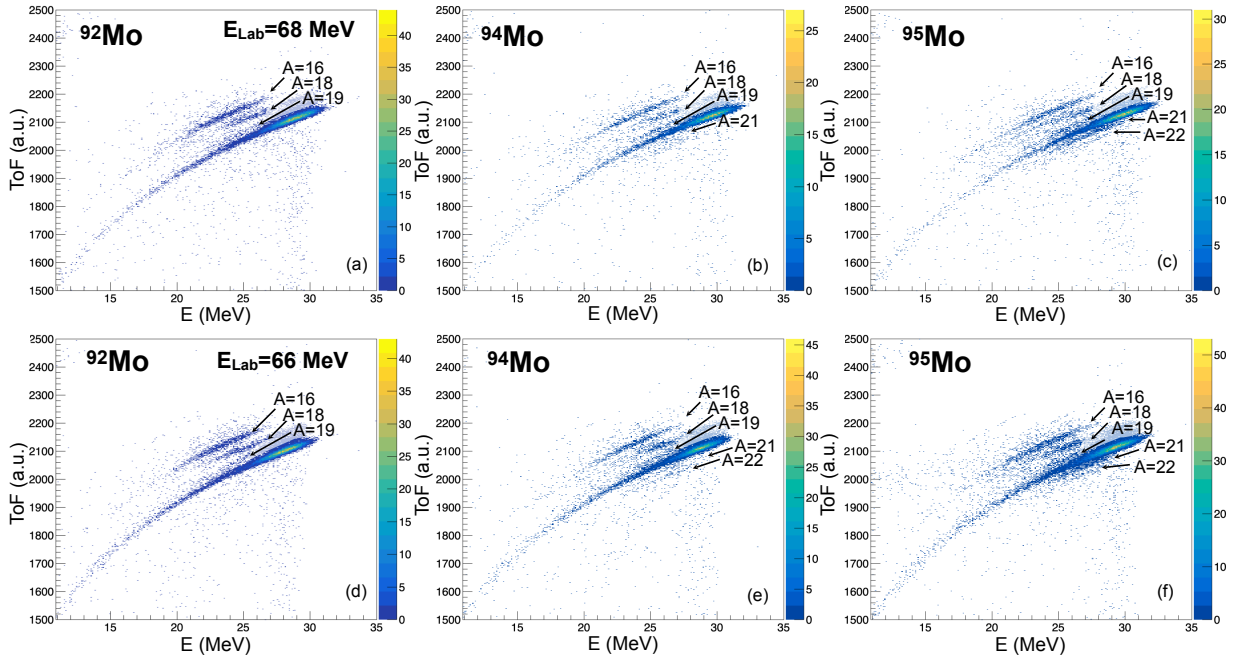


Figure 2: Transfer product identification in mass for the ^{20}Ne + ^{92,94,95}Mo systems at beam energies of 68 MeV (upper panels) and 66 MeV (lower panels).

Overall, the measurements show that the transfer pattern for the ^{92}Mo target remains relatively stable over the studied energy range, whereas the reactions involving ^{94}Mo and ^{95}Mo display the onset of additional neutron pickup channels at lower energies. The analysis of the data is currently ongoing. In particular, the extraction of the Q-value distributions for the different transfer channels will allow the contribution of each process to be quantified and will provide insight into the role of transfer-induced dissipation in shaping the quasielastic barrier distributions.

Bibliography

[1] E. Piasecki *et al.* Phys. Rev. C **80** (2009) 054613.
[2] E. Piasecki *et al.*Phys. Rev. C **85** (2012) 054608.
[3] A. Trzcińska *et al.* Phys. Rev. C **92** (2015) 034619.
[4] A. Trzcińska *et al.* Phys. Rev. C **102** (2020) 034617.
[5] G. Colucci *et al.*, Acta Phys. Pol. **17**(2023) 3-A23.
[6] A. Stefanini *et al.*, Phys. Lett. B **728**, (2014) 639.
[7] G. Scamps and K. Hagino, Phys. Rev. C **92**, (2015) 054614.
[8] T. Tanaka *et al.*, Phys. Rev. Lett. **124**, (2020) 052502.
[9] K. Cook *et al.*, Nat. Commun. **49**, (2023) 7988.
[10] G. Colucci *et al.* Phys. Rev. C **109** (2024) 064625.
[11] G. Colucci *et al.* European Physical Journal Web of Conferences **306** (2024) 01018.

C.10 First results from the T-INSIDE experiment

N.S. Martorana[1], G. Cardella[1], E. De Filippo[1], E. Geraci[1,2,3], C. Guazzoni[4], P. Russotto[5], L. Acosta[6], A. Barbon[1,2], A. Castoldi[4], G. Colucci[7], G. D'Agata[1,2], B. Gnoffo[1,2], J.G. Gonzàlez Linares[6], T. Kurtukian-Nieto[6], F. La Via[8], C. Maiolino[5], E.V. Pagano[5], S. Pirrone[1], G. Politi[1,2], M. Pozzi[4], K. Rani[7], F. Risitano[1,3,9], F. Rizzo[2,5], M. Trimarchi[1,9], A. Trzcińska[7], S. Tudisco[5], M. Wolińska-Cichocka[7], C. Zagami[2,3,5]

1) INFN Sezione di Catania, Catania, Italy
2) Department of Physics and Astronomy, University of Catania, Catania, Italy
3) The Sicilian Center of Nuclear Physics and Physics of Matter
4) DEIB Politecnico di Milano and INFN Sezione di Milano, Milano, Italy
5) INFN Laboratori Nazionali del Sud, Catania, Italy
6) Instituto de Estructura de la Materia, CSIC, Spain
7) Heavy Ion Laboratory, University of Warsaw, Warszawa, Poland
8) Institute for Microelectronics and Microsystems (IMM), National Research Council (CNR), Catania, Italy
9) Dipartimento MIFT, Università di Messina, Italy

Abstract

This contribution presents preliminary results from the T-INSIDE (timing investigation in SiC detectors) experiment, aimed at evaluating the fast timing capabilities of Silicon Carbide (SiC) detectors, combined with dedicated fast electronics i.e.: "front-end". The experiment was carried out at the Heavy Ion Laboratory using a ^{12}C beam, accelerated to 73 MeV, and a natural carbon target. Segmented SiC detectors (2×2 pixels, 100 μm thick) coupled with fast front-end electronics were tested through a kinematic coincidence technique. A timing resolution of about 124 ps per pixel was obtained for an energy loss of 43 MeV on a single pixel, demonstrating the potential of SiC detectors for time-of-flight applications.

Introduction

Precise time-of-flight (ToF) measurements can play an important role in the identification of Radioactive Ion Beams (RIBs), which enable studies of nuclear structure, reaction dynamics, nuclear astrophysics and applications in medical physics [1]. The in-flight production method, one of the techniques widely used to produce RIBs, typically generates a cocktail beam composed of different ion species, requiring an event-by-event identification. The ΔE-ToF technique is widely used for this purpose, as it allows the offline selection of the ion of interest for the specific study. However, existing systems show limitations in terms of timing resolution and sustainable rate. As a relevant example, at the FRIBS facility of INFN-LNS, systems based on MCP and DSSSD detectors achieved timing resolutions of 300-400 ps and were limited to rates of about 200 kHz for medium mass ions as carbon, with significantly worse performance, after several days of irradiation with heavier ions such as Ni, at ≈ 30 kHz [1]. Several experiments were nevertheless successfully performed with such systems, including studies of nuclear clustering and pygmy dipole resonance [1, 2].
The development of new facilities, such as FraISe@INFN-LNS, capable of delivering RIBs with intensities up to 10^7 pps, introduces new requirements for beam diagnostics and tagging systems [1, 2, 4]. In particular, detectors must combine radiation hardness, excellent timing resolution and spatial granularity in order to extract the beam profile, and the possibility to determine the isotopic composition of the cocktail beam using the ΔE-ToF method. Moreover, fast timing capability opens the way to allow the determination of the RIB energy via ToF measurements with an energy resolution of about 0.5%, representing a significant improvement compared to the 2-3% energy resolution, typical of the in-flight method. Silicon Carbide (SiC) detectors represent a promising solution for the development of diagnostic and tagging systems, due to their radiation hardness,

fast timing response, and good energy resolution. Within this technological framework, dedicated R&D activities have been carried out over the past 8 years, focusing on the development and characterization of SiC detectors for the identification of RIBs. Details about this characterization may also be found in Ref. [4]. In this context, the T-INSIDE experiment was performed to evaluate the timing capability of segmented SiC detectors, coupled with a custom fast frontend electronics [3], using a kinematic coincidence technique.

Experimental setup and preliminary first results

The experiment was performed using a ^{12}C beam at an incident energy of 73 MeV impinging on a natural carbon target. Two SiC detectors, segmented into 2×2 pixels (1 cm^2 area, 100 μm thick), were installed inside the ICARE chamber. The measurement exploits the kinematic coincidence between target-like and projectile-like fragments, produced in elastic and inelastic scattering processes. This configuration allows the simultaneous detection of correlated reaction products and the extraction of timing information from the time difference between the signals of the two SiC pixels in coincidence events. The detectors were coupled with fast front-end electronics and the output waveforms were digitized using a CAEN DT5742 digitizer, at 1GS/s sampling frequency. The timing information of each SiC pixel was evaluated using a crossing time at 35% of the waveform signal amplitude. Figure 1 shows a picture of the SiC detectors, coupled to the fast front-end electronics, mounted inside the ICARE chamber. The arrow indicates the position of the target support, shown in the upper part of the figure.

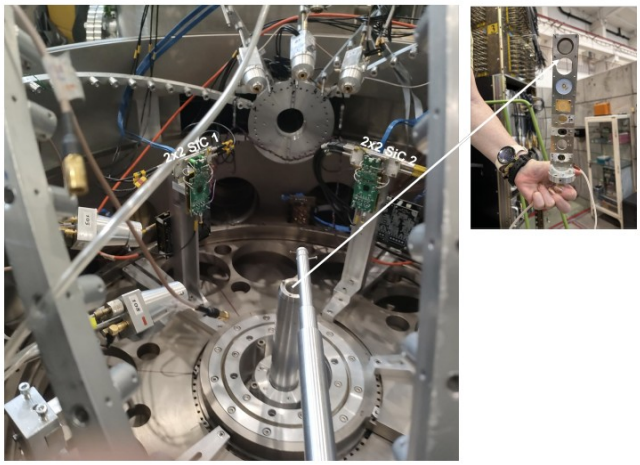


Figure 1: Experimental setup of the T-INSIDE measurement.

During the experiment detectors were placed at different angles in order to probe the timing performance as a function of fragments energy. The analysis reported here focuses on the configuration in which both detectors were placed at $\theta \approx 43°$, corresponding to an energy loss of about 34 MeV in each pixel. In this configuration, the coincidence events correspond to the detection of $^{12}C_{gs}$ in one pixel and $^{12}C^*$ (4.44 MeV) in the other. The time difference between signals in coincidence events was evaluated and fitted with a Gaussian function. Figure 2 shows the results obtained.

A value of $\sigma_{tot} = 175$ ps was obtained with the Gaussian fit. Assuming equal and independent contributions, the single-pixel resolution is given by $\sigma_{det} = \sigma_{tot}/\sqrt{2}$, resulting in about 124 ps at an energy loss of 34 MeV for each SiC pixel. The results obtained are very promising, especially considering that the analysis is still preliminary. In addition, data need to be corrected for systematic contributions due to energy spread and time-of-flight path difference.

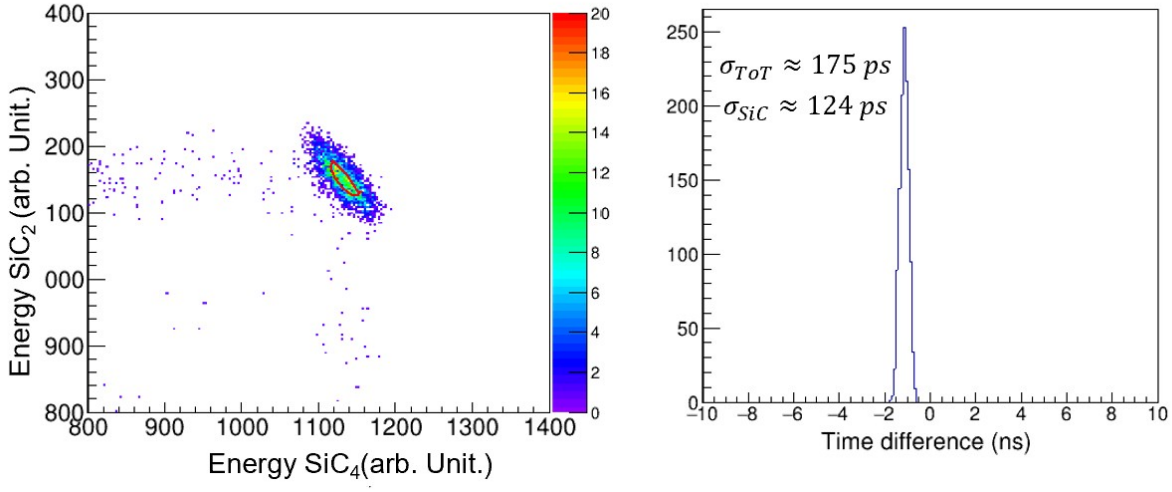


Figure 2: (left) Kinematic plot of coincidence events. (right) Time difference distribution obtained within the cut shown as a red ellipse in the right panel.

Conclusions

The T-INSIDE experiment demonstrates that SiC detectors coupled with fast front-end electronics can achieve timing resolutions well below 200 ps. These results support the use of SiC detector arrays in next-generation RIB facilities, where precise ToF measurements are required for beam identification. More accurate analyses are ongoing and will focus on detector calibration and correction of systematic effects.

Acknowledgments

This work was partially funded by the European Union (NextGeneration EU) through MUR-PNRR project SAMOTHRACE (ECS00000022). The authors are grateful to the technical staff of the HIL for the production of the carbon beam. This project has received funding from the European Union's Horizon Europe Research and Innovation programme under Grant Agreement No 101057511 (EURO-LABS) and Spanish MICIU PID2023-147569NB-C21. This work was performed thanks to the efforts of the CHIRONE collaboration.

Bibliography

[1] N.S. Martorana et al., Frontiers in Physics **10** (2022) and references therein.
[2] P. Russotto et al., Journal of Physics: Conference Series **1014** (2018) 012016 and references therein.
[3] A. Castoldi et al., IEEE Transactions on Nuclear Science **70** (2023) 1431.
[4] N.S. Martorana et al., Nucl. Instrum. Methods A **1086** (2026) 171356 and references therein.

C.11 Collective excitations of neutron-deficient Hg isotopes within the framework of the mean-field theory

L. Próchniak
Heavy Ion Laboratory, University of Warsaw, Warszawa, Poland

There are around 40 isotopes of mercury with half-lives greater than 1 ms, including 7 stable ones. This long chain of isotopes offers a good possibility to study the evolution of nuclear properties following a change in the neutron number. More experimental data are available for the neutron-deficient isotopes, while for the neutron-rich ones, even with longer half-lives, data are scarcer, mainly due to problems with the production of these isotopes. For several years there has been significant interest, both experimental and theoretical, in the region of the $^{182\text{-}186}$Hg isotopes. One reason for this is the interesting phenomenon of odd-even staggering of the mean charge radius. Moreover, these nuclei are close to the ^{186}Pb isotope for which a multiple shape coexistence was reported [1]. Hence, there were efforts to check whether a similar phenomenon could be found in the Hg isotopes; see, e.g., [2].

In this report, I present theoretical results concerning some collective properties of even-even Hg isotopes with masses $A = 178-192$. The main theoretical tool used was the General Bohr Hamiltonian (GBH) with mass parameters (inertial functions) and a potential energy obtained from the mean-field theory based on the UDF2 energy density functional. This functional, proposed originally in [3] and modified in [4], differs from the previous ones, UNEDF0 and UNEDF1, in the treatment of the pairing interaction. First, the Lipkin-Nogami method is not used. Second, the strength of the pairing interaction is not globally fixed but can be chosen for a given region of interest. On the other hand, additional data on single-particle levels were used to fit the UDF2 parameters. In the present calculations, the pairing interaction was modelled by the so-called mixed δ interaction (see e.g. [4]) with $V_\mathrm{n} = -260$ MeV and $V_\mathrm{p} = -270$ MeV.

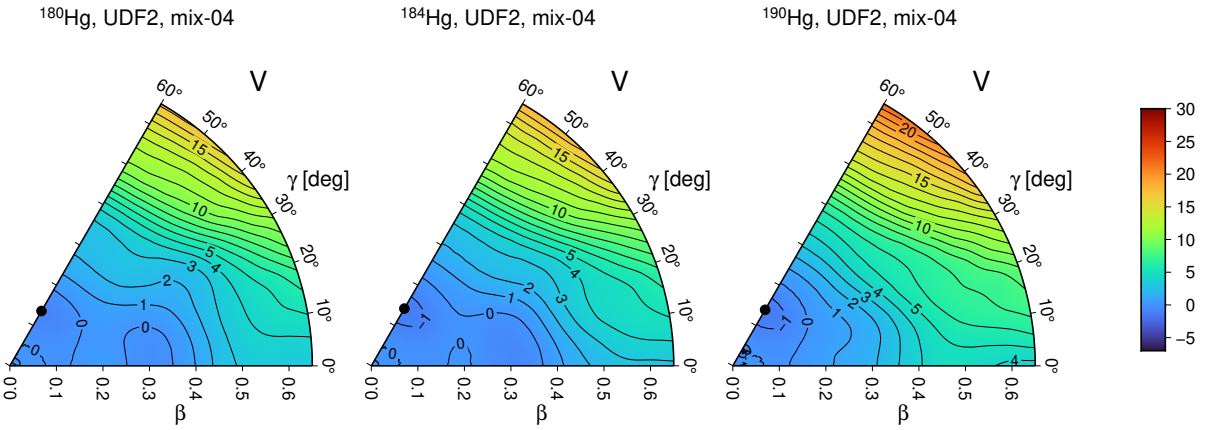


Figure 1: Theoretical potential energy relative to a spherical shape calculated with the UDF2 functional.

Mean-field calculations with constraints on the mass quadrupole moments were performed for 155 points in the sextant $0 \leq \beta \leq 0.7$, $0 \leq \gamma \leq 60$ deg. The results of the ADTHFB theory were used to calculate mass parameters and potential energy. Collective energy levels and B(E2) transition probabilities were then obtained from the GBH model [5]. In addition, I present results for the charge quadrupole invariant $[[QQ]^2Q]^0 \sim \beta^3 \cos 3\delta$ (for a discussion cf. [6]) calculated for the

lowest three 0^+ states, which give some information on the nonaxiality of a nucleus in a given state.

Plots of the potential energy for ^{180,184,190}Hg isotopes are shown in Fig. 1. The potential energy for all isotopes has a shallow minimum for a rather small oblate deformation and, more importantly, a very weak dependence on the γ nonaxiality variable. As can be seen in Fig. 2, energies of the ground state band and $2^+_{2,3}$, $0^+_{2,3}$ levels show a good agreement with experiment. It is worth noting that this remarkably good agreement was obtained within the model without any parameters fitted to spectroscopic data. In the case of E2 electromagnetic transitions, the overall agreement is reasonable but, as can be seen in Fig. 3, there are significant discrepancies, e.g., for the $2^+_1 \to 0^+_1$ transition for ^{182,184}Hg.

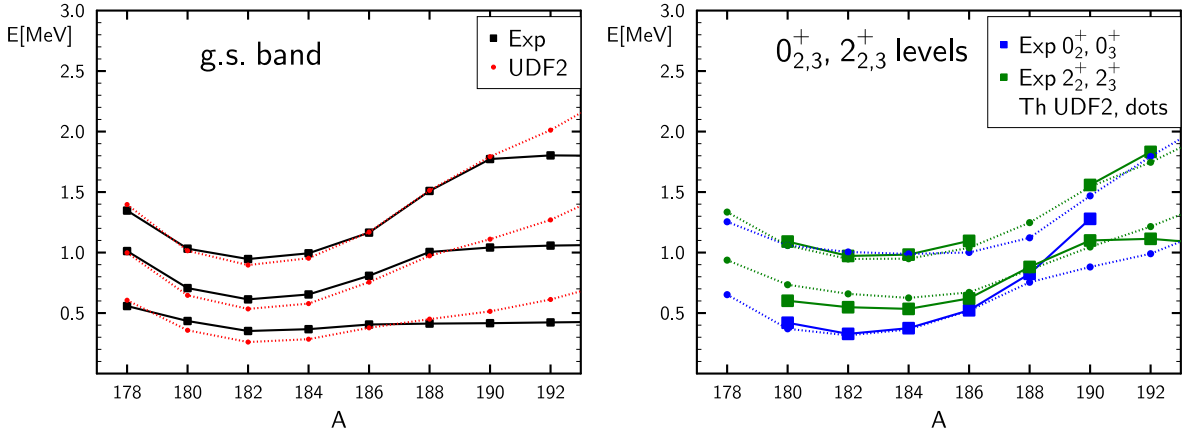


Figure 2: Selected energy levels in $^{178\text{-}192}$Hg. Experimental data from [7].

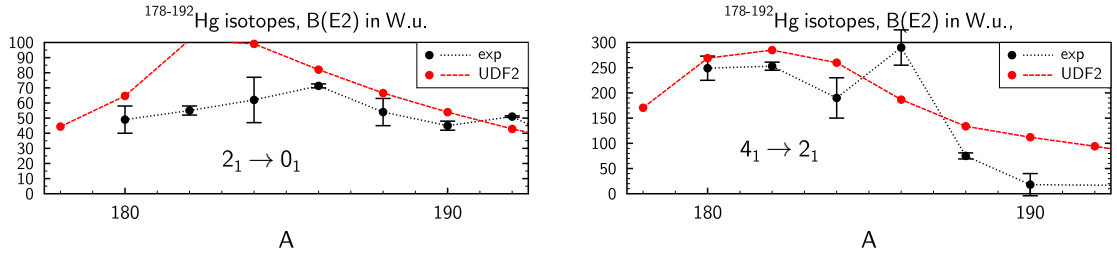


Figure 3: B(E2) probabilities for the $2^+_1 \to 0^+_1$ and $4^+_1 \to 2^+_1$ transitions in $^{178\text{-}192}$Hg.

To show the theoretical prediction of nonaxiality, I use the quantity $\langle \cos 3\delta \rangle$, which is calculated from the charge quadrupole invariants as

$$\langle \cos 3\delta \rangle = \langle [[QQ]^2 Q]^0 \rangle / \langle [QQ]^0 \rangle^{3/2} \tag{1}$$

Then, $\langle \delta \rangle$ is estimated as $\mathrm{acos}\,(\langle \cos 3\delta \rangle)/3$. Values of these quantities are plotted in Fig. 4. The tentative conclusion from the present calculations is that differences in the average nonaxiality for the lowest 0^+ states across all the considered isotopes are much too small to expect any features of multiple shape coexistence.

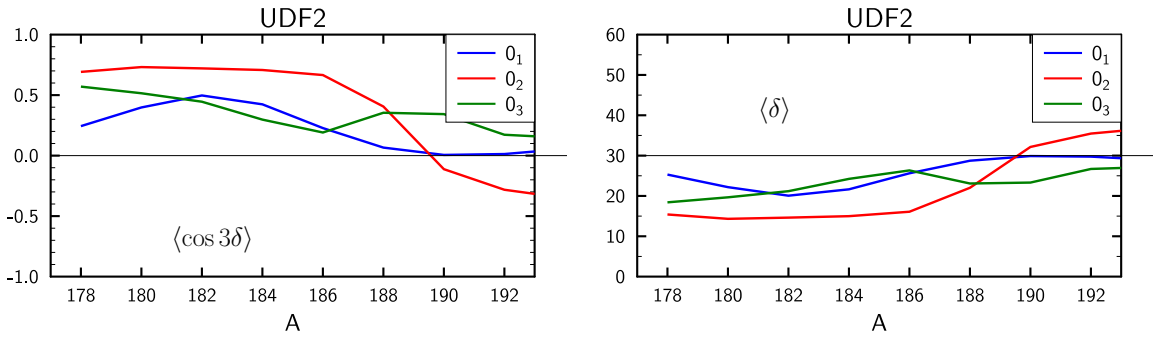


Figure 4: Theoretical values of $\langle\cos 3\delta\rangle$ and $\langle\delta\rangle$ for the three lowest 0^+ levels in $^{178\text{-}192}$Hg.

Bibliography

[1] J. Ojala *et al*, Comm. Phys. **5** (2022) 213; Andreyev *et al*, Nature, **405** (2000) 430
[2] N. Bree *et al*, Phys. Rev. Lett. **112** (2014) 162701 (2014); K. Wrzosek-Lipska *et al*, Eur. Phys. J. A **55** (2019) 130; M. Stryjczyk *et al*, Phys. Rev. C **108** (2023) 014308 (2023)
[3] M. Kortelainen *et al*, Phys. Rev. C **89** (2014) 054314
[4] M. Chen, T. Li, J. Dobaczewski and W. Nazarewicz, Phys. Rev. C **103**, 034303 (2021)
[5] L. Próchniak, S.G. Rohoziński, J. Phys. G: Nucl. Phys. **36** (2009) 123101
[6] J. Srebrny *et al*, Nucl. Phys. A **766** (2006) 25
[7] Data from the NNDC database, revision as of September 2025.

C.12 Coulomb excitation of ^{90}Zr

P. Dey[1,2], P. J. Napiorkowski[1], A. Kundu[3], R. Palit[2], U. Garg[4], M. Kumar Raju[5], Vishal Malik[2], V. Nanal[2], S. Pal[2], D. Sindhu[2], S. Thorat[2]

1) Heavy Ion Laboratory, University of Warsaw, Warszawa, Poland
2) Tata Institute of Fundamental Research, Mumbai, India
3) Saha Institute of Nuclear Physics, Kolkata, India
4) Department of Physics and Astronomy, University of Notre Dame, Notre Dame, USA
5) GITAM School of Science, GITAM University, Visakhapatnam, India

Octupole collectivity in atomic nuclei, less frequent than the axially symmetric quadrupole deformation, is a structural feature associated with an reflection-asymmetric shapes [1]. Signatures of this type of collectivity in even-even nuclei are experimentally observed low-lying 3_1^- state and a large $B(E3)$ strength of the corresponding $E3$ transition to the ground state. In addition to nuclei with the "octupole-magic numbers" $Z, N = 34, 56, 88, 134$, several spherical nuclei in the vicinity of a shell-closures show enhanced $B(E3)$ strength [2], originating primarily from octupole oscillations. Recent precision measurement of a large $B(E3)$ in one of the Zr-isotopes [3] encourages the study of its most spherical isotope, ^{90}Zr ($N = 50$) to benchmark the correlation between the shell-closing effect and octupole asymmetry. However, the reported $B(E3)$ values for ^{90}Zr from different probe-determinations exhibit a nearly four-fold spread [2, 4], implying the need for a fresh measurement using a model-independent technique such as Coulomb excitation.

The excited states of ^{90}Zr were populated through the Coulomb excitation technique at TIFR, Mumbai using an 88-MeV ^{32}S beam provided by the TIFR-BARC Pelletron Linac Facility. An enriched, self-supporting ^{90}Zr foil of 1.23 mg/cm^2 thickness was used as the target. The selected beam energy satisfied the criterion for safe Coulomb excitation [5] with negligible nuclear interaction. An annular double sided Si-detector (ADSSD), aligned with the beam axis, was placed upstream inside the target chamber at a distance of 2.6 cm from the target position. The ADSSD is an S3 type detector manufactured by Micron Semiconductor Ltd. which is segmented into 24 rings and 32 sectors on either side. For the detection of γ rays emitted from the de-excited ^{32}S and/or ^{90}Zr nuclei, 16 Compton-suppressed clover HPGe detectors from the Indian National Gamma Array (INGA) at TIFR, Mumbai were used [6]. At the data acquisition stage, a synchronization method was implemented between two crates housing 12-bit, 100-MHz digitizer modules (for clover detectors) and 14-bit, 100-MHz modules (for ADSSD), to which the electronic signals from the corresponding detectors were fed. The digitized events were sorted into one- and two-fold energy and time histograms using a suitably modified version of the "MultipARameter time-stamp-based COincidence Search program" (MARCOS) code [7], and were further analyzed using RADWARE and ROOT analysis packages.

Since the γ rays were emitted from the decay of excited states in the projectile and target nuclei in their in-flight motion, Doppler correction of γ rays was needed. The velocities of scattered ^{32}S and recoiling ^{90}Zr extracted from the kinematical correlation were high enough to create sizable Doppler broadening for the observed γ ray transitions from both nuclei, which was then corrected for beam energy loss through half the target thickness. The γ ray spectra were further cleaned using three-fold conditions that include (1) energy of the backscattered projectile-like ^{32}S ions, (2) time-tagging information between the clover HPGe detectors and the ADSSD rings, and (3) time-tagging information between ADSSD rings and sectors. Proper subtraction of random coincidence events originating from the background of any of the aforementioned conditions was incorporated. The final spectra used in the subsequent analysis were generated by obtaining true events C_f through the relation,

$$C_f = C_{p1,p2,p3} - C_{p1,p2,b3} - C_{p1,b2,p3} + C_{p1,b2,b3} - C_{b1,p2,p3} + C_{b1,p2,b3} + C_{b1,b2,p3} - C_{b1,b2,b3} \quad (1)$$

where $C_{p1,p2,p3}$ denotes events with "peaks" of all three conditions, while $C_{p1,p2,b3}$ denotes events with "peaks" of conditions 1 and 2, "background" of condition 3, and so on.

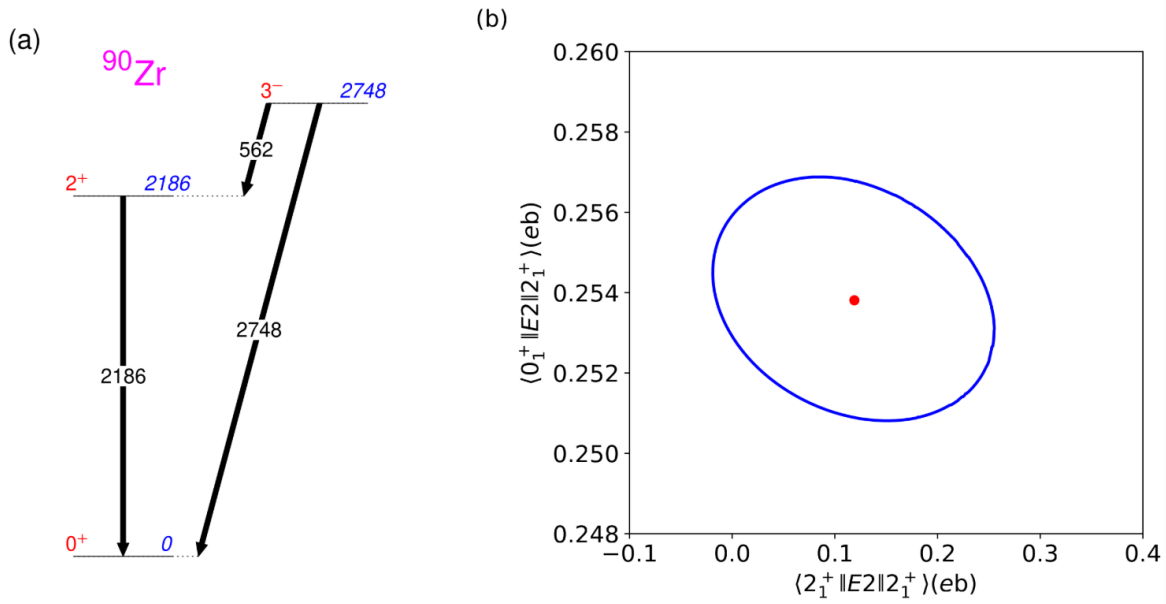


Figure 1: (a) Partial level scheme of ^{90}Zr showing states and transitions relevant to this work. (b) Contour of $\chi^2_{\min} + 1$ (blue line) around the $\chi^2_{\min}$ (red point) in the plane of the $\langle 0^+_1 \| E2 \| 2^+_1 \rangle$ and $\langle 2^+_1 \| E2 \| 2^+_1 \rangle$ matrix elements of ^{90}Zr from the GOSIA+GOSIA2 analysis.

Electromagnetic matrix elements were determined using the semiclassical coupled-channels codes GOSIA [8] and GOSIA2 [9] by simultaneously treating both projectile and target excitations with Doppler-corrected yields of the relevant transitions from the γ-ray spectra. Since no experimental value for the $\langle 2^+_1 \| E2 \| 2^+_1 \rangle$ matrix element of ^{90}Zr was available, we employed GOSIA2 considering excitations up to 2^+_1 in ^{32}S and ^{90}Zr as the first step. The lifetimes of these states, and yields of the $2^+_1 \rightarrow 0^+_1$ transitions – 2230 keV (for ^{32}S) and 2186 keV (for ^{90}Zr) – were given as experimental data. The absolute normalization was performed w.r.t. ^{32}S excitation by allowing its $\langle 0^+_1 \| E2 \| 2^+_1 \rangle$ and $\langle 2^+_1 \| E2 \| 2^+_1 \rangle$ matrix elements to vary. The global minimum of the two-dimensional χ^2 surface, $\chi^2_{\min}$ constructed in the plane of the $\langle 0^+_1 \| E2 \| 2^+_1 \rangle$ and $\langle 2^+_1 \| E2 \| 2^+_1 \rangle$ matrix elements of ^{90}Zr provided an initial estimate of $\langle 2^+_1 \| E2 \| 2^+_1 \rangle$ of ^{90}Zr [10]. This value was provided in the GOSIA analysis of ^{90}Zr in the next step where excitation of the 3^-_1 state was added (Fig. 1). The reported $E3(3^-_1 \rightarrow 0^+_1)/E1(3^-_1 \rightarrow 2^+_1)$ intensity ratio [11] was also given and all relevant matrix elements of ^{90}Zr were extracted. In the following step, a GOSIA2 analysis was performed similar to the first step, but this time with the inclusion of the 3^-_1 state of ^{90}Zr. Again, $\langle 2^+_1 \| E2 \| 2^+_1 \rangle$ was extracted from the new value of $\chi^2_{\min}$, and the GOSIA+GOSIA2 calculations were repeated until full convergence of all matrix elements was achieved.

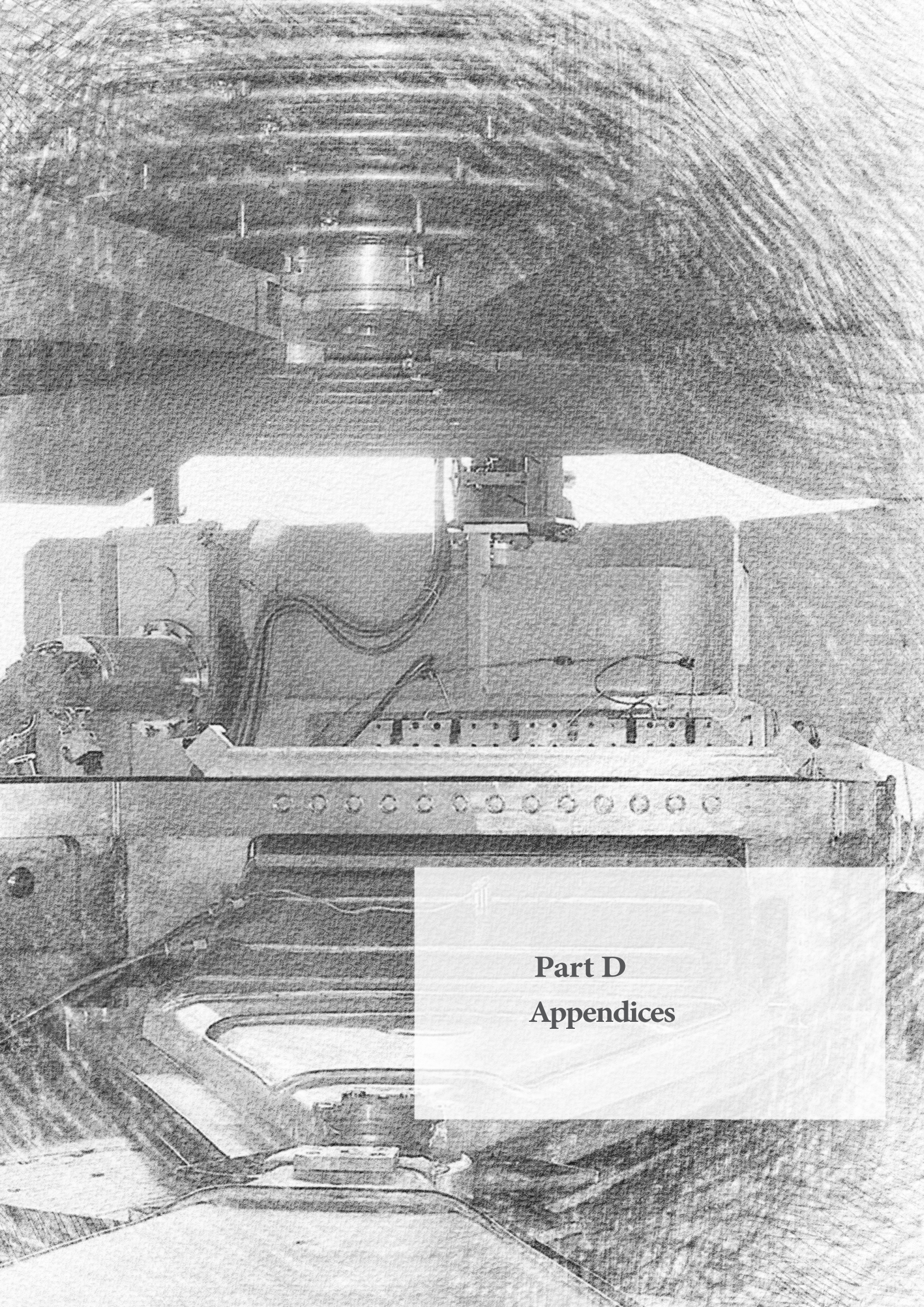
Acknowledgements

The authors are grateful to the staff at the TIFR-BARC Pelletron Linac Facility for smooth operation of the accelerator during the experiment. Support from B. S. Naidu, S. V. Jadhav and A. T. Vazhappilly for setting up the experimental apparatus is acknowledged.

Bibliography

[1] P. A. Butler, W. Nazarewicz, Rev. Mod. Phys. **68** (1996) 349–421.
[2] T. Kibedi, R. H. Spear, At. Data and Nucl. Data Tabl. **80** (2002) 35–82.
[3] Ł. Iskra *et al.*, Phys. Lett. B **788** (2019) 396–400.
[4] Ł. Iskra *et al.*, Phys. Rev. C **110** (2024) 064312.
[5] D. Cline, Annu. Rev. Nucl. Part. Sci. **36** (1986) 683–716.

[6] R. Palit, P. Dey, A. Kundu, Eur. Phys. J. A **61** (2025) 74.
[7] R. Palit *et al.*, Nucl. Inst. and Meth. A **680** (2012) 90-92.
[8] T. Czosnyka, D. Cline, C. Wu, Bull. Amer. Phys. Soc. **28** (1982) 745.
[9] M. Zielińska *et al.*, Eur. Phys. J. A **52** (2016) 99.
[10] P. Dey *et al.*, Acta Phys. Pol. B Proc. Suppl. **19**, (2026) 1-A19.
[11] P. E. Garrett *et al.*, Phys. Rev. C **68** (2003) 024312.



Part D
Appendices

D.1 List of experiments performed at HIL in 2025

A list of the experiments performed in 2025 is presented in the following pages.
The following acronyms of institution names are used in the list:

- HIL — Heavy Ion Laboratory, University of Warsaw, Warszawa, Poland;
- ATOMKI — HUN-REN ATOMKI, Debrecen, Hungary;
- DEIB PM Milano — DEIB Politecnico di Milano, Milano, Italy;
- DPA UC Catania — Department of Physics and Astronomy, University of Catania, Catania, Italy;
- FP UW — Faculty of Physics, University of Warsaw, Warszawa, Poland;
- IEM CSIC Spain — Instituto de Estructura de la Materia, CSIC, Spain;
- INFN SC Catania —INFN Sezione di Catania, Catania, Italy;
- INFN-LNS Catania — LNS, INFN e Università di Catania, Catania, Italy;
- INFN SM Milano — INFN. Sezione di Milano, Milano, Italy;
- INP PAN Kraków — Institute of Nuclear Physics PAN, Kraków, Poland;
- NCNR Świerk — National Centre for Nuclear Research, Świerk, Poland;
- SINP Kolkata — Saha Institute of Nuclear Physics, Kolkata, India;
- SPKLNS NETCU WFIINT SNSEPE SU — Shandong Provincial Key Laboratory of Nuclear Science, Nuclear Energy Technology and Comprehensive Utilization, Weihai Frontier Innovation Institute of Nuclear Technology, School of Nuclear Science, Energy and Power Engineering, Shandong University, Jinan, China;
- WRI IT US Weihai — Weihai Research Institute of Industrial Technology, Shandong University, Weihai, China;

For each experiment the following information is provided: ion, energy, setup/beam line information, date, proposal number, subject, spokespersons and institutions.

^{12}C — 73 MeV — EAGLE 10.06 – 13.06
HIL128 — Fast timing at HIL - commisioning. (A. Špaček)
HIL, INP PAN Kraków

^{12}C — 78-80 MeV — ICARE 24.06 - 27.06
HIL122 —T-INSIDE (Timing Investigation in SiC Detectors. (N. S. Martorana, E. Geraci)
INFN SC Catania, INFN-LNS Catania, INFN SM Milano, DEIB PM Milano, PA UC Catania, IEM CSIC Spain, HIL

^{11}B —50 MeV — EAGLE 01.07 – 12.07
HIL120 —Search for a new chiral nucleus in the 80 mass region: ^{72}As. (C. Liu, S. Y. Wang)
SPKLNS NETCU WFIINT SNSEPE SU, WRI IT US Weihai, HIL, INP PAN Kraków, NCNR Świerk

^{20}Ne — EAGLE, ICARE, Radiobiology 19.10 – 25.10
HIL001 — Student Workshop.
HIL

^{32}S — 88 MeV — EAGLE-SiLCA 02.12 – 12.12
HIL000 — Coulomb excitation of ^{104}Pd. (K. Hadyńska-Klęk)
HIL, ATOMKI, INP PAN Kraków, FP UW, SINP Kolkata

D.2 Degrees and theses completed or in progress during 2025

D.2.1 DSc degrees of HIL staff members

Mateusz Filipek, Faculty of Physics, University of Warsaw
From radiobiology to radiotherapy: dose homogeneity in cells after alpha irradiation in measurements and Monte Carlo simulations
Supervisors: dr hab. Z. Szefliński and dr hab. B. Brzozowska. Expected completion date: 2026.

Grzegorz Wałpuski, Faculty of Biology, University of Warsaw
Badanie wpływu promieniowania jonizującego na procesy fizjologiczne ujednokomórkowych glonów z gromady Cyanidiophyceae
Study of the influence of ionizing radiation on physiological processes in single-celled algae from the class Cyanidiophyceae
Supervisors: dr hab. Z. Szefliński and dr hab. M. Zienkiewicz. Expected completion date: 2027.

Iwona Piętka, Heavy Ion Laboratory, University of Warsaw
Badanie współistnienia kształtów w jądrze ^{110}Cd metodą wzbudzeń kulombowskich
Study of multiple shape coexistence in ^{110}Cd using the Coulomb-excitation method
Supervisor: dr hab. L. Próchniak and dr K. Wrzosek-Lipska. Expected completion date: 2027.

D.2.2 MSc and BSc theses supervised by HIL staff members

Patryk Elak, Faculty of Physics, University of Warsaw
Porównanie metod pomiarowych natężenia wiązki ciężkich jonów z cyklotronu U-200P
Comparison of methods for measuring the intensity of the heavy ion beam from the U-200P cyclotron
Supervisor: prof. dr hab. T. Rząca-Urban, dr P. Napiorkowski, dr M. Paluch-Ferszt. Thesis completed in July 2025.

Agata Krzysiek, Faculty of Physics, University of Warsaw
Wzbudzenie kulombowskie ^{60}Ni
Coulomb excitation of ^{60}Ni
Supervisor: dr K. Hadyńska-Klęk. Expected completion date: 2026.

Grzegorz Szymanek, Faculty of Physics, University of Warsaw
Wstępna analiza koincydencji cząstka–gamma z pomiaru wzbudzenia kulombowskiego ^{104}Pd na wiązce ^{32}S w SLCJ UW
Preliminary analysis of particle-gamma coincidences from the Coulomb excitation of ^{104}Pd by a ^{32}S beam at HIL UW
Supervisor: dr K. Hadyńska-Klęk. Thesis completed in September 2025.

Grzegorz Szymanek, Faculty of Physics, University of Warsaw
Wzbudzenie kulombowskie ^{104}Pd
Coulomb excitation of ^{104}Pd
Supervisor: dr K. Hadyńska-Klęk. Expected completion date: 2026.

Wiktoria Dworak, Faculty of Chemistry, University of Warsaw
Synteza i kontrola jakości radiofarmaceutyków ^{18}F
Synthesis and quality control of ^{18}F radiopharmaceuticals
Supervisor: dr hab. K. Kilian. Thesis completed in September 2025.

Katarzyna Głazowska, Faculty of Chemistry, University of Warsaw
Synteza radiofarmaceutyku 18FAZA na syntezerze Synthra RN
Synthesis of the radiopharmaceutical 18FAZA with the Synthra RN synthesizer
Supervisor: dr hab. K. Kilian. Thesis completed in July 2025.

Alicja Milewska, Faculty of Chemistry, University of Warsaw
Ocena wydajności syntezy ^{18}F-MISO w zależności od stopnia zalkalizowania środowiska reakcji
Evaluation of the efficiency of ^{18}F-MISO synthesis depending on the degree of alkalization of the reaction medium
Supervisor: dr hab. K. Kilian. Expected completion date: 2026.

Krystian Kluska, Faculty of Chemistry, University of Warsaw
Synteza i charakterystyka radiobiokoniugatu opartego na przeciwciele monoklonalnym i emiterze beta- ^{177}Lu do celowanej terapii potrójnie ujemnego raka piersi
Synthesis and characterization of a radiobioconjugate based on a monoclonal antibody and a ^{177}Lu beta emitter for targeted therapy of triple-negative breast cancer
Supervisor: dr hab. K. Kilian and prof. Agnieszka Majkowska-Pilip. Expected completion date: 2026.

Katarzyna Gałązka, Faculty of Chemistry, University of Warsaw
Synteza radiofarmaceutyku ^{18}F Fluorotymidyna (FLT) na syntezerze Synthra RN
Synthesis of the radiopharmaceutical ^{18}F Fluorothymidine (FLT) with a Synthra RN synthesizer
Supervisor: dr hab. K. Kilian. Expected completion date: 2026.

Hanna Adamiak, Faculty of Physics, University of Warsaw
Synteza radiofarmaceutyku ^{18}F Fluorotymidyna (FES) na syntezerze Synthra RN
Synthesis of the radiopharmaceutical ^{18}F Fluorothymidine (FES) with a Synthra RN synthesizer
Supervisor: dr hab. K. Kilian. Expected completion date: 2026.

Julianna Hausman, Faculty of Chemistry, University of Warsaw
Oznaczanie związków polifenolowych w oleju kawowym
Determination of polyphenolic compounds in coffee oil
Supervisor: dr hab. A. Sentkowska. Thesis completed in February 2025.

Julianna Hausman, Faculty of Chemistry, University of Warsaw
Chromatografia HILIC jako alternatywna metoda chromatograficznego oznaczania niesteroidowych leków przeciwzapalnych
HILIC chromatography as an alternative method for chromatographic determination of nonsteroidal anti-inflammatory drugs
Supervisor: dr hab. A. Sentkowska. Expected completion date: 2026.

Michał Janiszewski, Faculty of Chemistry, University of Warsaw
Chromatograficzne oznaczanie selenu w miodzie-opracowanie nowej metodyki ekstrakcji i konserwacji próbek
Chromatographic determination of selenium in honey - development of a new methodology for sample extraction and preservation
Supervisor: dr hab. A. Sentkowska. Thesis completed in June 2025.

Aniela Jakubowska, Faculty of Chemistry, University of Warsaw
Zastosowanie chromatografii HILIC do oznaczenia związków biologicznie aktywnych w fermencie chlebowym
Application of HILIC chromatography for the determination of B vitamins in bread ferment
Supervisor: dr hab. A. Sentkowska. Thesis completed in February 2025.

Aniela Jakubowska, Faculty of Chemistry, University of Warsaw
Chromatograficzne oznaczanie antocyjanów w produktach spożywczych
Chromatographic determination of anthocyanins in food products
Supervisor: dr hab. A. Sentkowska. Expected completion date: 2026.

Adam Malinowski, Faculty of Physics, University of Warsaw
W poszukiwaniu stanów wzbudzonych ^{57}Cu z układem EAGLE-NEDA-DIAMANT
In search of excited states of ^{57}Cu with the EAGLE-NEDA-DIAMANT setup
Supervisor: dr hab. M. Palacz. Thesis completed in July 2025.

Zuzanna Napora, Faculty of Chemistry, University of Warsaw
Jednodomenowe przeciwciało anty-HER2 znakowane teranostycznym ^{177}Lu – charakterystyka fizykochemiczna i biologiczna
Single-domain anti-HER2 antibody labelled with theranostic ^{177}Lu – physicochemical and biological characterization
Supervisors: dr hab. K. Kilian and dr hab. M. Pruszyński. Thesis completed in July 2025.

Michał Przystaś, Faculty of Chemistry, University of Warsaw
Kinetyka powstawania i zanikania ognisk naprawczych gamma-H2AX w komórkach glejaka eksponowanych na promieniowanie jonizujące
Kinetics of formation and disappearance of gamma-H2AX repair foci in glioma cells exposed to ionizing radiation Supervisors: dr hab. dr hab. A. Sentkowska and dr U. Kaźmierczak. Thesis completed in July 2025.

Agnieszka Oleksiuk, Faculty of Chemistry, University of Warsaw
Jednodomenowe przeciwciało anty-HER2 znakowane teranostycznym ^{161}Tb – charakterystyka fizykochemiczna i biologiczna
Single-domain anti-HER2 antibody labelled with theranostic ^{161}Tb – physicochemical and biological characterization
Supervisors: dr hab. K. Kilian and prof. M.Pruszyński. Expected completion date: 2026.

Patrycja Jasińska, Faculty of Chemistry, University of Warsaw
Porównanie wnikania porfiryn i kompleksów metaloporfirynowych do komórek HeLa
Comparison of the penetration of porphyrins and metalloporphyrin complexes into HeLa cells
Supervisors: dr hab. K. Kilian and dr Joanna Trzcińska-Danielewicz. Expected completion date: 2026.

Justyna Sykuła, Faculty of Chemistry, University of Warsaw
Badanie akumulacji porfiryn w liniach komórkowych glejaka M059K i M059J
Porphyrin accumulation study in glioma cell lines M059K and M059J
Supervisors: dr hab. K. Kilian and dr U. Kaźmierczak. Expected completion date: 2026.

Natalia Szoblik, Faculty of Chemistry, University of Warsaw
Wykorzystanie ekstraktu z morwy białej (Morus alba L.) do syntezy nanocząstek selenu
Application of white mulberry extract (Morus alba L.) for the synthesis of selenium nanoparticles
Supervisor:dr hab. A. Sentkowska. Thesis completed in February 2026.

D.3 Publications

[1] A. Agrawal, V. V. Alenkov, P. Aryal, J. Beyer, B. Bhandari, R. S. Boiko, K. Boonin, O. Buzanov, C. R. Byeon, N. Chanthima, M. K. Cheoun, J. S. Choe, S. Choi, S. Choudhury, J. S. Chung, F. A. Danevich, M. Djamal, D. Drung, C. Enss, A. Fleischmann, A. M. Gangapshev, L. Gastaldo, Y. M. Gavrilyuk, A. M. Gezhaev, O. Gileva, V. D. Grigorieva, V. I. Gurentsov, C. Ha, D. H. Ha, E. J. Ha, D. H. Hwang, E. J. Jeon, J. A. Jeon, H. S. Jo, J. Kaewkhao, C. S. Kang, W. G. Kang, V. V. Kazalov, S. Kempf, A. Khan, S. Khan, D. Y. Kim, G. W. Kim, H. B. Kim, H.-J. Kim, H. J. Kim, H. L. Kim, H. S. Kim, M. B. Kim, S. C. Kim, S. K. Kim, S. R. Kim, W. T. Kim, Y. D. Kim, Y. H. Kim, K. Kirdsiri, Y. J. Ko, V. V. Kobychev, V. Kornoukhov, V. V. Kuzminov, D. H. Kwon, C. H. Lee, D. Lee, E. K. Lee, H. J. Lee, H. S. Lee, J. Lee, J. Y. Lee, K. B. Lee, M. H. Lee, M. K. Lee, S. W. Lee, Y. C. Lee, D. S. Leonard, H. S. Lim, B. Mailyan, E. P. Makarov, P. Nyanda, Y. Oh, S. L. Olsen, **S.I. Panasenko**, H. K. Park, H. S. Park, K. S. Park, S. Y. Park, O. G. Polischuk, H. Prihtiadi, S. Ra, S. S. Ratkevich, G. Rooh, E. Sala, M. B. Sari, J. Seo, K. M. Seo, B. Sharma, K. A. Shin, V. N. Shlegel, K. Siyeon, J. So, N. V. Sokur, J. K. Son, J. W. Song, N. Srisittipokakun, V. I. Tretyak, R. Wirawan, K. R. Woo, H. J. Yeon, Y. S. Yoon, Q. Yue, A. Collaboration. *Improved limit on neutrinoless double beta decay of 100Mo from AMoRE-I.* Phys. Rev. Lett. 134(2025) 082501.

[2] A. Agrawal, V. V. Alenkov, P. Aryal, H. Bae, J. Beyer, B. Bhandari, R. S. Boiko, K. Boonin, O. Buzanov, C. R. Byeon, N. Chanthima, M. K. Cheoun, J. S. Choe, S. Choi, S. Choudhury, J. S. Chung, F. A. Danevich, M. Djamal, D. Drung, C. Enss, A. Fleischmann, A. M. Gangapshev, L. Gastaldo, Y. M. Gavrilyuk, A. M. Gezhaev, O. Gileva, V. D. Grigorieva, V. I. Gurentsov, C. Ha, D. H. Ha, E. J. Ha, D. H. Hwnag, E. J. Jeon, J. A. Jeon, H. S. Jo, J. Kaewkhao, C. S. Kang, W. G. Kang, V. V. Kazalov, S. Kempf, A. Khan, S. Khan, D. Y. Kim, G. W. Kim, H. B. Kim, H. J. Kim, H. J. Kim, H. L. Kim, H. S. Kim, M. B. Kim, S. C. Kim, S. K. Kim, S. R. Kim, W. T. Kim, Y. D. Kim, Y. H. Kim, K. Kirdsiri, Y. J. Ko, V. V. Kobychev, V. Kornoukhov, V. V. Kuzminov, D. H. Kwon, C. H. Lee, D. Y. Lee, E. K. Lee, H. J. Lee, H. S. Lee, J. Lee, J. Y. Lee, K. B. Lee, M. H. Lee, M. K. Lee, S. W. Lee, Y. C. Lee, D. S. Leonard, H. S. Lim, B. Mailyan, E. P. Makarov, P. Nyanda, Y. Oh, S. L. Olsen, **S.I. Panasenko**, H. K. Park, H. S. Park, K. S. Park, S. Y. Park, O. G. Polischuk, H. Prihtiadi, S. Ra, S. S. Ratkevich, G. Rooh, M. B. Sari, J. Seo, K. M. Seo, B. Sharma, K. A. Shin, V. N. Shlegel, K. Siyeon, J. So, N. V. Sokur, J. K. Son, J. W. Song, N. Srisittipokakun, V. I. Tretyak, R. Wirawan, K. R. Woo, H. J. Yeon, Y. S. Yoon, Q. Yue, A. Collaboration. *Development of MMC-based lithium molybdate cryogenic calorimeters for AMoRE-II.* Eur. Phys. J. C 85(2025) 172.

[3] A. Agrawal, V. V. Alenkov, P. Aryal, J. Beyer, B. Bhandari, R. S. Boiko, K. Boonin, O. Buzanov, C. R. Byeon, N. Chanthima, M. K. Cheoun, J. S. Choe, S. Choi, S. Choudhury, J. S. Chung, F. A. Danevich, M. Djamal, D. Drung, C. Enss, A. Fleischmann, A. M. Gangapshev, L. Gastaldo, Y. M. Gavrilyuk, A. M. Gezhaev, O. Gileva, V. D. Grigorieva, V. I. Gurentsov, C. Ha, D. H. Ha, E. J. Ha, D. H. Hwnag, E. J. Jeon, J. A. Jeon, H. S. Jo, J. Kaewkhao, C. S. Kang, W. G. Kang, V. V. Kazalov, S. Kempf, A. Khan, S. Khan, D. Y. Kim, G. W. Kim, H. B. Kim, H.-J. Kim, H. J. Kim, H. L. Kim, H. S. Kim, M. B. Kim, S. C. Kim, S. K. Kim, S. R. Kim, W. T. Kim, Y. D. Kim, Y. H. Kim, K. Kirdsiri, Y. J. Ko, V. V. Kobychev, V. Kornoukhov, V. V. Kuzminov, D. H. Kwon, C. H. Lee, D. Lee, E. K. Lee, H. J. Lee, H. S. Lee, J. Lee, J. Y. Lee, K. B. Lee, M. H. Lee, M. K. Lee, S. W. Lee, Y. C. Lee, D. S. Leonard, H. S. Lim, B. Mailyan, E. P. Makarov, P. Nyanda, Y. Oh, S. L. Olsen, **S.I. Panasenko**, H. K. Park, H. S. Park, K. S. Park, S. Y. Park, O. G. Polischuk,

H. Prihtiadi, S. Ra, S. S. Ratkevich, G. Rooh, E. Sala, M. B. Sari, J. Seo, K. M. Seo, B. Sharma, K. A. Shin, V. N. Shlegel, K. Siyeon, J. So, N. V. Sokur, J. K. Son, J. W. Song, N. Srisittipokakun, V. I. Tretyak, R. Wirawan, K. R. Woo, H. J. Yeon, Y. S. Yoon, Q. Yue, A. Collaboration. *Projected background and sensitivity of AMoRE-II.* Eur. Phys. J. C 85(2025).

[4] C. J. Appleton, P. J. Woods, A. Algora, J. A. Victoria, B. Rubio, D. S. Ahn, J. Agramunt, H. Baba, S. Bae, C. G. Bruno, M. L. Cortes, T. Davinson, P. Doornenbal, Y. Fujita, N. Fukuda, E. Ganioglu, C. J. Griffin, V. Guadilla, J. Ha, O. Hall, T. Isobe, D. Kahl, M. Kanenko, G. Kiss, S. Kubono, I. Kuti, M. Labiche, J. Lee, Y. Litvinov, J. Liu, F. Molina, E. Nacher, D. Nishimura, S. Nishimura, S. E. A. Orrigo, Z. Podolyak, K. P. Rykaczewski, H. Sakurai, H. Shimizu, Y. Shimizu, H. Suzuki, D. Sohler, T. Sumikama, J. L. Tain, H. Takeda, A. Tolosa-Delagado, **M. Wolińska-Cichocka**. *Measurements of β-delayed proton emitters in the region of 100Sn.* Phys. Rev. C 112(2025) 034310.

[5] M. Araszkiewicz, A. Korgul, K. Tyminska, **U. Kaźmierczak**, K. Dyka, P. Chuchala, R. Grzela, P. Kaminska, R. Kuczma, B. Paterczyk, A. Stankiewicz-Drogon, B. Wielgus-Kutrowska, A. Kustra, M. Fryc, P. Bednarczyk, K. Maliszewska-Olejniczak. *Expression of dna-damage response genes after exposure to high let particles used in bnct in glioblastoma cells with altered radiosensitivity.* Sci. Rep. 16(2025) 2822.

[6] D. Brugnara, G. Montagnoli, A. M. Stefanini, M. Del Fabbro, P. A. A. Jorquera, G. Andreetta, F. Angelini, M. Balogh, J. Benito, G. Benzoni, A. Bonhomme, S. Bottoni, S. Carollo, **G. Colucci**, L. Corradi, S. Courtin, R. Depalo, A. Ertoprak, E. Fioretto, F. Galtarossa, A. Goasduff, B. G. Servin, A. Gottardo, A. Gozzelino, M. Heine, M. Mazzocco, R. Menegazzo, D. Mengoni, B. Million, E. Monpribat, R. N. d. Alamo, J. Pellumaj, R. M. P. Vidal, E. Pilotto, S. Pigliapoco, M. Polettini, F. Recchia, M. Rocchini, K. Rezynkina, D. Stramaccioni, S. Szilner, **A. Trzcińska**, J. J. V. Dobon, L. Zago, I. Zanon. *Fusion dynamics far below the barrier for 12C+28Si.* Nucl. Phys. A 1063(2025) 123195.

[7] C. Ciampi, J. D. Frankland, D. Gruyer, N. Le Neindre, S. Mallik, R. Bougault, A. Chbihi, L. Baldesi, S. Barlini, E. Bonnet, B. Borderie, A. Camaiani, G. Casini, I. Dekhissi, D. Dell'Aquila, J. A. Duenas, Q. Fable, F. Gramegna, C. Gouyet, M. Henri, B. Hong, S. Kim, **A. Kordyasz**, T. Kozik, M. J. Kweon, I. Lombardo, O. Lopez, L. Manduci, T. Marchi, K. Mazurek, S. H. Nam, J. Park, M. Parlog, G. Pasquali, S. Piantelli, G. Poggi, A. Rebillard-Soulie, R. Revenko, S. Valdre, G. Verde, E. Vient. *Model-independent measurement of isospin diffusion in Ni-Ni systems at intermediate energy.* Phys. Rev. C 111(2025) 044601.

[8] C. Ciampi, S. Mallik, F. Gulminelli, D. Gruyer, J. D. Frankland, N. Le Neindre, R. Bougault, A. Chbihi, L. Baldesi, S. Barlini, B. Borderie, A. Camaiani, G. Casini, I. Dekhissi, J. A. Duenas, Q. Fable, F. Gramegna, M. Henri, B. Hong, S. Kim, **A. Kordyasz**, T. Kozik, I. Lombardo, O. Lopez, T. Marchi, S. H. Nam, J. Park, M. Parlog, G. Pasquali, S. Piantelli, G. Poggi, S. Valdre, G. Verde, E. Vient. *Constraining the nuclear symmetry energy with Fermi-energy heavy ion collisions.* Phys. Lett. B 868(2025) 139815.

[9] C. Ciampi, S. Piantelli, G. Casini, J. D. Frankland, L. Baldesi, S. Barlini, B. Borderie, R. Bougault, A. Camaiani, A. Chbihi, D. Dell'aquila, J. A. Duenas, Q. Fable, C. Frosin, T. Genard, F. Gramegna, D. Gruyer, M. Henri, B. Hong, S. Kim, **A. Kordyasz**, T. Kozik, M. J. Kweon, J. Lemarie, N. LE Neindre, I. Lombardo, O. Lopez, T. Marchi, K. Mazurek, S. H. Nam, J. Park, J. H. Park, M. Parlog, G. Pasquali, G. Poggi, A. Rebillard-soulie, A. A. Stefanini, S. Upadhyaya, S. Valdre, G. Verde, E. Vient, M. Vigilante. *Isospin transport*

phenomena in heavy ion collisions at fermi energies: An overview on the most recent results from the first INDRA-FAZIA experiment. Nuovo Cimento C 48(2025) 51.

[10] **G. Colucci**, **A. Trzcińska**, **E. Piasecki**, **M. Wolińska-Cichocka**, A. Barbon, G. D'agata, E. DE Filippo, Z. K. Czerski, R. Dubey, E. Geraci, B. Gnoffo, **K. Hadyńska-Klęk**, **G. Jaworski**, **M. Kisieliński**, P. Koczon, M. Kondzielska, **M. Kowalczyk**, Y. Leifels, B. Lommel, **M. Matuszewski**, N. S. Martorana, V. Pagano, E., L. Quattrocchi, F. Risitano, P. Russotto, **J. Samorajczyk-Pyśk**, **A. Stolarz**, G. Tiurin, M. Trimarchi, W. H. Trzaska, **A. Tucholski**, C. Zagami, **B. Zalewski**. *Role of dissipation on the quasielastic barrier distributions: The case of 20 Ne.* Nuovo Cimento C 48(2025) 46.

[11] **G. Colucci**, **A. Trzcińska**, **E. Piasecki**, **M. Wolińska-Cichocka**, A. Barbon, Z. K. Czerski, G. D'Agata, E. De Filippo, R. Dubey, E. Geraci, B. Gnoffo, **K. Hadyńska-Klęk**, **G. Jaworski**, **M. Kisieliński**, P. Koczon, M. Kondzielska, **M. Kowalczyk**, Y. Leifels, B. Lommel, **M. Matuszewski**, N. S. Martorana, V. Pagano, E., L. Quattrocchi, F. Risitano, P. Russotto, **J. Samorajczyk-Pyśk**, **A. Stolarz**, G. Tiurin, M. Trimarchi, W. H. Trzaska, **A. Tucholski**, C. Zagami, **B. Zalewski**. *Role of dissipation on the quasielastic barrier distributions of the 20Ne+92,94,95Mo systems.* Nucl. Phys. A 1063(2025) 123197.

[12] M. Das, S. Sharma, E. Y. Beyene, A. Bilewicz, **J. Choiński**, N. Chug, C. Curceanu, E. Czerwiński, K. V. Eliyan, J. Hajduga, S. Jalali, K. Kacprzak, T. Kaplanoglu, Ł. Kapłon, K. Kasperska, A. Khreptak, G. Korcyl, T. Kozik, K. Kubat, D. Kumar, A. K. Venadan, E. Lisowski, F. Lisowski, J. Medrala-Sowa, S. Moyo, W. Mryka, S. Niedźwiecki, P. Pandey, S. Parzych, A. Porcelli, B. Rachwał, E. P. del Rio, M. Rädler, A. Rominger, K. Shi, M. Skurzok, A. Stolarz, T. Szumlak, P. Tanty, K. T. Ardebili, S. Tiwari, R. Walczak, E. Ł. Stępień, P. Moskal. *First positronium imaging using 44Sc with the J-PET scanner: a case study on the NEMA-Image Quality Phantom.* IEEE Trans. Radiation and Plasma Med. Sci. (2025) article in press.

[13] J. M. Deltoro, A. Goasduff, F. J. Egea, V. Gonzalez, A. Gadea, R. M. Perez-Vidal, I. Lazarus, M. Kogimtzis, L. Mcnicholl, **M. Palacz**, **G. Jaworski**, J. J. Valiente-Dobon, J. Nyberg, S. Casans, A. E. Navarro-Anton, E. Sanchis, A. Boujrad, E. Clement, T. Huyuk, R. Illicachi, O. Stezowski, V. Modamio. *Implementation of a double trigger condition system based on charge comparison and TOF measurement for the NEDA detector array.* Nucl. Sci. Tech. 36(2025) 30.

[14] J. M. Deltoro, **G. Jaworski**, A. Goasduff, V. Gonzalez, A. Gadea, **M. Palacz**, J. J. Valiente-Dobon, J. Nyberg, S. Casans, A. E. Navarro-Anton, E. Sanchis, G. de Angelis, A. Boujrad, S. Coudert, T. Dupasquier, S. Erturk, O. Stezowski, R. Wadsworth. *Reconstruction of pile-up events using a one-dimensional convolutional autoencoder for the NEDA detector array.* Nucl. Sci. Tech. 36(2025) 32.

[15] C. Fransen, A. Blazhev, F. Dunkel, J. Jolie, C. D. Lakenbrink, R. Novak, F. von Spee, C. Mueller-Gatermann, M. P. Carpenter, G. Savard, T. Lauritsen, W. Reviol, D. Seweryniak, T. Grahn, P. Greenlees, J. Pakarinen, P. Rahkila, P. Ruotsalainen, J. Saren, **T. Abraham**, **K. Hadyńska-Klęk**, **G. Jaworski**, **M. Komorowska**, **P. J. Napiorkowski**, **M. Palacz**, **P. Sekrecka**, **J. Srebrny**, **A. Tucholski**, **K. Wrzosek-Lipska**, A. Nalecs-Jawecki, B. Cederwall, M. D. Monasterio, H. Iwasaki, A. Sanchez, A. Korichi. *The recoil distance doppler-shift technique: A valuable method for nuclear structure studies far from the valley of stability.* Acta Phys. Pol. B Proc. Suppl. 18(2025) A30.

[16] F. Galtarossa, A. Gottardo, L. Zago, M. Balogh, E. Pilotto, G. Pasqualato, D. Mengoni, P. A. Jorquera, G. Andreetta, F. Angelini, L. Baldesi, J. Benito, G. Benzoni, S. Bottoni,

D. Brugnara, A. Camaiani, S. Carollo, J. Collado, G. Corbari, M. D'Andrea, G. De Angelis, M. Del Fabbro, D. Dell'Aquila, J. Diklic, F. Dunkel, F. Ercolano, A. Ertoprak, A. Gadea, A. Giaz, A. Goasduff, B. Gngora-Servin, A. Gozzelino, **K. Hadyńska-Klęk**, C. Hiver, Z. Huang, M. Kaci, H. Kleis, S. M. Lenzi, I. Lombardo, N. Marchini, H. Mayr, R. Menegazzo, N. Miani, A. Nannini, D. R. Napoli, R. N. del Alamo, J. Pellumaj, R. M. Perez-Vidal, S. Pigliapoco, M. Polettini, F. Recchia, L. Redigolo, K. Rezynkina, M. Rocchini, M. Sedlak, A. =Špaček, F. Spee, G. Spina, D. Stramaccioni, J. J. Valiente-Dobon, I. Zanon, G. Zhang. *Lifetime measurement after direct transfer reactions with AGATA at LNL.* EPJ Web of Conf. 324(2025) 00029.

[17] A. Giaz, O. Wieland, G. Benzoni, C. Boiano, S. Brambilla, B. Million, F. C. L. Crespi, S. Bottoni, A. Bracco, F. Camera, G. Corbari, D. Genna, S. Leoni, M. Luciani, G. Spina, S. Riboldi, M. Kmiecik, M. Ciemała, A. Maj, P. Bednarczyk, N. Cieplicka-Oryńczak, B. Fornal, J. Grębosz, L. W. Iskra, J. Lukasik, M. Matejska-Minda, K. Mazurek, W. Parol, P. Pawlowski, C. Schmitt, B. Sowicki, M. Zięblński, **K. Hadyńska-Klęk**, **P. J. Napiorkowski**, C. Hiver, I. Matea, J. Wilson, D. Stramaccioni, M. Balogh, M. N. Harakeh, M. Lewitowicz, P. Miriot-Jaubert, N. Benouaret. *Search for pdr and isgqr in A ≈ 60 and A=120 mass regions.* Acta Phys. Pol. B Proc. Suppl. 18(2025) A34.

[18] A. Grudniak, J. Folcik, J. Szmytke, **A. Sentkowska**. *Mechanism of antioxidant activity of selenium nanoparticles obtained by green and chemical synthesis.* Int. J. Nanomed. 20(2025) 2797.

[19] D. Gruyer, L. Baldesi, S. Barlini, B. Borderie, R. Bougault, A. Camaiani, G. Casini, A. Chbihi, C. Ciampi, J. A. Duenas, Q. Fable, D. Fabris, J. D. Frankland, C. Frosin, T. Genard, F. Gramegna, M. Henri, B. Hong, S. Kim, **A. Kordyasz**, T. Kozik, M. J. Kweon, N. LE Neindre, I. Lombardo, O. Lopez, T. Marchi, K. Mazurek, S. H. Nam, J. Park, M. Parlog, G. Pasquali, S. Piantelli, G. Poggi, A. Rebillard-soulie, A. A. Stefanini, S. Upadhyaya, S. Valdre, G. Verde, E. Vient, M. Vigilante. *Recent highlights from INDRA and FAZIA.* Nuovo Cimento C 48(2025) 43.

[20] J. Henderson, J. Heery, M. Rocchini, M. Siciliano, N. Sensharma, A. D. Ayangeakaa, R. V. F. Janssens, T. M. Kowalewski, Abhishek, P. D. Stevenson, E. Yuksel, B. A. Brown, T. R. Rodriguez, L. M. Robledo, C. Y. Wu, S. Kisyov, C. Muller-Gatermann, V. Bildstein, L. Canete, C. M. Campbell, S. Carmichael, M. P. Carpenter, W. N. Catford, P. Copp, C. Cousins, M. Devlin, D. T. Doherty, P. E. Garrett, U. Garg, L. P. Gaffney, **K. Hadyńska-Klęk**, D. J. Hartley, S. F. Hicks, H. Jayatissa, S. R. Johnson, D. Kalaydjieva, F. Kondev, D. Lascar, T. Lauritsen, G. Lotay, N. Marchini, M. Matejska-Minda, S. Nandi, A. Nannini, C. O'Shea, S. Pascu, C. J. Paxman, A. Perkoff, E. E. Peters, Z. Podolyak, A. Radich, R. Rathod, B. J. Reed, P. H. Regan, W. Reviol, E. Rubino, R. Russell, D. Seweryniak, J. R. Vanhoy, G. L. Wilson, **K. Wrzosek-Lipska**, S. W. Yates, I. Zanon. *Deformation and collectivity in doubly magic 208Pb.* Phys. Rev. Lett. 134(2025) 062502.

[21] C. Hiver, J. N. Wilson, G. Pasqualato, M. Lebois, G. Charles, A. Lopez-martens, I. Matea, J. Ljungvall, K. Hauschild, K. Stoyachev, C. Cannes, S. Delpech, D. Rogrigues, S. Oberstedt, P. H. Regan, S. E. Poulton, E. B. O'sullivan, W. Catford, S. Pascu, **P. J. Napiorkowski**, **K. Hadyńska-Klęk**, **K. Wrzosek-Lipska**, **J. Samorajczyk-Pyśk**, T. Milanovic, S. Ilic, D. Knezevic, M. Beuschlein, D. Gjestvang, G. Torvund, E. M. Gandolfo, A. Maj, L. W. Iskra, P. Bednarczyk, M. Ciemała, B. Fornal, M. Kmiecik, M. Zięblński, S. Bottoni, A. Bracco, S. Brambilla, F. Camera, F. Crespi, S. Leoni, A. Algora, M. Staniou, S. Calinescu, C. Schmitt, O. Dorvaux, S. Kihel, N. Dzysiuk, O. Stezowski, M. Lewitowicz. *High-resolution studies of isomeric states in 236U with the nu-Ball2 spectrometer.* Acta Phys. Pol. B Proc. Suppl.

18(2025) A25.

[22] Z. Huang, C. M. Petrache, B. F. Lv, Y. X. Liu, G. X. Zhang, A. Astier, S. Guo, H. J. Ong, G. L. Zhang, N. T. Zhang, X. H. Zhou, D. Mengoni, D. Bazzacco, A. Boso, A. Goasduff, F. Recchia, D. Testov, F. Galtarossa, **G. Jaworski**, D. R. Napoli, S. Riccetto, M. Siciliano, J. J. Valiente-Dobon, C. Andreoiu, F. H. Garcia, I. Kuti, D. Sohler, **T. Marchlewski**, **A. Tucholski**. *New short-lived isomer in 128Xe.* Phys. Rev. C 111(2025) 054302.

[23] C. E. Jones, A. M. Bruce, D. Reygadas, N. Marginean, R. Marginean, G. Aggez, T. Beck, M. Boromiza, M. Brunet, R. B. Cakirli, R. L. Canavan, A. Chalil, C. Clisu, N. Florea, E. R. Gamba, E. Ganioglu, I. Gheorghe, J. P. Greene, **K. Hadyńska-Klęk**, J. Kleemann, S. Lalkovski, R. Lica, T. J. Mertzimekis, C. Mihai, R. Mihai, A. Mitu, R. Neveling, A. Oprea, Z. Podolyak, P. H. Regan, L. Sahin, C. Sotty, L. Stan, I. Stiru, S. Toma, A. Turturica, S. Ujeniuc, P. Van Isacker, A. P. Weaver. *Lifetime measurements in 102Mo interpreted in the interacting boson model and the X(5) symmetry.* Phys. Rev. C 111(2025) 034325.

[24] B. Khamidullin, S. G. Belogurov, V. Chudoba, A. M. Abakumov, S. A. Krupko, **P. J. Napiorkowski**, **S.I Panasenko**, P. G. Sharov, **B. Zalewski**. *Scintillation detector GADAST for the investigation of proton radioactivity reactions.* J. Instrum. 20(2025) C08031.

[25] R. Li, D. Verney, G. De Gregorio, R. Mancino, I. Matea, L. Coraggio, N. Itaco, M. N. Harakeh, C. Delafosse, F. Didierjean, L. A. Ayoubi, H. Al Falou, G. Benzoni, F. Le Blanc, V. Bozkurt, M. Ciemała, I. Deloncle, M. Fallot, C. Gaulard, A. Gottardo, V. Guadilla, J. Guillot, **K. Hadyńska-Klęk**, F. Ibrahim, N. Jovancevic, A. Kankainen, M. Lebois, T. Martinez, **P. J. Napiorkowski**, B. Roussiere, Y. G. Sobolev, I. Stefan, S. Stukalov, D. Thisse, G. Tocabens. *Simultaneous impacts of nuclear shell structure and collectivity on β decay: Evidence from $^{80}Ga_{49}$.* Phys. Rev. C 111(2025) 034303.

[26] R. Li, D. Verney, I. Matea, M. N. Harakeh, C. Delafosse, F. Didierjean, S. Ebata, L. A. Ayoubi, H. Al Falou, G. Benzoni, F. Le Blanc, V. Bozkurt, M. Ciemała, I. Deloncle, M. Fallot, C. Gaulard, A. Gottardo, V. Guadilla, J. Guillot, **K. Hadyńska-Klęk**, F. Ibrahim, N. Jovancevic, A. Kankainen, M. Lebois, T. Martinez, **P. J. Napiorkowski**, B. Roussiere, Y. G. Sobolev, I. Stefan, S. Stukalov, D. Thisse, G. Tocabens. *β-delayed spectroscopy of 80ge48 and competition between gamow-teller and first-forbidden transitions in $^{80g+m}Ga_{49}$ β decay.* Phys. Rev. C 112(2025) 044306.

[27] M. Matejska-Minda, P. Bednarczyk, M. Ciemała, N. Cieplicka-Oryńczak, I. Dedes, D. Duda, B. Fornal, J. Grębosz, **K. Hadyńska-Klęk**, L. W. Iskra, **G. Jaworski**, M. Kmiecik, **M. Komorowska**, **M. Kowalczyk**, P. Kulessa, I. Kuti, A. Maj, **A. Malinowski**, J. Molnar, **P. J. Napiorkowski**, **M. Palacz**, **S.I. Panasenko**, **I.Z. Piętka**, **J. Samorajczyk-Pyśk**, **P. Sekrecka**, B. Sowicki, **A. Špaček**, **A. Tucholski**, **K. Wrzosek-Lipska**, M. Zięblíński. *Ancillary detectors for the EAGLE array - new opportunities to study nuclear structure at hil uw.* Acta Phys. Pol. B Proc. Suppl. 18(2025) 2A42.

[28] P. Miriot-Jaubert, M. Vandebrouck, I. Matea, D. Dore, N. L. Achouri, L. Al Ayoubi, D. Beaumel, P. Bednarczyk, Y. Blumenfeld, A. Bogenschutz, A. Bracco, S. Brambilla, S. Calinescu, F. Camera, D. C. Ott, W. Catford, M. Ciemała, A. Corsi, F. Crespi, Y. Demane, W. Dong, O. Dorvaux, J. Dudouet, M. Dupuis, D. Etasse, S. Erturk, A. M. Frelin, J. Gerl, J. Gibelin, M. N. Harakeh, D. Jenkins, S. Kihel, M. Kmiecik, M. Lebois, X. Ledoux, S. Leoni, M. Lewitowicz, M. Mac Cormick, A. Maj, T. Martinez, I. Mazumdar, V. Nanal, **P. J. Napiorkowski**, A. Perez de Rada Fiol, S. Peru, D. Ramos, E. Rey-Herme, C. Schmitt, M. Stanoiu, O. Stezowski, C. Theisen, D. Thisse, L. Thulliez, G. Tocabens, J. Wilson, M. Zięblíński, M. Zielińska. *First study of the pygmy dipole resonance via neutron inelastic*

scattering at GANIL-SPIRAL2/NFS: Benchmarking the method on the 12C 2+ excited state. Acta Phys. Pol. B Proc. Suppl. 18(2025) A35.

[29] G. Montagnoli, M. Del Fabbrol, A. M. Stefanini, M. Balogh, A. Goasduff, G. Andreettal, E. Angelinil, J. Benito, A. Bonhomme, D. Brugnara, **G. Colucci**, L. Corradi, S. Courtin, R. Depalo, A. Ertoprak, E. Fioretto, E. Galtarossa, B. G. Servin, A. Gottardo, A. Gozzelino, M. Heine, M. Mazzoccol, D. Mengoni, B. Million, E. Monpribat, R. N. Del Alamol, I. Pellumaj, R. M. P. Vida, S. Pigliapoco, E. Pilottol, M. Polettini, K. Rezynkina, M. Rocchini, D. Stramaccioni, S. Szilner, **A. Trzcińska**, J. V. Dobon, L. Zago, I. Zanon. *Recent data on fusion far below the barrier for 12C+28Si.* EPJ Web of Conf. 324(2025) 00008.

[30] P. Moskal, A. Khreptak, **J. Choiński**, P. Jones, I. Kadenko, A. Majkowska-Pilip, R. Palit, **A. Stolarz**, R. Walczak, E. Stepien. *Endorsing titanium-scandium radionuclide generator for PET and positronium imaging.* Acta Phys. Pol. A 148(2025) S152.

[31] I. A. Muzalevskii, N. B. Shulgina, A. A. Bezbakh, V. Chudoba, S. A. Krupko, S. G. Belogurov, D. Biare, I. A. Egorova, A. S. Fomichev, E. M. Gazeeva, V. Gorshkov, A., V. Grigorenko, L., G. Kamiński, M. Khirk, O. Kiselev, D. A. Kostyleva, M. Y. Kozlov, B. Mauyey, I. Mukha, E. Y. Nikolskii, Y. L. Parfenova, **W. Piątek**, A. M. Quynh, A. Serikov, S. I. Sidorchuk, P. G. Sharov, R. S. Slepnev, V. Stepantsov, S., A. Swiercz, P. Szymkiewicz, G. M. Ter-Akopian, **B. Zalewski**. *Population of tetraneutron continuum in reactions of 8he on deuterium.* Phys. Rev. C 111(2025) 014612.

[32] R. Palit, **P. Dey**, A. Kundu. *Nuclear structure and reaction studies with digital INGA.* Eur. Phys. J. A 61(2025) 74.

[33] A. Paluch, **M. Paluch-Ferszt**, M. Kalisz, M. Gryniewicz-Jaworska. *Anomaly detection and security threats in internet of things: A study of data integrity in the measurement process.* Adv. Sci. Tech. Res. J. 19(2025) 415.

[34] J. Park, R. A. Lopez, J. Cederkall, C. Fahlander, P. Golubev, A. Knyazev, E. Rickert, **J. Iwanicki**, **K. Wrzosek-Lipska**, A. Blazhev, P. Reiter, D. Rosiak, M. Seidlitz, N. Warr, P. A. Butler, L. P. Gaffney, T. Berry, D. M. Cox, J. Pakarinen, T. Kroll, C. Henrich, M. Schilling, C. Stahl, M. von Schmid, G. Rainovski, C. Berger, C. Berner, R. Gernhauser, A. Illana, H. De Witte, M. Górska, T. Habermann, S. Saha, G. de Angelis, M. J. G. Borge, O. Tengblad, T. Otsuka, Y. Tsunoda. *First measurement of the quadrupole moment of the 21+state in 110Sn.* Phys. Rev. Lett. 135(2025) 222502.

[35] S. Piantelli, A. Camaiani, G. Poggi, A. Ono, C. Frosin, L. Baldesi, S. Barlini, B. Borderie, R. Bougault, G. Casini, C. Ciampi, M. Cicerchia, A. Chbihi, D. Dell'aquila, J. A. Duennas, Q. Fable, D. Fabris, J. D. Frankland, T. Genard, D. Gruyer, M. Henri, B. Hong, M. J. Kweon, S. Kim, **A. Kordyasz**, T. Kozik, I. Lombardo, O. Lopez, T. Marchi, K. Mazurek, S. H. Nam, J. Lemarie, N. Leneindre, P. Ottanelli, M. Parlog, J. Park, G. Pasquali, A. Rebillard-soulie, B. H. Sun, A. A. Stefanini, S. Terashima, S. Upadhyaya, S. Valdre, G. Verde, E. Vient, M. Vigilante. *Study of the in medium cross-section and of the clustering process by means of the Bayesian technique applied to a nuclear reaction at Fermi energy.* Nuovo Cimento C 48(2025) 55.

[36] **E. Piasecki**, **G. Colucci**, **A. Trzcińska**, **M. Wolińska-Cichocka**. *The influence of dissipation on the quasielastic barrier distributions of some nuclear systems.* EPJ Web of Conf. 324(2025) 00007.

[37] K. Piasecki, **E. Piasecki**, **G. Colucci**, **J. Choiński**, H. M. Jia, **M. Kisieliński**, **M. Kowalczyk**, C. J. Lin, **M. Matuszewski**, N. R. Ma, **A. Trzcińska**, **M. Wolińska-Cichocka**, **B. Zalewski**, L. Yang, H. Q. Zhang. *Beam position monitoring system based on SiC detectors.* Eur. Phys. J. A 61(2025) 212.

[38] **I.Z Piętka**, **K. Wrzosek-Lipska**, P. E. Garrett, M. Zielińska, **L. Próchniak**, A. Nannini, M. Rocchini, **T. Abraham**, P. Aguilera, Z. T. Ahmed, J. M. Allmond, F. Angelini, M. Balogh, F. L. B. Garrote, J. Benito, H. Bidaman, V. Bildstein, D. Brugnara, S. Buck, C. Burbadge, S. Carollo, J. Cederkall, M. Chiari, R. Coleman, G. Colombi, **G. Colucci**, A. D. Varela, D. T. Doherty, S. Dutt, F. Ercolano, A. Ertoprak, R. Escudeiro, F. Galtarossa, A. Goasduff, B. Gongora-Swevin, A. Gottardo, A. Gozzelino, B. Greaves, K. Hadyńska-Klęk, J. Heery, S. F. Hicks, Z. Huang, D. Hymers, A. Illana, **J. Iwanicki**, **G. Jaworski**, B. Jigmeddorj, D. Kalaydjieva, **M. Kisieliński**, R. Kjus, **M. Komorowska**, N. Kopec, M. Kowalczyk, J. Kowalska, K. Z. Krutul-Bitowska, R. Kumar, A. M. Quynh, N. Marchini, **T. Marchlewski**, K. R. Mashtakov, M. Matejska-minda, D. Mengoni, C. Michelagnoli, **P. J. Napiorkowski**, D. R. Napoli, B. Olaizola, **M. Palacz**, S. Pannu, E. Pasquali, J. Pellumaj, E. E. Peters, R. M. Perez-Vidal, S. Pigliapoco, E. Pilotto, F. Recchia, K. Rezynkina, E. Sahin, **J. Samorajczyk-Pyśk**, M. Saxena, M. Sedlak, **J. Srebrny**, **A. Stolarz**, K. Stoychev, C. E. Svensson, **A. Tucholski**, **A. Trzcińska**, S. Valbuena, J. J. Valiente-Dobon, J. L. Wood, S. W. Yates, L. Zago, I. Zanon, G. Zhang, T. Zidar. *Probing low-energy states in 110Cd using Coulomb excitation.* Acta Phys. Pol. B Proc. Suppl. 18(2025) A26.

[39] K. Pyrzyńska, **K. Kilian**. *Porphyrin-based sorbents for the enrichment and removal of metal ions.* Molecules 30(2025) 2238.

[40] J. Ruotsalainen, A. Jaries, M. Stryjczyk, A. Kankainen, B. Andel, M. Araszkiewicz, O. Beliuskina, A. M. Bruce, S. Cannarozzo, S. Chinthakayala, S. Doshi, T. Eronen, A. Fijałkowska, L. M. Fraile, P. Garczynski, Z. Ge, D. Grigorova, **G. Jaworski**, A. Korgul, T. Krakowski, J. Kurpeta, S. Lalkovski, M. L. Exposito, I. D. Moore, L. M. Motilla, M. Mougeot, H. Penttila, A. Raggio, W. Rattanasakuldilok, J. Saren, K. Solak. *Probing the quantum phase transition near $N \approx 60$ via mass measurements of technetium isotopes.* Phys. Rev. C 112(2025) 064302.

[41] **A. Sentkowska**, J. Folcik, J. Szmytke, A. Grudniak. *Is there any correlation between green synthesis parameters and the properties of obtained selenium nanoparticles?* Molecules 30(2025) 2865.

[42] M. Singha, R. Yokoyama, R. Grzywacz, A. Keeler, T. T. King, J. Agramunt, N. T. Brewer, S. Go, J. Liu, S. Nishimura, P. Parkhurst, V. H. Phong, M. M. Rajabali, B. C. Rasco, K. P. Rykaczewski, D. W. Stracener, A. Tolosa-Delgado, K. Vaigneur, **M. Wolińska-Cichocka**. *YSO implantation detector for beta-delayed neutron spectroscopy.* Nucl. Instrum. Methods Phys. Res. A 1073(2025) 170239.

[43] **A. Špaček**, A. Herzan, M. Sedlak, M. Venhart, F. A. Ali, A. N. Andreyev, K. Auranen, S. Banovska, M. Balogh, R. J. Carroll, D. M. Cox, J. G. Cubiss, T. Davis, M. C. Drummond, J. L. Easton, T. Grahn, A. Gredley, P. T. Greenlees, J. Henderson, U. Jakobsson, D. T. Joss, R. Julin, S. Juutinen, G. Kantay, J. Kliman, J. Konki, E. A. Lawrie, M. Leino, V. Matousek, A. K. Mistry, C. G. Mcpeake, D. O'Donnell, R. D. Page, J. Pakarinen, P. Papadakis, J. Partanen, P. Peura, P. Rahkila, A. Repko, P. Ruotsalainen, M. Sandzelius, J. Saren, B. Saygi, D. Seweryniak, C. Scholey, J. Sorri, S. Stolze, A. Thornthwaite, I. S. Timchenko, J. Uusitalo, M. Veselsky, S. Vielhauer, F. P. Wearing. *Fine structure in the α decay of 179Hg*

and 177Au. Eur. Phys. J. A 61(2025) 43.

[44] A. M. Stefanini, G. Montagnoli, M. Del Fabbro, F. Fontana, P. Aguilera, G. Andreetta, D. Brugnara, **G. Colucci**, L. Corradi, E. Fioretto, F. Galtarossa, A. Goasduff, B. G. Servin, A. Gozzelino, M. Heine, G. Harmant, D. Mengoni, M. Luciani, K. Rezynkina, S. Rocca, D. Stramaccioni. *Low-energy fusion of doubly magic nuclei: The notable case of 16O+48Ca.* Phys. Rev. C 111(2025) 064620.

[45] H. Suzuki, N. Fukuda, H. Takeda, Y. Shimizu, D. S. Ahn, T. Komatsubara, A. Algora, B. Rubio, J. A. Victoria, J. L. Tain, A. Tolosa, J. Agramunt, E. Nacher, S. E. A. Orrigo, V. Guadilla, G. Kiss, D. Sohler, I. Kuti, T. Davinson, O. B. Hall, D. Kahl, C. G. Bruno, C. J. Appleton, P. J. Woods, S. Nishimura, H. Baba, D. Nishimura, T. Isobe, M. Kaneko, S. Kubono, H. Sakurai, H. Shimizu, T. Sumikama, P. Doornenbal, M. L. Cortes, Z. Podolyak, E. Ganioglu, Y. Fujita, F. Molina, J. Liu, J. Lee, K. P. Rykaczewski, **M. Wolińska-Cichocka**, M. Labiche, C. J. Griffin, S. Bae, J. Ha, Y. A. Litvinov, K. Kusaka, Y. Yanagisawa, M. Ohtake, N. Fukunishi, S. Michimasa. *Discovery of 98Sn produced by the projectile fragmentation of a 345-MeV/nucleon 124Xe beam.* Prog. Theor. Exp. Phys. 2025(2025) 053D02.

[46] A. Tolosa-Delgado, J. L. Tain, M. Reichert, A. Arcones, M. Eichler, B. C. Rasco, N. T. Brewer, K. P. Rykaczewski, R. Yokoyama, R. Grzywacz, I. Dillmann, J. Agramunt, D. S. Ahn, A. Algora, H. Baba, S. Bae, C. G. Bruno, R. C. Folch, F. Calvino, P. J. Coleman-Smith, G. Cortes, T. Davinson, C. Domingo-Pardo, A. Estrade, N. Fukuda, S. Go, C. J. Griffin, J. Ha, O. Hall, L. Harkness-Brennan, T. Isobe, D. Kahl, M. Karny, L. H. Khiem, G. G. Kiss, M. Kogimtzis, A. Korgul, S. Kubono, M. Labiche, I. Lazarus, J. Liang, J. Lee, J. Liu, G. Lorusso, K. Matsui, K. Miernik, F. Montes, B. Moon, A. I. Morales, N. Nepal, S. Nishimura, R. D. Page, M. Piersa-Silkowska, V. H. Phong, Z. Podolyak, V. F. E. Pucknell, P. H. Regan, Y. Saito, H. Sakurai, Y. Shimizu, J. Simpson, P. A. . Soderstrom, D. W. Stracener, T. Sumikama, R. Surman, H. Suzuki, M. Takechi, H. Takeda, A. Tarifeno-Saldivia, S. L. Thomas, **M. Wolińska-Cichocka**, P. J. Woods, X. X. Xu. *Impact of newly measured β-delayed neutron emitters around 78Ni on light element nucleosynthesis in the neutrino wind following a neutron star merger.* Phys. Rev. Lett. 134(2025) 172701.

[47] **A. Tucholski**, Z. Patyk. *Magnetic field at nucleus for ionized atoms.* Nucl. Phys. A 1059(2025) 123073.

[48] S. Valdre, A. Camaiani, G. Verde, S. Piantelli, G. Casini, N. Le Neindre, L. Baldesi, S. Barlini, M. Bini, A. Boiano, E. Bonnet, B. Borderie, R. Bougault, A. Chbihi, C. Cialdai, C. Ciampi, D. Dell'Aquila, J. Duenas, P. Edelbruck, Q. Fable, D. Fabris, J. D. Frankland, C. Frosin, F. Gramegna, D. Gruyer, M. Henri, B. Hong, S. Kim, **A. Kordyasz**, T. Kozik, M. Kweon, I. Lombardo, O. Lopez, T. Marchi, K. Mazurek, A. Olmi, A. Ordine, P. Ottanelli, J. Park, M. Parlog, G. Pasquali, M. G. Pellegriti, G. Poggi, A. Rebillard-Soulie, L. Redigolo, F. Salomon, M. Scaringella, A. A. Stefanini, G. Tobia, G. Tortone, S. Upadhyahya, E. Vient, M. Vigilante. *FAZIA: A new generation array for nuclear dynamics and EoS experiments at intermediate energies.* Int. J. Mod. Phys. A 40(2025) 2444008.

[49] G. Walpuski, A. Rafalski, M. Galas, **Z. Szefliński**, M. Zienkiewicz. *Influence of ploidy on radiation resilience in extremophilic alga Galdieria sulphuraria under extreme ionizing conditions.* Environ. Exp. Bot. 240(2025) 106231.

[50] **B. Zalewski**, M. S. Golovkov, **K. Rusek**, S. G. Belogurov, A. A. Bezbakh, V. Chudoba, E. M. Gazeeva, V. Gorshkov, A., G. Kamiński, N. Keeley, S. A. Krupko, B. Mauyey, I. A. Muzalevskii, **P. J. Napiorkowski**, **W. Piątek**, A. Serikov, S. I. Sidorchuk, R. S. Slepnev,

P. G. Sharov, N. Sokolowska, G. M. Ter-Akopian, **A. Trzcińska**, R. Wolski. *Influence of deuteron breakup on d+ 6He elastic scattering.* Phys. Rev. C 111(2025) 054616.

D.4 Seminars

D.4.1 Seminars organised at HIL

A. Sentkowska — Heavy Ion Laboratory, University of Warsaw, Warszawa, Poland — 15 January 2025

Nano selen - dlaczego tak ważny?

Nano selenium – why is it so important?

A. Kordyasz — Heavy Ion Laboratory, University of Warsaw, Warszawa, Poland — 12 February 2025

Badanie wielkiej odporności radiacyjnej cienkich 21 μm self-biased detektorów krzemowych pracujących bez napięcia polaryzacji tak jak baterie słoneczne

Investigation of the high radiation resistance of thin 21 μm self-biased silicon detectors operating without bias voltage, similar to solar cells

P. Dey — Heavy Ion Laboratory, University of Warsaw, Warszawa, Poland — 9 April 2025

Exploration of single-particle and collective excitations in nuclei around the A=90 region

C. Kamaran — Akdeniz University, Antalya, Turkey — 14 May 2025

Innovations in advamced nanomaterials for energy storage and conversion systems

M. Janiszewski — Faculty of Chemistry, University of Warsaw, Warszawa, Poland — 11 June 2025

Chromatograficzne oznaczanie selenu w miodzie - opracowanie nowej metodyki ekstrakcji i konserwacji próbek

Chromatographic determination of selenium in honey – development of a new extraction and sample preservation methodology

M. Maryański — Gdańsk University of Technology, Poland — 15 October 2025

Żele polimerowe jako trójwymiarowe dozymetry fantomowe i detektory śladowe promieniowania jonizującego, w tym hadronów

Polymer gels as three-dimensional phantom dosimeters and track detectors for ionizing radiation, including hadrons

R. Wolski — Institute of Nuclear Physics PAN, Kraków, Poland — 4 November 2025

Study of nuclear structure in the continuum using the (d,p) reaction with radioactive beams

I.S. Badambaevith — Uzbekistan Acad. of Sci. Inst. of Nucl. Phys., Tashkent, Uzbekistan — 3 December 2025

The Role of Nuclear Transfer Reactions in Astrophysics

D.4.2 Seminars co-organised by HIL

Warsaw Nuclear Physics Seminar

Seminars organised jointly by the divisions of Nuclear Physics and Nuclear Structure Theory of the Faculty of Physics, University of Warsaw and the Heavy Ion Laboratory, University of Warsaw

I. Michelon — ISOLDE, CERN, Geneve, Switzerland 16 January 2025
Beta-decay spectroscopy with beams of laser-polarised nuclei at VITO ISOLDE

M. Zielińska — IRFU, CEA, Université Paris-Saclay, Gif-sur-Yvette, France 23 January 2025
Exploring quadrupole and octupole collectivity in ^{106}Cd via unsafe Coulomb excitation

J. Orliński — Faculty of Physics, University of Warsaw, Warszawa, Poland 27 February 2025
Transverse flow of strange hadrons in heavy ion collisions at a beam kinetic energy of a few GeV measured in HADES

A. Kusina — The H. Niewodniczański Inst. of Nucl. Phys. PAN, Kraków, Poland 6 March 2025
Quark and gluon distributions in nuclei at high energy and their connection with correlated nucleon pairs

M. Grodzicka-Kobyłka — National Centre for Nuclear Research 13 March 2025
Fotopowielacze krzemowe w detekcji promieniowania gamma i neutronów – zasady działania i zastosowania
Silicon photomultipliers in gamma-ray and neutron detection – principles of operation and applications

K. W. Fornalski — Faculty of Physics, Warsaw Univ. of Technology 20 March 2025
W kręgu biofizyki radiacyjnej: niskie dawki promieniowania a odpowiedź adaptacyjna organizmu
In the realm of radiation biophysics: low doses of radiation and the organism's adaptive response

A. Ruciński — The H. Niewodniczański Inst. of Nucl. Phys. PAN, Kraków, Poland 27 March 2025
Secondary radiation measurements and applications in proton and ion beam therapy range monitoring

Y. Jaganathen — National Centre for Nuclear Research 3 April 2025
Demystifying the Fusion Mechanism in Heavy-Ion Collisions: A Six-Dimensional Langevin Dissipative Dynamics Approach

J. Henderson — Department of Physics, University of Surrey, Guildford, UK 10 April 2025
Coulomb excitation with radioactive and stable beams

J. Łukasik — The H. Niewodniczański Inst. of Nucl. Phys. PAN, Kraków, Poland 24 April 2025
Symmetry Energy at High Densities from Heavy Ion Collisions: ASY-EOS II experiment using KRAB detector and the R3B infrastructure

M. Pfützner — Faculty of Physics, University of Warsaw, Warszawa, Poland — 15 May 2025
Promieniotwórczość dwuprotonowa: historia, status i perspektywy
Two-proton radioactivity: history, current status, and prospects

J. Wilson — Lab. de Physique des 2 infinis Irène Joliot-Curie, Orsay, France — 22 May 2025
Prompt and delayed γ ray emission as an experimental probe of fission

J. Menéndez — The Institute of Cosmos Science, University of Barcelona, Spain — 29 May 2025
Exploring nuclear shapes within the shell model: new perspectives

M. Ciemała — The H. Niewodniczański Inst. of Nucl. Phys. PAN, Kraków, Poland — 5 June 2025
Wysokoenergetyczne struktury w widmach promieniowania gamma zmierzone w reakcji fuzji–rozszczepienia $^{238}U + {}^{8}B$
High-energy structures in gamma-ray spectra measured in the $^{238}U + {}^{8}B$ fusion–fission reaction

W. Urban — Faculty of Physics, University of Warsaw, Warszawa, Poland — 12 June 2025
Zagadka niskoenergetycznych stanów 0^+ w jądrach parzysto-parzystych A$\sim$150
The puzzle of low-energy 0^+ states in even–even nuclei with A$\sim$150

K. Hadyńska-Klęk — Heavy Ion Laboratory, University of Warsaw, Warszawa, Poland — 2 October 2025
Probing nuclear structure and deformation in the vicinity of ^{40}Ca and ^{56}Ni

S. Trojanowski — National Centre for Nuclear Research — 9 October 2025
Forward Collider Neutrinos and Implications for Hadronic Physics

K. Rani — Heavy Ion Laboratory, University of Warsaw, Warszawa, Poland — 16 October 2025
Reaction Studies from below to well above the Coulomb Barrier energies

J. Choiński — Heavy Ion Laboratory, University of Warsaw, Warszawa, Poland — 23 October 2025
30-lecie Środowiskowego Laboratorium Ciężkich Jonów w Uniwersytecie Warszawskim - mało znany fakt jego zaangażowania w produkcję radioizotopów medycznych
The 30th anniversary of the Heavy Ion Laboratory at the University of Warsaw – a little-known fact about its involvement in medical radioisotope production

L. Kosarzewski — Faculty of Physics, Warsaw Univ. of Technology — 30 October 2025
Obrazowanie kształtów jąder atomowych w relatywistycznych zderzeniach ciężkich jonów w eksperymencie STAR
Imaging nuclear shapes in relativistic heavy-ion collisions in the STAR experiment

H. Zbroszczyk — Faculty of Physics, Warsaw Univ. of Technology — 6 November 2025
Observation of the antimatter hypernucleus at STAR

E. Masha — Helmholtz-Zentrum Dresden-Rossendorf, Germany 20 November 2025
Stellar fusion in an underground lab: New measurements from the Felsenkeller

O. Le Noan — IPHC, Strasbourg, France 27 November 2025
Electric Dipole Response and the Nature of the Pygmy Dipole Resonance in light Nuclei from a Shell-Model Perspective

Y. Jaganathen — National Centre for Nuclear Research 11 December 2025
Suppression of genuine ternary fission in heavy and superheavy nuclei: A self-consistent perspective

R. Ryblewski — The H. Niewodniczański Inst. of Nucl. Phys. PAN, Kraków, Poland 18 December 2025
Spin hydrodynamics in relativistic heavy-ion collisions

D.4.3 External seminars given by HIL staff

K. Hadyńska-Klęk 05 February 2025
Perspectives of the PARIS project at the Heavy Ion Laboratory in Warsaw
PARIS Collaboration Meeting - Open Session "Future of PARIS – LNL Legnaro and beyond", Bormio, Italy

G. Colucci 19 February 2025
Role of dissipation in nuclear Fusion reactions
Seminar – Chinese Institute of Atomic Energy (CIAE), Pekin, Chiny

P. Dey 11 March 2025
Octupole collectivity in zirconium isotopes around A=90 region
Conference on Frontiers in Gamma Ray Spectroscopy (FIG2025), TIFR Mumbai, India

A. Špaček 13 March 2025
Expanding the EAGLE Array at HIL: The FLASH Campaign for Fast-Timing Spectroscopy
Fast timing for nuclear structure and applications (FAST'25) workshop – Madrid, Spain

K. Hadyńska-Klęk 24 April 2025
Probing nuclear deformation in the ^{40}Ca and ^{56}Ni mass regions using the Coulomb excitation method
University of Barcelona, Barcelona, Spain

K. Hadyńska-Klęk 21 May 2025
Forging tools to understand nuclear deformation in light and medium mass nuclei
Sezione di Firenze and University of Florence, Sesto Fiorentino, Italia

K. Wrzosek-Lipska 26 May 2025
Probing multiple shape coexistence in Cd isotopes using Coulomb excitation
The 29^{th} International Nuclear Physics Conference (INPC 2025), Daejeon, Korea

K. Kilian 29 May 2025
Radioizotopy i promieniowanie jonizujące w poszukiwaniu leków i diagnostyki
Radioisotopes and ionizing radiation in the search for drugs and diagnostics

Aspekty regulatorowe w opracowaniu i wdrażaniu radiofarmaceutyków, Warszawa

A. Sentkowska 05 June 2025
Nano selen - dlaczego tak ważny?
Nano selenium - why so important?
Seminar of the Department of Biomedical Physics, University of Warsaw, Warszawa

K. Hadyńska-Klęk 11 June 2025
Shapes and collectivity near magic nuclei: Coulomb excitation of ^{62}Ni
AGATA Prepac Workshop, INFN LNL, Legnaro, Italia

A. Sentkowska 18–20 August 2024
Green synthesis of selenium nanoparticles - pros and cons
European Advanced Materials Congress, Stockholm, Sweden

K. Hadyńska-Klęk 5 September 2025
A guide on how to travel around the world with Coulomb excitation tools in a suitcase
The Mazurian Lakes Conference on Physics, Poland

G. Colucci 11 September 2025
Dissipation in the quasielastic barrier distributions of ^{20}Ne + ^{92,94,95}Mo: the role of transfer channels
Heavy Ion Accelerator Symposium on Nuclear Physics and its Applications (HIAS 2025) – Canberra, Australia

L. Próchniak 18 September 2025
A journey into the mercury region
31st Nuclear Physics Workshop, Lublin, Poland

J. Srebrny 18 September 2025
Quadrupole Triaxiality Softness: From a simple phenomenological model to a fully microscopic General Bohr Hamiltonian
31st Nuclear Physics Workshop, Lublin, Poland

J. Choiński 25 September 2025
The 30^{th} anniversary of the Heavy Ion Laboratory of the University of Warsaw and its contribution to the production of medical radioisotopes
2^{nd} Symposium on new trends in nuclear and medical physics Marian Smoluchowski Institute of Physics, Jagiellonian University, Kraków, Poland

K. Wrzosek-Lipska 14 October 2025
Studying multiple shape coexistence in Cd isotopes through Coulomb excitation
Isospin, STructure, Reactions and energy Of Symmetry (ISTROS) Conference, Casta Papiernicka, Slovakia

K. Hadyńska-Klęk 14 October 2025
Probing nuclear deformation in the vicinity of ^{40}Ca and ^{56}Ni
Isospin, Structure, Reactions and energy Of Symmetry (ISTROS) Conference, Casta Papiernicka, Slovakia

L. Próchniak 14 October 2025
Quadrupole excitations within the self-consistent mean-field theory
Isospin, STructure, Reactions and energy Of Symmetry (ISTROS) Conference, Casta Papiernicka, Slovakia

A. Špaček 16 October 2025
Expanding the EAGLE array at HIL: The FLASH campaign for fast-timing spectroscopy
Isospin, STructure, Reactions and energy Of Symmetry (ISTROS) Conference, Casta Papiernicka, Slovakia

M. Palacz 27 October 2025
The EAGLE HPGe detector array
FLASH (Fast-Timing LaBr3 Array for Spectroscopy at HIL) Workshop, Warsaw, Poland

K. Hadyńska-Klęk 27 October 2025
SilCA – a particle detector array for Coulomb excitation studies
FLASH (Fast-Timing LaBr3 Array for Spectroscopy at HIL) Workshop, Warsaw, Poland

A. Špaček 27 October 2025
Commissioning experiment
FLASH (Fast-Timing LaBr3 Array for Spectroscopy at HIL) Workshop, Warsaw, Poland

P. J. Napiorkowski 29 October 2025
Irradiation station for heavy ion beams from the Warsaw Cyclotron
Nuclear Physics and Innovative Technologies, Warsaw, Poland

J. Choiński 29 October 2025
The Heavy Ion Laboratory of the University of Warsaw and its contribution to the production of medical radioisotopes
Nuclear Physics and Innovative Technologies, Warsaw, Poland

A. Sentkowska 29 October 2025
Chemistry and nanotechnology at HIL-recent achievements and future perspectives
Nuclear Physics and Innovative Technologies, Warsaw, Poland

I. Piętka 29 October 2025
Low-background gamma spectroscopy
Nuclear Physics and Innovative Technologies, Warsaw, Poland

K. Wrzosek-Lipska 25 November 2025
Multiple shape coexistence in Cd isotopes studied with Coulomb excitation
The African Nuclear Physics Conference 2025 (ANPC 2025), Cape Town, iThemba LAB, South Africa

D.4.4 Poster presentations

K. Kilian 17 June 2025
Assessment of porphyrin cellular uptake in cancer cells
Annual Congress of the European Association for Cancer Research (EACR 2025), Lisbon, Portugal

K. Kilian 18 June 2025
Characterization of radiolabelled single-domain anti-HER2 antibodies as potential radioimmunotherapeutics for breast cancer
Annual Congress of the European Association for Cancer Research (EACR 2025), Lisbon, Portugal

I. Piętka 4 September 2025
Coulomb excitation of ^{110}Cd studied with AGATA at LNL
The Mazurian Lakes Conference on Physics, Poland

A. Špaček 4 September 2025
Expanding the EAGLE Array at HIL: The FLASH Campaign for Fast-Timing Spectroscopy
The Mazurian Lakes Conference on Physics, Poland

P. Dey 4 September 2025
Measurements of octupole collectivity in $^{90,\ 91}$Zr
The Mazurian Lakes Conference on Physics, Poland

C. Hiver 4 September 2025
Complex simulations of the heavy ion detection mechanism for the modernized version of the Recoil Filter Detector at HIL UW
The Mazurian Lakes Conference on Physics, Poland

P. Sekrecka 4 September 2025
In beam gamma-ray spectroscopy of ^{134}Sm
The Mazurian Lakes Conference on Physics, Poland

J. Choiński, A. Stolarz 05 November 2025
First experimental demonstration of positronium lifetime imaging with ^{44}Sc using the J-PET Scanner
The 2025 IEEE MIC conference, Yokohama, Japan

J. Choiński, A. Stolarz 07 November 2025
Simulation studies of a brain PET insert for total body J-PET tomography
The 2025 IEEE MIC conference, Yokohama, Japan

D.4.5 Lectures for students and student laboratories

K. Hadyńska-Klęk 27-29 January 2025
Quadrupole sum rules and nuclear shapes
EURO-LABS – InTraNS – Florence Training Workshop on Coulomb Excitation, Florence, Italy

K. Wrzosek-Lipska 27-29 January 2025
GOSIA practical sessions
EURO-LABS – InTraNS – Florence Training Workshop on Coulomb Excitation, Florence, Italy

K. Wrzosek-Lipska 27 January 2025
Introduction to GOSIA
EURO-LABS – InTraNS – Florence Training Workshop on Coulomb Excitation, Florence, Italy

K. Wrzosek-Lipska 28 January 2025
Normalization in Coulomb excitation experiments
EURO-LABS – InTraNS – Florence Training Workshop on Coulomb Excitation, Florence, Italy

K. Wrzosek-Lipska 29 January 2025
The role of complementary data
EURO-LABS – InTraNS – Florence Training Workshop on Coulomb Excitation, Florence, Italy

K. Wrzosek-Lipska May 2025
Badanie kształtów jąder atomowych metodą wzbudzeń kulombowskich
Studying the shapes of atomic nuclei using the Coulomb excitation method
Koło Naukowe Fizyki Jądrowej i Cząstek Elementarnych Wydziału Fizyki UW

Z. Szefliński 10 April 2025
Wpływ ploidalności na przebieg choroby popromiennej u ekstremofilnej algi Galdieria sulphuraria
The influence of ploidy on the course of radiation sickness in the extremophilic alga Galdieria sulphuraria
Faculty of Physics, Warsaw University of Technology, Warszawa, Poland

Z. Szefliński 06 June, 06 November 2025
Fizyka w diagnostyce medycznej PET-SPECT
Physics in PET-SPECT medical diagnostics
Faculty of Physics, University of Warsaw, Warszawa, Poland

P. J. Napiorkowski 19 October 2025
30 lat wiązki ciężkich jonów
30 years of heavy ion beams
XIX Ogólnopolskie Warsztaty Akceleracji i Zastosowań Ciężkich Jonów

A. Stolarz 20 October 2025
Tarcze do badań w fizyce jądrowej
Targets for research in nuclear physics

XIX Ogólnopolskie Warsztaty Akceleracji i Zastosowań Ciężkich Jonów

M. Palacz 20 October 2025
Detekcja promieniowania gamma, cząstek naładowanych i neutronów
Detection of gamma rays, charged particles and neutrons
XIX Ogólnopolskie Warsztaty Akceleracji i Zastosowań Ciężkich Jonów

K. Kilian 21 October 2025
Radiofarmaceutyki do pozytonowej tomografii emisyjnej (PET)
Radiopharmaceuticals for positron emission tomography (PET)
XIX Ogólnopolskie Warsztaty Akceleracji i Zastosowań Ciężkich Jonów

K. Hadyńska-Klęk 21 October 2025
Spektroskopia gamma na wiązce
Gamma beam spectroscopy
XIX Ogólnopolskie Warsztaty Akceleracji i Zastosowań Ciężkich Jonów

O. Nassar 22 October 2025
Akceleracja ciężkich jonów i elementy optyki jonowej
Heavy ion acceleration and ion optics components
XIX Ogólnopolskie Warsztaty Akceleracji i Zastosowań Ciężkich Jonów

K. Rusek 23 October 2025
Reakcje jądrowe
Nuclear reactions
XIX Ogólnopolskie Warsztaty Akceleracji i Zastosowań Ciężkich Jonów

U. Kaźmierczak winter semester of the academic year 2024/25
Biofizyka - laboratorium
Biophysics - laboratory

U. Kaźmierczak summer semester of the academic year 2024/25
SDNSP - Rozwój naukowy – zajęcia indywidualne z promotorem (warsztat naukowca)
SDNSP - Scientific development - individual classes with a supervisor (scientist workshop)

K. Kilian summer semester of the academic year 2024/25
Pracownia radiofarmaceutyków
Laboratory of Radiopharmaceuticals
Faculty of Physics, University of Warsaw, Warszawa, Poland

K. Kilian winter semester of the academic year 2024/25
Metody izotopowe i chemia radiofarmaceutyków
Isotope methods and radiopharmaceutical chemistry
Faculty of Physics, University of Warsaw, Warszawa, Poland

K. Kilian winter semester of the academic year 2024/25
Metody izotopowe i chemia radiofarmaceutyków
Isotope methods and radiopharmaceutical chemistry
Faculty of Chemistry, University of Warsaw, Warszawa, Poland

K. Kilian summer semester of the academic year 2024/25
Radiofarmaceutyki – synteza, wytwarzanie i zastosowania
Radiopharmaceuticals – synthesis, production and applications
Faculty of Chemistry, University of Warsaw, Warszawa, Poland

A. Sentkowska winter semester of the academic year 2024/25
Differential spectrophotometric - determination of acylated anthocyanins in ivy - exercises within the Environmental Analysis Laboratory
Faculty of Chemistry, University of Warsaw, Warszawa, Poland

D.4.6 Science popularization lectures

M. Paluch-Ferszt Dni Kampusu Ochota (DOKO) 22.03.2025

Promieniowanie jonizujące w służbie ochrony zdrowia i życia - historia i teraźniejszość
Ionizing radiation in the service of health and life protection - history and present

M. Paluch-Ferszt 29 Festiwal Nauki 24.09.2025

Promieniowanie jonizujące w służbie ochrony zdrowia i życia - historia i teraźniejszość
Ionizing radiation in the service of health and life protection - history and present

K. Kilian, P. J. Napiorkowski Wykład otwarty dla uczniów liceów i techników 15.11.2025

Obrazowanie medyczne, czyli pokaż kotku co masz w środku
Medical imaging, or Kitty, show me what's inside

A. Sentkowska Dni Kampusu Ochota (DOKO) 22.03.2025

Kawa, herbata a może...wino? Co pić aby „delikatnie" się odmłodzić?
Coffee, tea or maybe... wine? What to drink to "gently" rejuvenate yourself?

A. Sentkowska Lecture for HIL guests 27.10.2025

Czy na pewno wiesz jak parzyć herbatę? O zdolnościach antyutleniających słów kilka
Do you really know how to brew tea? A few words about its antioxidant properties

Z. Szefliński 29 Festiwal Nauki 23.09.2025

Słońce-atom-wiatr
Sun-atom-wind

Z. Szefliński 29 Festiwal Nauki 24.09.2025

Radon wokół nas
Radon around us

Z. Szefliński LXI LO Specjalne im. Janiny Zawadowskiej 21.10.2025

Radon wokół nas
Radon around us

Z. Szefliński LXI LO Specjalne im. Janiny Zawadowskiej 21.10.2025

Słońce-atom-wiatr
Sun-atom-wind

Z. Szefliński I LO im. A Mickiewicza, Węgrów 28.10.2025

Radon wokół nas
Radon around us

Z. Szefliński I LO im. A Mickiewicza, Węgrów 28.10.2025

Słońce-atom-wiatr
Sun-atom-wind

Z. Szefliński LXI Liceum Artes Liberales, Warszawa, 05.11.2025

Radon wokół nas
Radon around us

D.5 Honours and Awards

The Rector of the University of Warsaw distinction award for scientific achievements 2025:

dr Giulia Colucci

Tomek Czosnyka Honorary Award 2025 Presented to:

dr Katarzyna Hadyńska-Klęk

The Rector of the University of Warsaw awards 2025:

Eliza Balcerowska,
Jarosław Choiński,
Ewa Sobańska.
Nurullo Sobirov,
Mariusz Szperkiewicz,
Anna Ratyńska,
Kamil Makowski,
Bogusław Paprzycki,
Michalina Komorowska,
Mariusz Matuszewski,
Robert Ratyński,
Justyna Samorajczyk-Pyśk,
Łukasz Standyło.

D.6 Laboratory staff

Director: Paweł Napiorkowski
Deputy directors: Jarosław Choiński, Krzysztof Kilian
Scientific Leader: Krzysztof Rusek
Financial executive: Eliza Balcerowska

Senior scientists:

Andrzej Kordyasz[a], Marcin Palacz, Ernest Piasecki[b], Leszek Próchniak, Aleksandra Sentkowska, Anna Stolarz, Zygmunt Szefliński

Scientific staff and engineers:

Tomasz Abraham, Andrzej Bednarek, Giulia Colucci, Piku Dey, Jarosław Falkowski[c], Katarzyna Hadyńska-Klęk, Corentin Hiver[d], Grzegorz Jaworski, Grzegorz Kamiński[e], Urszula Kaźmierczak, Maciej Kisieliński, Michalina Komorowska, Marian Kopka, Michał Kowalczyk[f], Joanna Kowalska, Katarzyna Krutul-Bitowska[e], Jan Miszczak, Olga Nassar, Wojciech Okliński, Krzysztof Olejarczyk, Monika Paluch-Ferszt, Serhii Panasenko, Mateusz Pęgier, Bogdan Radomyski, Kavita Rani, Justyna Samorajczyk-Pyśk, Paulina Sekrecka, Andrej Špaček, Julian Srebrny[a], Łukasz Standyło, Agnieszka Trzcińska, Andrzej Tucholski, Marzena Wolińska-Cichocka, Katarzyna Wrzosek-Lipska,

Doctoral candidates:

Patrycja Kamińska, Adam Malinowski, Iwona Piętka,

Technicians:

Mariusz Antczak, Tomasz Bracha, Tomasz Drzycimski[g], Piotr Jasiński, Wiesław Kalisiewicz, Robert Kopik, Wojciech Kozaczka, Piotr Krysiak, Krzysztof Łabęda, Kamil Makowski, Mariusz Matuszewski, Bogusław Paprzycki, Krzysztof Pietrzak, Robert Ratyński, Mariusz Szperkiewicz, Łukasz Świątek

Administration and support:

Anna Błaszczyk-Duda[a], Agnieszka Borowik, Rafał Klęk[h], Aleksandra Lewandowska[i], Mirosław Makos, Jolanta Matuszczak, Andrzej Młociński, Dariusz Noceń, Olga Oborska[j], Anna Odziemczyk[j], Piotr Orłowski, Jolanta Ormaniec[i], Jarosław Pniewski[k], Anna Ratyńska, Ewa Sobańska, Nurullo Sobirov, Lidia Strzelczyk, Andrzej Suchecki, Edyta Szeląg, Lech Szeląg, Magdalena Zawal, Andrzej Żuryński.

Voluntary scientists:

Jędrzej Iwanicki, Andrzej Kordyasz[l], Jan Kownacki, Julian Srebrny[l], Andrzej Wojtasiewicz.

---

[a] until 31 July
[b] until 2 September
[c] since 1 November
[d] since 1 February
[e] on leave
[f] until 30 June
[g] since 1 June
[h] until 31 May
[i] since 1 October
[j] until 31 December
[k] since 1 March
[l] since 1 September

D.7 Laboratory Council

1. Mgr Eliza Balcerowska
Heavy Ion Laboratory
University of Warsaw, Warszawa

2. Prof. dr hab. Ewa Bulska
Biological and Chemical Research Centre
University of Warsaw, Warszawa

3. Dr Jarosław Choiński
Heavy Ion Laboratory
University of Warsaw, Warszawa

4. Dr Urszula Kaźmierczak
Heavy Ion Laboratory
University of Warsaw, Warszawa

5. Dr hab. Krzysztof Kilian
Heavy Ion Laboratory
University of Warsaw, Warszawa

6. Prof. dr hab. Stanisław Kistryn
(**Member of the Council Presidium**)
M. Smoluchowski Institute of Physics
Jagiellonian University, Kraków

7. Dr hab. Agnieszka Korgul, prof. UW
(**Deputy Chairman of the Council**)
Faculty of Physics
University of Warsaw, Warszawa

8. Dr hab. Michał Kowal, prof. NCBJ
The National Centre for Nuclear Research
Świerk

9. Prof. dr hab. Adam Maj
(**Chairman of the Council**)
The Henryk Niewodniczański
Institute of Nuclear Physics
Polish Academy of Sciences, Kraków

10. Dr Paweł Napiorkowski
Heavy Ion Laboratory
University of Warsaw, Warszawa

11. Dr hab. Marcin Palacz
Heavy Ion Laboratory
University of Warsaw, Warszawa

12. Dr hab. Leszek Próchniak
(**Member of the Council Presidium**)
Heavy Ion Laboratory
University of Warsaw, Warszawa

13. Prof. dr hab. n. med. i n. o zdr. Marek Saracyn
(**Member of the Council Presidium**)
Faculty of Medicine, University of Warsaw,
Military Institute od Medicine - National Research Institute.

14. Dr hab. Aleksandra Sentkowska
Heavy Ion Laboratory
University of Warsaw, Warszawa

15. Dr Agnieszka Trzcińska
Heavy Ion Laboratory
University of Warsaw, Warszawa

D.8 Programme Advisory Committee

PAC members 2020 - 2025

- Piotr Bednarczyk (Institute of Nuclear Physics Polish Academy of Sciences, Kraków, Poland)
- Gilles de France (GANIL, Caen, France)
- Nicholas Keeley (National Centre for Nuclear Research, Świerk, Poland)
- Chiara Mazzocchi (Faculty of Physics, University of Warsaw, Warszawa, Poland)
- Marco Mazzocco (University of Padova, Padova, Italy)
- Leszek Próchniak (Heavy Ion Laboratory, University of Warsaw, Warszawa, Poland)
- **Władysław Trzaska - chair** (Department of Physics, University of Jyväskylä, Finland)

PAC members 2025 - 2028

- Michał Ciemiała (Institute of Nuclear Physics Polish Academy of Sciences, Kraków, Poland)
- Emmanuel Clement (GANIL, Caen, France)
- Chiara Mazzocchi (Faculty of Physics, University of Warsaw, Warszawa, Poland)
- Marco Mazzocco (University of Padua)
- Javier Menéndez (University of Barcelona)
- Krzysztof Rusek (Heavy Ion Laboratory, University of Warsaw, Warszawa, Poland)
- Władysław Trzaska (Department of Physics, University of Jyväskylä, Finland)

The international Programme Advisory Committee of the Heavy Ion Laboratory usually meets twice a year, in spring and autumn. The deadline for submitting proposals is 3 - 4 weeks before a PAC meeting. PAC approved experiments are scheduled at the meetings of the Users' Committee, which also serves as a link between cyclotron users and the Laboratory. The Users' Committee is chaired by Jarosław Perkowski (University of Łódź).

D.9 HIL external users

From 2023, HIL external users must register before arrival. Since then, **235** users have been registered until the end of 2025. In 2025 there were **55** new registrations and the total number of valid registration in 2025 was **148**. The Laboratory was visited by **52** HIL external users and visitors from **22** scientific institutions, including 26 people from 9 institutes in Poland, 15 people from 8 institutions in the European Union and associated countries and 11 people from 5 institutes in other countries.
HIL was also visited by **1024** people from the DRD Collaboration Meeting (CERN), GANIL, NCNR Świerk, Faculty of Biology, Faculty of Physics University of Warsaw, Cardinal Stefan Wyszyński University, Education Center, International School, 3 primary schools, 32 secondary schools and during open days.

HIL external users and visitors were from:

Poland

- AGH University of Science and Technology, Kraków, Poland
- Faculty of Chemistry, University of Warsaw, Warszawa, Poland
- Faculty of Physics, University of Warsaw, Warszawa, Poland
- Faculty of Physics and Applied Computer Science, University of Lodz, Łódź, Poland
- Gdańsk University of Technology, Gdańsk, Poland
- Institute of Nuclear Physics Polish Academy of Sciences, Kraków, Poland
- National Centre for Nuclear Research, Świerk, Poland
- University of Gdańsk, Gdańsk, Poland
- Warsaw University of Technology, Warszawa, Poland

European Union and associated countries

- DEIB Politecnico di Milano, Milano, Italy
- Department of Physics and Astronomy, University of Catania, Catania, Italy
- HUN-REN Institute for Nuclear Research, ATOMKI, Debrecen, Hungary
- INFN Sezione di Catania, Catania, Italy
- INFN. Sezione di Milano, Milano, Italy
- Instituto de Estructura de la Materia, CSIC, Spain
- LNS, INFN e Università di Catania, Catania, Italy
- Trinity College Dublin, Ireland

Other countries

- Akdeniz University, Antalya, Turkey
- Saha Institute of Nuclear Physics, Kolkata, India
- Shandong Provincial Key Laboratory of Nuclear Science, Nuclear Energy Technology and Comprehensive Utilization, Weihai Frontier Innovation Institute of Nuclear Technology, School of Nuclear Science, Energy and Power Engineering, Shandong University, Jinan, China
- Uzbekistan Academy of Science Inst. of Nuclear Physics,Tashkent, Uzbekistan
- Weihai Research Institute of Industrial Technology, Shandong University, Weihai, China

List of Authors

Abraham T., 11, 25, 51, 64
Acosta L., 76
Al Daas D., 51
Allmond J.M., 64
Andreoiu C., 56
Antczak M., 11, 18, 27
Astier A., 56

Barbon A., 73, 76
Basak S., 56
Beckers M., 56
Bednarczyk P., 54
Bednarek A., 23
Bello Garrote F.L., 64
Bhat I. M., 56
Bidaman H., 64
Bildstein V., 64
Blazhev A., 51
Bracha T., 16, 25
Briscoe A., 56
Buck S., 64
Burbadge C., 64

Cardella G., 76
Castoldi A., 76
Cederwall B., 51
Cheng Y., 70
Chen Q.B., 59
Chiari M., 64
Choiński J., 11, 16, 18, 25
Ciemała M., 54
Coleman R., 64
Colombi G., 64
Colucci G., 31, 54, 56, 64, 67, 70, 73, 76
Czerski Z.K, 73

D'Agata G., 73, 76
de France G., 54
Dey P., 67, 82
De Filippo E., 73, 76
Diaz Varela A., 64
Didik A., 51
Doherty D.T., 64
Doncel Monasterio M., 51
Droste Ch., 59
Duan K.D., 56
Dubey R., 73
Duda D., 67
Dunkel F., 56
Dutt S., 64
Dworak W., 41

Fijałkowska A., 54, 67
Fransen C., 51, 56, 59

Garg U., 82
Garrett P.E., 64
Geraci E., 73, 76
Gnoffo B., 76
Goasduff A., 54, 56, 67
Gonzàlez Linares J.G., 76
Grahn T., 51, 56
Greaves B., 64
Grochalska W., 27
Grodner E., 56, 59, 61
Grębosz J., 51, 54, 56, 61, 67
Guadilla V., 54
Guazzoni C., 76
Guo S., 56
Górecki A., 18
Głazowska K., 44

Hadyńska-Klęk K., 28, 31, 51, 54, 56, 61, 64, 67, 73
Han X.C., 61
Heery J., 64
Heymer C., 51
Hiver C., 67
Hlebowicz M., 64
Hymers D., 64

Iwanicki J., 64, 67

Jakowinicz K., 67
Janiszewski M., 37
Jasiński P., 11, 18
Jaworski G., 51, 54, 56, 61, 64, 67, 73
Jia H.M., 70
Jigmeddorj B., 64
Jodidar P.M., 56
Jolie J., 51

Kalaydjieva D., 64
Kalisiewicz W., 11
Karanfil E., 54

Kilian K., 31, 35, 41, 44, 46
Kisieliński M., 23, 27, 64, 73
Koczoń P., 73
Komorowska M., 27, 28, 31, 51, 54, 56, 59, 61, 64, 67
Kondzielska M., 73
Kopeć N., 64
Kopik R., 11, 16, 18, 27
Kopka M., 11, 18
Kordyasz A.J., 23
Korgul .A, 54
Kornwebel L., 56
Kowalczyk M., 27, 31, 51, 54, 56, 59, 61, 64, 67, 73
Kowalska J.A., 16, 28, 31, 54, 64, 67
Kozaczka W., 11, 18
Krakó A., 54
Krutul-Bitowska K., 56, 64
Kruzsicz B., 56
Krysiak P., 11, 18
Krzysiek A., 51, 67
Kumar R., 64
Kumar Raju M., 82
Kundu A., 67, 82
Kurtukian-Nieto T., 76
Kuti I., 54, 56, 67

Lakenbrink C.-D., 51, 56, 59
La Via F., 76
Leifels Y., 73
Lin C.J., 70
Liu C., 61
Li G.Y., 61
Lommel B., 73
Lv B.F., 56
Łabęda K., 11, 18

Müller-Gatermann C., 51
Maiolino C., 76
Mai Quynh A., 64
Makowski K., 11, 18
Malinowski A., 27, 51, 54, 61, 67
Marchini N., 64
Marchlewski T., 64
Martorana N.S., 73, 76
Mashtakov K.R., 64
Matejska-Minda M., 54, 64
Matuszewski M., 11, 18, 27, 67, 73
Ma N.R., 70
McCarter A., 56
McDonalds N., 56
Michelagnoli C., 64
Miernik K., 54
Mierzejwski J., 67
Miszczak J., 11, 18, 25
Molnar J., 54
Mueller Gattermann C., 59

Nanal V., 82
Nannini A., 64
Napiorkowski P.J., 6, 31, 51, 54, 56, 64, 67, 82
Napora Z., 46
Nassar O., 16, 31
Nałęcz-Jawecki A., 51, 54, 56, 59
Novak R., 51

Okliński W., 27, 54, 67
Olaizola B., 64
Olejarczyk K., 18, 21
Oleszczuk F., 64
Otręba A., 54

Pagano E.V., 73, 76
Palacz M., 27, 28, 31, 51, 54, 56, 61, 64, 67
Palit R., 82
Palkowski M.M., 56
Paluch-Ferszt M., 31
Pal S., 82
Panasenko S., 67
Parkarinen J., 51
Pasquali E., 64
Peters E.E., 64
Petrache C.M., 56, 59
Piasecki E., 70, 73
Pietrzak K., 11, 18
Pirrone S., 76
Piętka I., 28, 31, 51, 54, 61, 64, 67
Poklepa W., 56
Politi G., 76
Pozzi M., 76
Pruszyński M., 46
Próchniak L., 59, 64, 79
Pyrzyńska K., 35
Pęgier M., 35

Quattrocchi L., 73

Radomyski B., 11, 16, 18
Rani K., 31, 70, 76
Ratyński R., 11, 18
Regulska M., 54
Risitano F., 76
Rizzo F., 76
Rocchini M., 64

Ruotsalainen P., 51
Rusek K., 31, 51
Russotto P., 73, 76

Sahin E., 64
Samorajczyk-Pyśk J., 31, 54, 56, 61, 64, 67, 73
Sarén J., 56
Saxena M., 64
Saygı B., 54
Sekrecka P., 31, 51, 54, 61, 67
Sentkowska A., 37, 39
Sindhu D., 82
Singh G., 67
Socha S., 67
Sohler D., 56
Solak K., 67
Spagnoletti P., 56
Srebrny J., 51, 56, 59, 61, 64
Standyło Ł., 11, 18, 23
Stolarz A., 16, 23, 28, 31, 54, 59, 61, 64, 67, 73
Sudlitz K., 18
Szoblik N., 39
Szperkiewicz M., 11, 18
Szymanek G., 67
Špaček A., 27, 28, 51, 54, 61, 67
Świątek Ł., 16

Thorat S., 82
Timar J., 56
Tiurin G., 73
Toniolo N., 54, 56, 67
Trimarchi M., 76
Trzaska W.H., 73
Trzcińska A., 31, 64, 70, 73, 76
Tucholski A., 51, 54, 56, 59, 64, 73
Tudisco S., 76

Uusikylä E.T.E., 51, 56
Uusitalo J., 56

Venhart M., 64
Vishal Malik, 82
von Spee F., 51, 56

Wang E.H., 61
Wang S.Y., 61
Wang Z.Y., 61
Wen P.W., 70
Wolińska-Cichocka M., 31, 70, 73, 76
Wood J. L., 64
Wrzosek-Lipska K., 28, 31, 51, 54, 56, 61, 64, 67
Wu F., 56

Xu W.Z., 61

Yang L., 70
Yates S. W., 64
Yeltepe E., 54

Zagami C., 76
Zalewski B., 73
Zeng W.B., 61
Zhang H.Q., 70
Zhang H.Y., 61
Zheng K.K., 56
Zidar T., 64
Zielińska M., 64

www.slcj.uw.edu.pl

RAPORT ROCZNY 2025
ŚRODOWISKOWE LABORATORIUM CIĘŻKICH JONÓW
UNIWERSYTET WARSZAWSKI